Molecular and cell biological analysis of the ESCRT system in *Arabidopsis thaliana*

Inaugural-Dissertation

zur
Erlangung des Doktorgrades
der Mathematisch-Naturwissenschaftlichen Fakultät
der Universität zu Köln

vorgelegt von

Mojgan Shahriari

Aus Iran

Köln 2008

Berichterstatter: Prof. Dr. Martin Hülskamp
Prof. Dr. Ute Höcker

Prüfungsvorsitzender: Prof. Dr. Siegfried Roth

Tag der mündlichen Prüfung: November 2008

Acknowledgment

It is a heart warming and rewarding experience to pay tribute to the people whose invaluable contributions helped me through out my time as a PhD researcher at cologne university, Köln.

My sincere and profound gratitude goes to Prof. Martin Hülskamp how gave me a chance to be a member of Botanical Institute III and Dr. Swen SChellmann for giving me an opportunity to join his group and for the trust that he put into me. It was a unique experience to work with him. His excellent scientific guidance helped me expanded my capabilities.

My special thanks go to my thesis Committee, Prof. Dr. Martin Hülskamp, Prof. Dr. Ute Höcker and Prof. Dr. Siegfried Roth.

I would like to acknowledge the assistance of the technicians of the department: Birgit Kernebeck, Britta Müller, Irene Klinkhammer, Bastian Welter and Uschi Claßen. The personal encouragement and actual help I received from them has made it possible to complete my studies during my time in the University of Cologne.

My special thanks go to the members of the ELCH Group: Christoph Spitzer, Aneta Sabovljevice, Channa Keshavaiah, Stefanie Herbeth, Florian Heßner, and Britta Müller for their extensive for nice comments and the many discussions and for creating a pleasant working atmosphere.

I am indebted to Dr. Schellmann, Dr. Roodbarkelari, Dr. Pesch, Dr. Horvath and Dr. Digiuni for the critical reading of the whole text and for the valuable contribution to the clearness of the manuscript.

And many thanks go to Katja Wester for her help on Confocal Microscopy

I would like to thank Ullrich Herrmann for his help on computer tasks

I would like to thank Niko Pawlowski and Rainer Häusler for helping me run the protein experiments.

I want to thank Ilona Zimmermann, Joachim Uhrig for helping me run yeast two hybrid technique.

My special thanks go to Gardeners of Botanic Institute, who prepared excellent plants for my research.

I would like to thank Simona, Channa, Aneta, Anderea, Jenny, Alex, Nora for creating such a great friendship at the office.
There are all the other people who have made Botanic III very special place over all those years: Andrea Schrader, Burcu Dartan, Cho-Chun Huang, Elena Galiana Jaime, Ullrich Herrmann, Marc Jakoby, Cordula Jörgens, Rachappa Balkunde, Valerie Mach, Philipp Thomas, Elena Galiana Jaime, Moola Mutondo, Victor Kirik, Angela Kirik, Rainer Saedler, Daniel Bouyer, and all the others who have passed through.
I would like to express my thanks to all members of Botanic III Institute who have helped me directly and indirectly in accomplishing this project and giving me a leaning environment to grow me personally as well as professionally.
I appreciated from SFB 635 for their financial support of my study.
I would like to thank everybody who was important to the successful realization of thesis, as well as expressing my apology that I could not mention personally one by one.
I cannot finish without saying how grateful I am with my family. My husband, Farshad, my daughter, Dorsa, my sister and my brothers all have given me a loving environment where to develop.
Finally, and most importantly, I wish to thank my parents, MohamadAli and Sakineh. They have always supported and encouraged me to do my best in life. To them I dedicate this thesis.

CONTENTS

ZUSAMMENEFASSUNG

Die „Endosomal sorting complex required for transport" (ESCRT) Maschinerie ermöglicht den Transport ubiquitinierter Proteine von Endosomen zu den Lysosomomen über die „Multivesicular bodies" (MVBs) in Hefe und Säugetieren. Die Komponenten der ESCRT-Maschinerie sind in drei Subkomplexe und assoziierte Proteine angeordnet. Die Komplexe spielen eine entscheidende Rolle in der Rezeptorregulation, retroviraler Knospung und Proteinsortierung. Die Dissoziation der ESCRT-Komplexe von der endosomalen Membran in der letzten Stufe der Sortierung wird von der AAA-ATPase Vps4 vermittelt. In meiner Doktorarbeit habe ich zwei Aspekte der Funktion des ESCRTs in *Arabidopsis thaliana* untersucht.

Die Analyse von Interaktionen zwischen ESCRT-homologen Proteinen in *Arabidopsis* mittels Hefe-2-Hybrid und BiFC-Untersuchungén zeigen, dass ein Interaktions-Netzwerk von ESCRT-Homologen in *Arabidopsis* existiert. Vps23/ELCH spielt eine zentrale Rolle in der ESCRT-Maschinerie. Es interagiert mit mutmaßlichen Upstream ESCRT-Komponenten sowie mit ESCRT II und ESCRT III. Im Rahmen dieser Studie habe ich ein TOM1-Homolog und ein Mitglied einer neuen Klasse pflanzenspezifischer FYVE-Proteine gefunden, welche mit ELCH interagieren. Dies legt nahe, dass sie an Stelle von Vps27 und HSE1, die nicht im *Arabidopsis*-Genom existieren, Cargo-Proteine rekrutieren.

Im zweiten Teil meiner Doktorarbeit habe ich die Rolle von AtSKD1 im ESCRT-Weg in *Arabidopsis* untersucht. Ich identifizierte ein Sequenzhomolog von Vps4 in *Arabidopsis* (*At*SKD1). Hefe-2-Hybrid und BiFC-Untersuchungén zeigten, das AtSKD1 sowohl an den ESCRT III – Komplex bindet als auch an regulatorische Proteine wie AtLIP5, Vps60 und Vps46. Zusätzlich kolokalisiert YFP-AtSKD1 in *Arabidopsis*-Protoplasten mit endosomalen Markern wie Ara6 und Ara7, wie auch mit FM4-64, einer endocytotischen Markerfärbung.

Die Expression von dominant negativen AtSKD1-Varianten induziert eine Veränderung im endosomalen System von *Arabidopsis*, welcher in vergrößerten Endosomen resultiert, die den „Klasse E"-Kompartimenten in Hefe gleichen. Expression von AtSKD1^{K178A}, AtSKD1^{E234Q}, AtSKD1^{K178AE234Q} in *Arabidopsis*-Trichomen führt zu multiplen Zellkernen ähnlich der Mutation der *Arabidopsis* ESCRT I Komponente Vps23/ELCH, was darauf hindeutet, das der MVB-Weg spezifisch die Zellteilung in Pflanzen reguliert.

Darüberhinaus führt AtSKD1 dominant negative zu Vakuolenfragmentation und Trichomtod.

Abstract

The Endosomal sorting complex required for transport (ESCRT) machinery facilitates the trafficking of ubiquitylated proteins from endosomes to lysosomes via the multivesicular bodies (MVBs) in yeast and mammals. Its components are arranged in three subcomplexes and associated proteins. The ESCRT complexes play critical roles in receptor downregulation, retroviral budding, and protein sorting. Disassembly of ESCRT complexes from endosomal membranes during the last stage of sorting is mediated by the AAA ATPaseVps4. In my thesis I have investigated two aspects of ESCRTs function in *Arabidopsis thaliana*.

Analysis of the interactions of ESCRT homologous proteins of *Arabidopsis* by yeast two hybrid and BiFC assays showed that an interaction network of the ESCRT homologues in *Arabidopsis* exists. Vps23/ELCH plays a central role in the plant ESCRT machinery. It directly interacts with putative upstream ESCRT components and also ESCRT II and ESCRT III. In this study I found a TOM1 homologue and a member of a novel class of plant specific FYVE proteins that interact with ELCH suggesting that they might recruit cargo protein in *Arabidopsis* instead of Vps27 and HSE1 which are not exist in *Arabidopsis* genome.

In the second part of my thesis I examined the role of AtSKD1 in ESCRT pathway in *Arabidopsis*. I identified one sequence homologue of Vps4 in *Arabidopsis* (*AtSKD1*). Yeast two hybrid and BiFC assays detected binding of AtSKD1 to the ESCRT III complex and regulatory proteins like AtLIP5, Vps60 and Vps46. In additio YFP-AtSKD1 colocalizes with endosomal markers such as Ara6 and Ara7, and endocytic marker dye FM4-64 in *Arabidopsis* protoplasts. Expression of dominant negative AtSKD1

variantsinduces changing in the endosomal system of *Arabidopsis* which resulted in enlarged endosomes resembling the yeast "class E" compartments. Expression of AtSKD1^{K178A}, AtSKD1^{E234Q}, AtSKD1^{K178AE234Q} in *Arabidopsis* trichomes multiple nuclei similar to mutation of the *Arabidopsis* ESCRT I component Vps23/ELCH indicating that the MVB pathway regulates specifically cell division in plants.

Furthermore, AtSKD1 dominant negative induce vacuole fragmentation and trichome death.

Publication, manuscript and in preparation papers of my PhD thesis:

Publication:
Christoph Spitzer, Swen Schellmann, Aneta Sabovljevic, **Mojgan Shahriari**, Channa Keshavaiah, Nicole Bechtold, Michel Herzog, Stefan Müller, Franz-Georg Hanisch and Martin Hülskamp. The *Arabidopsis* elch mutant reveals functions of an ESCRT component in cytokinesis. (Development. 2006, 133: 4679-4689)

Manscript: The *Arabidopsis thaliana* ESCRT protein interaction network is involved in cytokinesis

Inpreparation: Trichome specific expression of dominant negative *Arabidopsis* AtSKD1 versions leads to multinuclear trichome cells

Figure and table index

Figures

Table

Abbreviations and gene names

:	fused to (in the context of promoter-gene fusion constructs)
AD	Activation domain
A. thaliana	*Arabidopsis thaliana*
ATP	adenosine triphosphate
bp	base pairs
BD	Binding domain
bHLH	basic helix-loop-helix
BiFC	Bimolecular fluorescent complementation
C	DNA-content of a haploid genome
°C	degree Celsius
CaMV	*Cauliflower mosaic virus*
CCV	clathrin coated vesicles
CFP	cyan fluorescent protein
Da	dalton
DAPI	4',6-Diamidino-2-phenylindol
DNA	Deoxyribonuleic acid
DTT	dithiothreitol
E	Glutamic acid
EE	early endosome
EGFR	epidermal growth factor receptor
ELC	*ELCH*
ER	endoplasmatic reticulum
ESCRT	endosomal sorting complex required for targeting
et al.	et alterni [Lat.] and others
FDA	fluorescein diacetate
Fig.	Figure
FM4-64	N-(3-triethylammoniumpropyl)-4-(6-(diethylamino)phenyl)hexatrienyl) pyridinium dibromide
g	gram (s)
GL2	GLABRA2
k	kilo
kb	kilobase (s)
K	lysine
kDa	kilodalton
LE	late endosome
µ	mikro
MIT	microtubule interacting and trafficking
mM	millimolar
MVB	multi-vesicular body
mRNA	messenger ribonucleic acid
n	number
PCD	Programmed cell death
PCR	polymerase chain reaction
pH	negative decimal logarithm of H+ concentration
PI	propidium iodide

pro	promoter
RE	recycling endosome
Rpm	rounds per minute
SDS	sodium dodecyl sulfate
SKD1	Suppressor of K^+ TRANSPORT GROWTH DEFFECT1
Tris	Tris-(hydroxymethyl)-aminomethane
TSG101	*TUMOR SUSCEPTIBILITY GENE 101*
UBA	Ubiquitin Associated domain
UEV	Ubiquitin Enzyme Variant domain
UIM	ubiquitin interaction domain
V-ATPase	vacuolar-ATPase
VPE	vacuolar processing enzyme
Vps23p	yeast nomenclature for protein
VPS	*VACUOLAR PROTEIN SORTING*
VHA	cytosolic subunits of the vacuolar (H+) ATPase
VHA-a3	transmembrane subunits of the vacuolar (H+) ATPase
Wt	wild type
YFP	yellow fluorescent protein
%	percent

All gene- and mutant names are written in italics. WT-genes are written in capital letters. Proteins are written in non-italic letters.

1. Introduction

1.1 Endomembrane system in eukaryotes

In eukaryotes certain materials in the cell, including some proteins, are sorted by the functionally related cellular membranes of the endomembrane system. The eukaryotic cell system consists of the nuclear envelope; endoplasmic reticulum (ER) and Golgi apparatus, vesicles and other structures derived from them and the plasma membrane. The endomembrane system plays an important role in transport of materials around the cell, notably proteins and membranes which latter is called membrane trafficking (Hawes et al., 1999; Kim and Kim, 2000; Jurgens, 2004).

Many proteins are made on ribosomes bound to the endoplasmic reticulum (ER). Then they are inserted into the lumen of the ER, afterwards vesicles that bud from the ER membrane transport proteins to the cis-face of the Golgi apparatus. Within the Golgi, the proteins are modified and then send out from the trans-face of Golgi by new vesicles. These vesicles move through the cytoplasm fused to endosomes, then the vesicles with sorted proteins move to their final destinations (lysosome or plasma membrane) (Okita and Rogers, 1996; Jurgens, 2004). Delivery of protein occurs by direct connections between the compartments or via vesicular traffic in the endomembrane system by different pathways including biosynthetic routes; autophagy and endocytic transport route which are conserved in eukaryotic cells (Harter and Wieland, 1996; Matlack et al., 1998; Marty, 1999). In the biosynthetic route (secretory pathway) newly synthesized proteins are delivered from the ER, through the Golgi complex, and then either to the hydrolytic compartment, vacuoles in plants and yeast or lysosomes in animal cells, or for the secretion. Some other proteins are constantly being retrieved from later to earlier Golgi by small retrograde transport vesicles. These proteins are sorted in the *trans*-Golgi network into transport vesicles that immediately move to and fuse with the plasma membrane, release their contents by exocytose (Kirchhausen et al., 1997; Rohn et al., 2000).

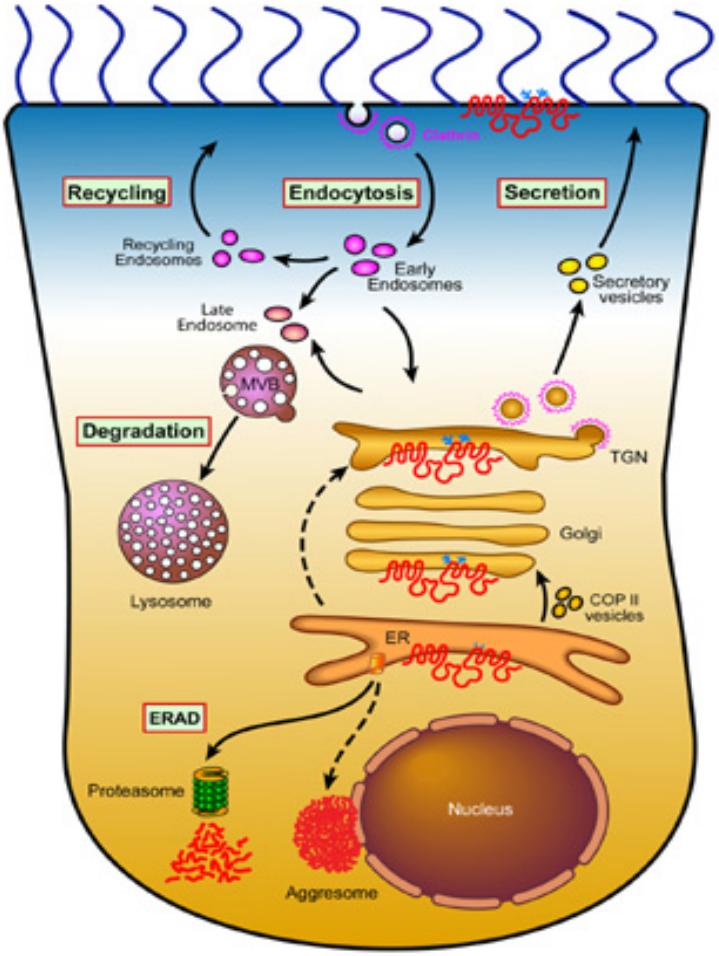

Fig1-1. Overview of the Endomembrane System. The endomembrane system contains compartments and trafficking components that are conserved among all eukaryotes. The biosynthetic pathway transports proteins from the endoplasmic reticulum (ER) through the Golgi complex to the cell surface. In the Golgi network, proteins are sorted and transported to the ***trans***-Golgi network or are sened back to earlier Golgi compartments for re-processing. Within the ***trans*** network, proteins are sorted for trafficking to either the plasma membrane, endosomes, or lysosomes (for degradation). Those proteins destined for the plasma membrane can also be recycled through the endosomes and send back to the membrane or the Golgi, as well as sorted to late endosomes and potentially to lysosomes/vacuole. Molecules can enter either constitutive secretory vesicles Material internalized from outside the cell reaches the early endosomes (EE) first and can be recycled back to the surface, either directly or via a perinuclear recycling endosome (RE) compartment or they are transported to late endosomes (LE) and to the lysosome/vacuole. Picture is taken from (taken from: www cellbio.med.unc.edu/grad/depttest/gentzsch.htm)

The endocytic pathway flows retrograde to the biosynthetic pathway. In the endocytic pathway materials are taken up from the cell surface and transported to the lysosome in animals or to the vacuole in plants and yeast for degradation. Alternatively they are recycled back to the cell surface. In the endocytic machinery the majority of molecules

are internalized from the plasma membrane and the extracellular environment by endocytosis (membrane vesicles derived from the plasma membrane) (Mukherjee et al., 1997) and transported to early endosomes, as the first station of the endocytic pathway (Kornfeld and Mellman, 1989; Mellman, 1996). Endocytosed proteins can follow different pathways from early endosomes, some of them either recycle back to the plasma membrane for further processing or are sorted into late endosomes. Proteins are internalized from the limiting membrane of the late endosome that then is called multivesicular body (MVB). MVBs are responsible for the accumulation and concentration of the cargo after receiving it from early endosomes and then transport it to lysosomes for degradation (Mukherjee et al., 1997). Sorted proteins are delivered from late endosomes to lysosomes by fusion of late endosomes with lysosomes. Proteins are digested in the lysosomes by lysosomal proteases at low pH (pH 5) (Figure 1-1) (Gruenberg et al., 1989; Mellman, 1996).

Protein transport to the eukaryotes vacuole is a complex process that appears to be involved in multiple pathways. Proteins destined for the vacuole enter the secretory pathway and are diverted by specific sorting signals to the vacuole (Miller et al., 1999). Transport of proteins through the secretory pathway is executed by vesicles. Genetic studies in yeast have identified a new pathway that specially sorts proteins destined for the vacuolar lumen which termed endosomal sorting complexes required for transport (ESCRT) pathway. A group of genes is crucial for this process. A subset of these genes encodes the ESCRT components which act sequentially on endosomal membranes.

1.2 Trafficking in the ESCRT system

The ESCRT pathway is responsible for sorting of proteins which are labeled with a single ubiquitin and delivers them to the vacuole (Odorizzi et al., 1998; Babst, 2005).

Ubiquitin functions as a sorting signal for the sorting of cargo by the MVB sorting machinery. Ubiquitylated proteins are sorted into internal vesicles of endosomes during the MVB pathway. Biogenesis of MVB vesicles and the recognition of ubiquitylated transmembrane proteins as cargo depend on a set of cytosolic proteins that are known as the class E vacuolar protein sorting proteins (Vps). In yeast class E Vps proteins are a group of 19 proteins (Babst, 2005) each of them has at least one ortholog in human.

The Class E Vps proteins are organized in three high molecular weight protein complexes, ESCRT I, II and III. In addition upstream and downstream related proteins function in the MVB sorting pathway. The ESCRT machinery is required for the formation of MVBs. ESCRT complexes combine transiently with endosomal membranes and are disassociated from endosomes by the action of Vps4. It is known from yeast, that the MVB sorting pathway internalizes ubiquitylated plasma-membrane proteins that are initially recognized by the Vps27-Hse1 complex. Vps27 belongs to a group of ESCRT complex which is called ESCRT 0. Vps27 binds to ubiquitylated cargo via an ubiquitin-interacting motif (UIM). The Vps27 protein also contains a FYVE domain which binds to the endosomal lipid, phosphatidylinosito l 3-phosphate (PI(3)P). Vps27 recruits ESCRT I. the Vps23 subunit of ESCRT I also interacts with ubiquitylated cargo directly via its Ubiquitin Enzyme Variant domain (UEV). The ESCRT II complex acts down stream of ESCRT I. It also interacts with ubiqutylated cargo via the N-terminal NZF zinc fingers of Vps36. The ESCRT III is recruited by the activity of ESCRT II. ESCRT III is composed of two subcomplexes. It is involved in MVB formation and cargo sorting. Prior to invagination of the limiting membrane the ubiquitin is removed from the cargo by the deubiquitylase Doa4 and the ESCRT complexes is disassembled from the endosomal membrane by the ATPase activity of the Vps4/SKD1 (Figure 2-1). Fusion of the MVB with the lysosomes/vacuole results in the delivery of the lumenal MVB vesicles to the hydrolytic environment of the lumen of the target compartment ultimately leading to degradation of endocytic cargo.

Deletion of each of the class E Vps genes leads to mislocalization of membrane proteins into the limiting membrane of the vacuole and accumulation of cargo proteins in large aberrant structure in the prevacuolar compartment close to the vacuole which is called the class E compartment (Raymond et al., 1992).

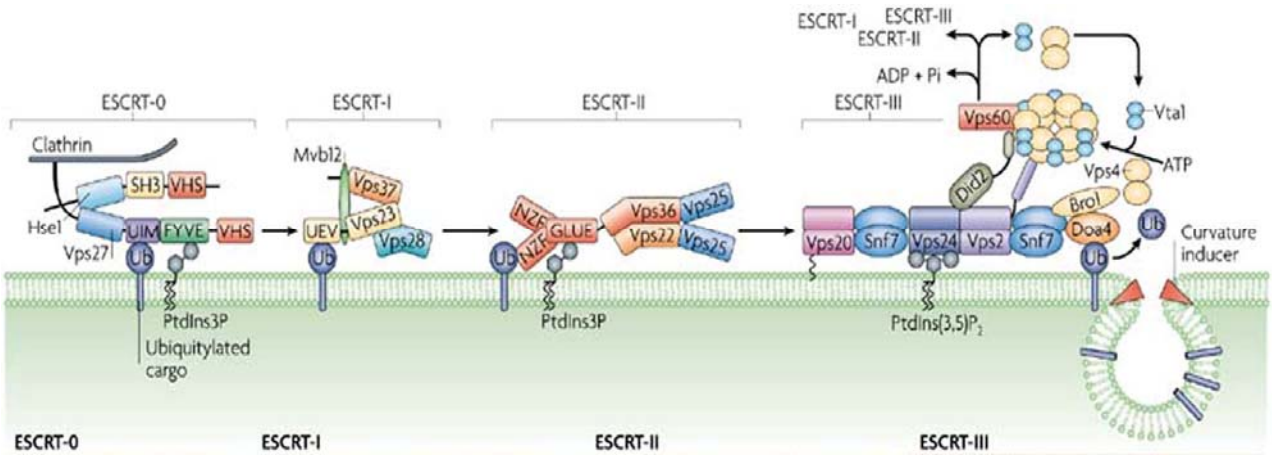

Fig2-1 Overview of ubiquitin- dependent sorting of protein by the ESCRT pathway
At the endosome Vps27-Hse1 (ESCRT 0) binds to ubiquitylated cargo proteins. ESCRT-I and ESCRT-II are recruited from the cytoplasm to the endosome by interacting with Vps27. Both ESCRT complexes bind to monoubiquitylated cargo proteins. ESCRT-I activates ESCRT-II, which in turn initiates the formation of ESCRT-III. The ESCRT-III complex concentrates the MVB cargo and recruits additional factors such as the deubiquitylating enzyme Doa4 and the AAA-type ATPase Vps4. Vps4 dissociates the ESCRT machinery and releases the ESCRTs for further rounds of sorting.
(Taken from Williams and Urbé., 2007)

1.2.1 The ESCRT pathway in plants

As in animal and yeast cells, the endosomal system in plant plays important roles in cellular functions. There are many similarities between the endosomal systems of all eukaryotic cells. Plant proteins like proteins of bacteria, yeast and mammals continually are degraded and replaced. Proteins are sorted and separated in different processes. In plants at least two kinds of vacuoles are known, storage vacuoles that store proteins that are accumulated after sorting in the Golgi apparatus. The other vacuole type is the lytic vacuole where endocytic proteins are sorted to in the MVB pathway for degradation (Winter and Hauser, 2006).

Homologues of most of the ESCRT components have been found in the *Arabidopsis thaliana* genome (Spitzer et al., 2006; Winter and Hauser, 2006). But no gene was detected with the full domain structure of Vps27 or HseI comparable to the one in yeast and mammals. However, there are nine genes that show similarity to the human TOM1 gene which is a known interactor of TSG101, a human homologue of Vps23 (Puertollano, 2005; Winter and Hauser, 2006). Analysis of the *Arabidopsis* Vps23 mutant

elch revealed that in plants the ESCRT pathway is relevant for regulation of cytokinesis (Spitzer et al., 2006).

1.2.2 Vps4 is an important subunit of the ESCRT machinery

Disassembly of the ESCRT complexes from the endosomal membrane is executed by Vps4. Vps4 is a class E Vps gene that was identified as a member of the family of AAA-type ATPases (Babst et al., 1997; Finken-Eigen et al., 1997; Scheuring and Schramm, 1997; Yoshimori et al., 2000). Vps4 is a soluble protein with 48 kDa molecular weight that is more or less conserved in eukaryotes. Some organisms have more than one Vps4 homologue, such as human that has two isoforms of Vps4, Vps4A and Vps4B. The endocytic functions of yeast Vps4 protein are conserved in mammalian Vps4B (Vajjhala et al., 2006). Yeast has only one Vps4 protein that shows 60% homology to both human proteins (Ogura and Wilkinson, 2001; Scott et al., 2005b). The Vps4 proteins have four domains: A N-terminal MIT domain (N-terminal microtubule interacting and trafficking) which is required for binding to the ESCRT III subunits, a highly conserved large AAA-ATPase domain with the ATP binding site, a small AAA-ATPase domain with a four-helix bundle, and the ß-domain, that contributes to the Vps4 oligomerization and binding to the Vps regulator Vta1/LIP5 (Yeo et al., 2003; Scott et al., 2005b; Nickerson et al., 2006).

Vps4 is classified in a class I of AAA-ATPase proteins that are present as dimers in the cytosol whereas at the endosomal membrane they are bound to ATP and form oligomers (Babst et al., 1998; Scott et al., 2005b). Recent studies reported that Vps4 is a double heptameric ring (Hartmann et al., 2008). Although most AAA-ATPase proteins are hexameric, the oligomerization form is depending on the conditions and protein species. AAA-ATPase cassettes are monomers comprised of one or two nucleotide binding domains. The oligomeric structures are the functional structures in these proteins. AAA-ATPase proteins are important regulators for a great variety of cellular functions including peroxisome biogenesis, vesicle mediated transport, control of cell division and gene expression. This great variety of cellular functions is based on a common mechanism: the energy dependent unfolding, remodeling and disassembly of proteins and protein complexes (Lupas and Martin, 2002).

The ATPase activity of Vps4 is required for Vps4 function in the vacuolar protein sorting pathway in which Vps4 catalyze the dissociation of the ESCRTs from the endosomal membrane (Babst et al., 1997; Babst et al., 1998; Yu et al., 2008). The binding of Vps4 to the membrane is regulated by its ATPase activity; Oligomerisation state and membrane association of Vps4 are regulated by the two class E proteins Vta1 and Vps46. Both bind to Vps4 in an ATP dependent manner. Hydrolysis of ATP to ADP decreases the stability of the oligomer and it disassembles into lower molecular weight dimers.

Two mutations have been described in either ATP binding or ATP hydrolysis domain that lead to ATP binding or ATP hydrolysis deficiency of Vps4. The ATPase defective mutants of Vps4 act as dominant negative and cause enlarged endosomal compartment which is called a class E phenotype. Mutated Vps4 steadily associates with ESCRT protein complexes on the membrane and blocks the dissociation of the complexes. This result in yeast is consisting with results for the human MVB pathway (Bishop and Woodman, 2000; Yoshimori et al., 2000; Tanaka et al., 2002; Azmi et al., 2006; Lottridge et al., 2006). Loss of Vps4 function also leads to aberrant multilamellar endosomal structure and missorting and secretion of vacuolar proteins (Hartmann et al., 2008).

In plants relatively little is known about function and regulation of the MVB pathway. A plant homolog of Vps4 is SKD1; mcSKD1 has been described for ice plant, an inducible holophyte (Jou et al., 2004). It is localized mainly in the endoplasmic reticulum-Golgi network and facilitates K^+ ion uptake (Jou et al., 2006). In the course of my thesis Haas et al have detected a sequence homologue of SKD1 in *Arabidopsis thaliana.*

1.3 Model systems to study the function of the ESCRT in plants

Analysis of the protein sorting in plants has strongly relied on the use of misexpression experiments. The ubiquitously active 35S promotor from the *Cauliflower Mosaic Virus* (*CaMV*) has been employed for carrying out misexpression experiments and the effect of a gene can be analyzed in a wide range of cell types. On the other hand ectopically expressing cell regulators can severely effect plant growth.

Haas et al and our results indicated overexpression of AtSKD1 dominant negatives under the control of the CaMV35S promoter is lethal in *Arabidopsi sthaliana* plants. It is difficult to distinguish whether the observed lethality is caused directly by the misexpression of AtSKD1 sorting proteins, or whether it is an indirect effect.

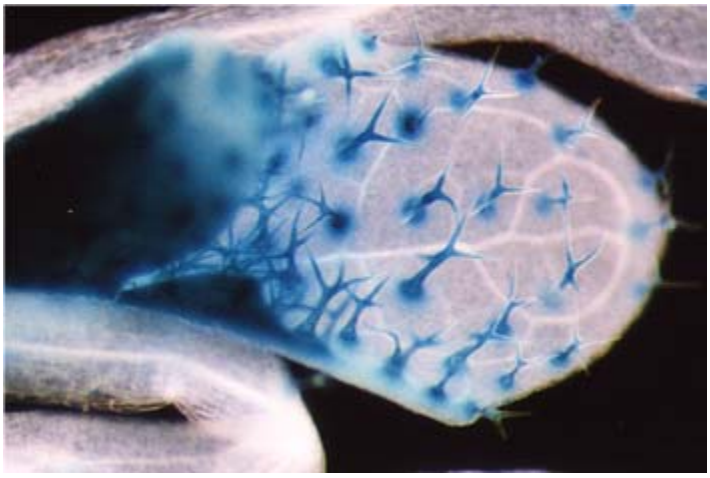

Fig 3-1 Expression pattern of pro*GLABRA2:GUS* in rosette leaves
(Taken from Roodbarkelari, unpublished data)

To analyze the AtSKD1 trcihomes can be a nice model cells. Trichomes in *Arabidopsis* are single-cell leaf hairs, which are initiated with a controlled distance to each other in the basal part of the young developing leaves. Incipient trichomes exit the mitotic program and switch to an endoreplication mode concurrently with outgrowth and initiation of branches.

Trichomes undergo approximately four rounds of endoreplication resulting in mature three-branched trichomes with a DNA content of approximately 32C (Hulskamp et al., 1999).

To study the role of Vps4 protein in the MVB pathway GL2 promoter was used. The GL2 gene plays an important role in trichome development. It is expressed from very early stages until late stages of trichome development in a largely trichome specific manner (Figure3-1) (Szymanski et al., 1998). We chose Gl2 than using the ubiquitously expresse 35S promoter, because trichomes are not necessary for viability of *Arabidopsis* plants. Thus, expression of sorting proteins under control of the *GLABRA2* promoter provided a good tool to analyze their function in an MVB sorting pathway.

Aim of this work

In this study I focused on two aspects: first in order to know whether the ESCRT protein degradation pathway exists in *Arabidopsis*. I have cloned all Vps candidate genes in pENTRY vector, then to destinations vectors. I determined protein-protein interaction network of all ESCRT candidate homologues in *Arabidopsis* using yeast two hybrid technique and bimolecular fluorescent complementation assays.

In the second part I analyzed the function of AtSKD1, a key protein of MVB sorting in *Arabidopsis thaliana*. The analysis focused on loss of function of AtSKD1 which was done by analyzing dominant negative AtSKD1, in protoplast which produce Class E compartment, and on cell type specific misexpression experiments in trichomes and roots.

2. Results

2.1 The ESCRT complex network in *Arabidopsis thaliana:*

Endosomal sorting of ubiquitylated transmembrane proteins is executed by members of the core ESCRT (endosomal sorting complex required for transport) sorting machinery which includes the subcomplexes ESCRT I, ESCRT II and ESCRT III. In yeast nineteen proteins are involved in endosomal protein sorting.

To analyze the interaction networks of the putative *Arabidopsis* ESCRT proteins BLAST searches were performed, resulting in 40 putative *Arabidopsis* homologues of Vacuolar protein sorting candidate genes (Spitzer et al., 2006; Winter and Hauser, 2006)(Table 1-2). To test possible functional connections the candidates were used in yeast two hybrid analyses.

2.2 Interaction assay of *Arabidopsis* putative ESCRT proteins

2.2.1 Yeast two hybrid assay as a technique to show the interactions of the *Arabidopsis* putative ESCRT proteins

The yeast two-hybrid technique uses two protein domains that have specific functions. The pACT vector contains a GAL4 transactivation domain fusion the pAS vector contains a GAL4 DNA-binding domain fusion that is capable of binding the GAL4 promoter. When both domains come into close proximity via an interaction of the tested proteins, they reconstitute a functional transcription factor that then activates a reporter gene. This allows protein-protein interactions to be recognized between the two combinations of fusion proteins and allows identification of possible self-interaction. Yeast two-hybrid assays typically use selective genes encoding proteins that enable amino acid synthesis such as histidine, leucine and tryptophan as reporter genes. The constructs including respective genes are therefore transformed to a yeast strain and interaction of the fusion proteins is determined by growth medium lacking leucine, tryptophan or histidine.

In order to investigate a possible functional connection between the ESCRT homologs of *Arabidopsis*, candidate genes were cloned into pENTRY and then into the destination vectors (pACT (prey) and pAS (bait)) using Gateway BP and LR reactions respectively. The Yeast two-hybrid assays were systematically performed to study protein-protein interaction using each protein as bait and as prey (Table 2-2). Both interactions within and between of ESCRT I, ESCRT II and ESCRT III components were analyzed by yeast two-hybrid assays. SNF1 and SNF4 were used as positive controls (Fields and Song, 1989) and the empty vectors were used as negative controls.

2.2.2. Split–YFP was used to prove the Yeast two hybrid data

To confirm the yeast two hybrid data, Bimolecular Fluorescence Complementation (BiFC) assays were used. BiFC is based on the formation of a fluorescent complex through the association of two fragments of a fluorescent protein. Each fragment was cloned in frame to N-terminus or C-terminus of a gene of interest, enabling expression of fusion proteins. Formation of the fluorescent complex requires the fragments of the fluorescent protein come into close proximity via specific interaction between the fusion proteins (Bracha-Drori et al., 2004).

To demonstrate the feasibility of BiFC in plants, two pairs of interacting proteins were utilized**.** Members of each protein pair were transiently co-expressed in *Arabidopsis* protoplast. Reconstitution of a fluorescing YFP chromophore occurred only when the in question proteins interacted. No fluorescence was detected following co-expression non-interacting protein pairs. Yellow fluorescence was detected in the endosomes and cytoplasm of protoplasm (Figure 5-2 B, F, J and N).

The BiFC assay was performed using transient expression in protoplasm cells and typically analyzed after over 16h. Negative controls were carried out for each experiment by cotransforming an empty vector containing only the appropriate split-YFP part together with the respective gene:split-YFP part fusion and by expression of the non-interacting transcription factors AtMYB51 in pSYNE and Bhlh133 in pSPYCE to exclude non-specific association caused by high local concentrations of non interacting partners (Gigolashvili et al., 2007).

Table 1-2: components of ESCRT- 0, -I,-II, -III complexes and downstream regulator proteins in *Arabidopsis*, yeast and mammals. Upstream proteins in yeast in term are called ESCRT0

Yeast	Mammals	*Arabidopsis*	*Arabidopsis*
ESCRT-0	**ESCRT-0**	**upstream ESCRT genes**	
Vps27	HRS	-	-
Hse1	STAM	-	-
		TOM1H-2[a]	At2g38410
		TOM1H-3[a]	At3g08790
		TOM1H-1	At5g01760
		TOM1H-4[a]	At1g76970
		TOM1H-5[a]	At2g21380
		TOM1H-6[a]	At5g63640
		TOM1H-7[a]	At5g16880
		TOM1H-8[a]	At1g06210
		TOM1H-9[a]	At2g22795
		FYVE-1[a]	At1g29800
		FYVE-2	At3g43230
		FYVE-3[a]	At4g11740
ESCRT-I	**ESCRT-I**	**ESCRT-I**	
Vps23/Stp22	TSG101	ELCH	At3g12400
		ELCH-like	At5g13860
Vps28	Vps28	Vps28	At4g05000
Vps28	Vps28	Vps28	At4g21560
Vps37	Vps37	Vps37	At3g53120
		Vps37	At2g36680
ESCRT-II	**ESCRT-II**	**ESCRT-II**	
Vps22	EAP30	Vps22	At4g27040
		Vps22	At3g31960
Vps25	EAP25	Vps25	At4g19003
VPS36	EAP45	VPS36	At5g04920
ESCRT-III	**ESCRT-III**	**ESCRT-III**	
		VPS2	At2g06530
VPS2	Chmp2	VPS2	At1g03950
		VPS2	At5g44560
Vps20	Champ6	Vps20	At5g63880
		Vps20	At5g09260
Vps24	Champ3	Vps24	At5g22950
		Vps24	At3g45000
Vps32	Champ4	Vps32	At2g19830
		Vps32	At4g29160
Downstream ESCRT complexes	**Downstream ESCRT complexes**	**Downstream ESCRT complexes**	
Vps4	SKD1	SKD1	At2g27600
Vta1	LIP5	LIP5	At4g26750
Doa4	Doa4	Doa4	At2g40930
Vps31	Bro1	Bro1	At1g15130
		RSP5	At4g12570
Vps46	Champ1	Vps46	At1g17730
		Vps46	At1g73030
Vps60	Champ5	Vps60	At3g10640
			At5g04850

2.2.3 ESCRT I Complex in *Arabidopsis thaliana*

ESCRT I is a heterotetrameric 350 kDa complex with a 1:1:1:1 stoichiometry of Vps23 (yeast) or TSG101 (human), Vps28 and Vps37 and Mvb12. ESCRT I transiently associates with endosomal membranes and acts in recognition of mono-ubiquitylated cargo proteins (Bowers et al., 2004); (Winter and Hauser, 2006).

Seven candidate genes which belong to the class E vacuolar sorting proteins were found for the ESCRT I complex in *Arabidopsis thaliana*. In *Arabidopsis thaliana* Vps23 has three homologues and Vps37 or Vps28 has two homologues (Table 1-2).

Three predicted Vps23 homologues are present in *Arabidopsis*. ELCH is the ortholog of Vps23 in yeast and TSG101 in human with a mass of 48.5 kDa. ELCH/Vps23 is an important component that binds to the ubiquitinated protein. In other hand it interacts with other Vps homolog proteins in the ESCRT pathway, similar to the interaction of the human Vps23 homolog TSG101 with Vps28 (Eastman et al., 2005; Spitzer et al., 2006) and Vps37 (Stuchell et al., 2004). Deficient *elch* function results in cytokinesis defects in *Arabidopsis* (Spitzer et al., 2006). Vps37 has two putative homologues in *Arabidopsis* (Winter and Hauser, 2006; Spitzer et al., 2006) which have a coiled coil and a Mod-r domain that is important for protein-protein interactions. There are two putative homologues of Vps28 in *Arabidopsis* which have a C-terminal and a N-terminal domain (Kostelansky et al., 2007)

In the yeast two-hybrid assays of the *Arabidopsis* Vps proteins; self interaction of Vps37 and ELCH (Figure 1-2) was detected.

Vps37 interacts with both homologues of Vps28, and with ELCH and the homolog of ELCH. Rest of interactions can be seen in figure 1-2.

BiFC could confirm our yeast two hybrids results. But Split YFP assays did not detect any interaction between ELCH and Vps28-1 (Figure 1-2)(Channa keshavaiah unpublished data).

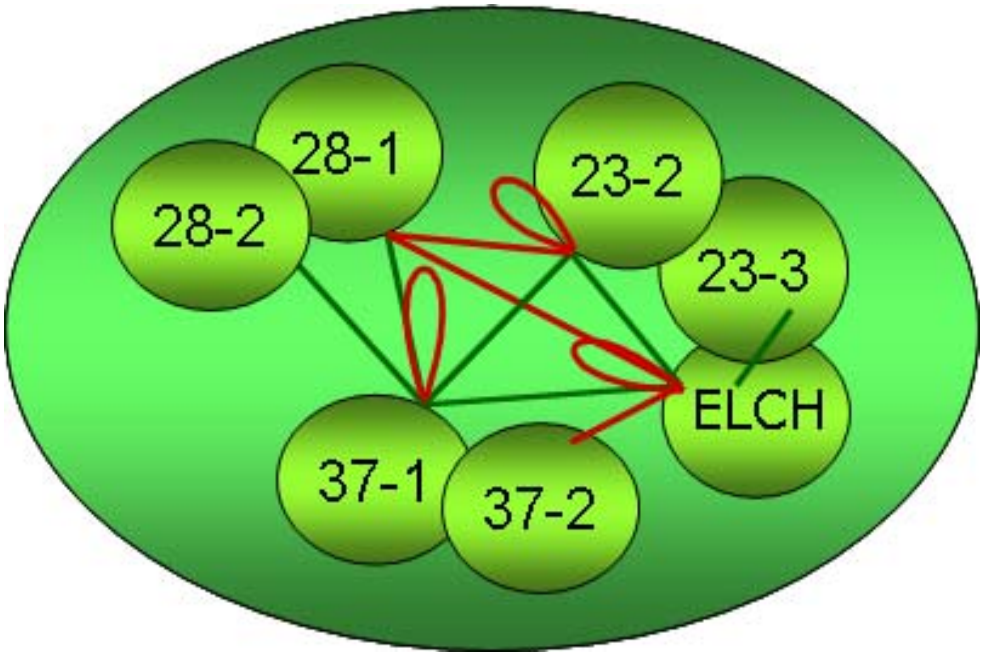

Fig 1-2: **Interactions within the ESCRT I complex**. Positive interactions found with yeast two hybrid assay (red) and BiFC (green) are shown as connecting lines. Self- interactions are indicated by loops.

2.2.4 Interaction assay of ESCRT II using Yeast two hybrids and Split YFP

ESCRT II is a heteromeric 138 kDa complex that transiently associates with endosomal membranes. The ESCRT II complex has three components Vps22/ EAP25, Vps25/ EAP 45, Vps36/ EAP30 in yeast and human (Winter and Hauser, 2006).

In *Arabidopsis* the ESCRT II complex consists of four components. One homologue of Vps22 interacts with Vps25 and Vps36. Based on a study in yeast, Vps25 is a small protein about 20 kDa that is highly conserved and widely expressed in eukaryotic organisims which interact with Vps36, whereas in *Arabidopsis* no interaction was detected between Vps25 and Vps36. Vps36 of the *Arabidopsis* and its human homolog lack the zinc finger domains which exist in yeast. Within ESCRT II subunits, Vps36 shows self interaction (Figure 2-2).

Split YFP assays could not detect any interaction between ESCRT II components (Aneta Sabovljevice unpublished data).

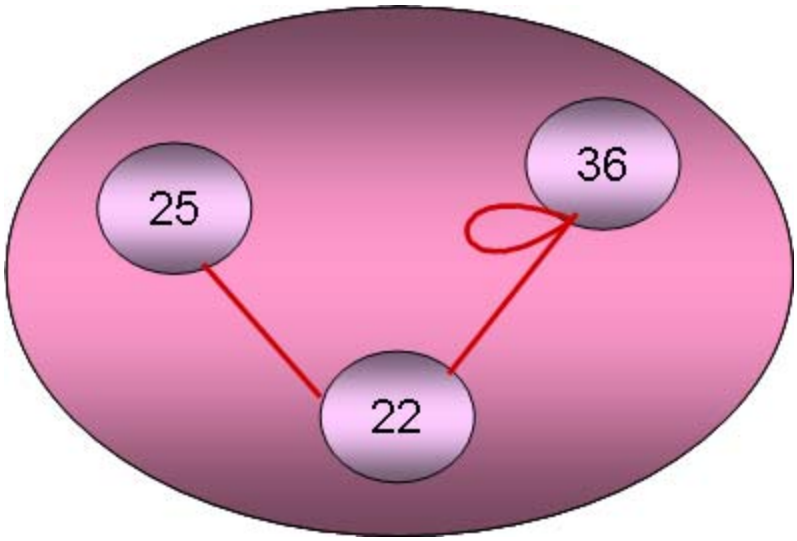

Fig 2-2: **Interactions within ESCRT II components**. All positive interactions found with yeast two hybrid assay (red) and BiFC (green) are shown as connecting lines. Self-interactions are indicated by loops.

2.2.5 Interaction assay of ESCRT III using Yeast two hybrids

ESCRT III has a role during the sorting process (Azmi et al., 2008). CHMP2A, CHMP3, CHMP4B and CHMP6, are homologues of ESCRT III components in human (Teo et al., 2004; Winter and Hauser, 2006). In yeast the ESCRT III complex is divided into two sub-complexes, the first sub-complexes contain Vps2 and Vps24, and the second contains Vps32/Snf7 and Vps20. In *Arabidopsis,* homologues of Vps20 interact with each other as well as with Vps32 homologues, while Vps20-1 interacts with both homologues of Vps32, but Vps20-2 only binds with Vps32-1 (Figure 3-2). Three members of the Vps2 component were identified in *Arabidopsis*. Yeast two-hybrid assays did not detect any interaction between Vps2 or Vps24 with other members of ESCRT III in *Arabidopsis*. Homologues of Vps2 (Vps2-1 and Vps2-2) showed interactions with ESCRT II components. While BiFC assay identified interactions between Vps2-3 with all components of ESCRT III complex.

Also BiFC assays could confirm yeast two hybrids interactions for Vps32-1 and Vps32-2 homologes with Vps20-1 and Vps20-2 homologues. The BiFC assays detected some new interactions within ESCRT III complex. Vps2-3 binds to homologues of Vps32 and also interacts with homologues of Vps 20. This assay revealed interaction between Vps24 with homologues of Vps20 and Vps32. The rest of interactions can be seen in figure 3-2

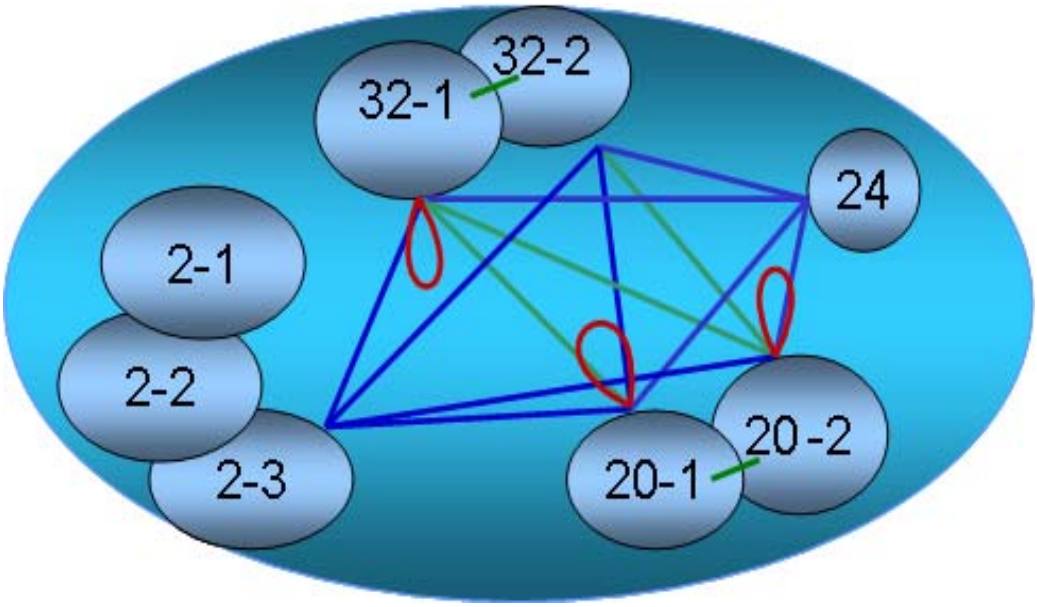

Fig. 3-2: **Interactions within ESCRT III components**. All positive interactions found with BiFC (blue), yeast two hybrid (red) yeast two hybrid and BiFC (green) are shown as connecting lines. Self- interactions are indicated by loops

2.1.6 Protein-protein interaction of putative upstream components and ESCRT-I by Yeast two-hybrid and BiFC assay

In yeast, monoubiquitylated membrane proteins are recognized by ubiquitin-binding proteins such as Vps27, HRS. HSE or STAM are mammalian orthologes of Vps27 that containing N-terminal VHS and GAT domains that are necessary for efficient binding of respectively cargos and transport of monoubiqutinated cargo proteins to the MVB pathway (Scott et al., 2005a) these proteins are divided in another complex which called ESCRT 0 (Alam and Sundquist, 2007; Leung et al., 2008). In the *Arabidopsis* a class of nine genes has been identified that share a VHS domain with Vps27 and HseI (Table 1-2). This class has also a GAT domain which is similar to the animal TOM1L which interacts with TSG101 (Puertollano, 2005). The GAT domain of TOM1L binds to ubiquitin, similar to the ubiquitin binding domain (UIM) of Vps27 and HseI in yeast (Prag et al., 2005; Winter and Hauser, 2006). TOM1L lacks the FYVE domain of Vps27, which is important for membrane binding.

Based on BLAST searches using the FYVE domain of yeast Vps27, one class of three genes of FYVE proteins could be identified in the *Arabidopsis* genome (Table 1-2). Yeast two-hybrid assays could detect interactions between ELCH and FYVE-2 and TOM1H-1. As well as between the ELCH homologues (Vps23-2) of the ESCRT I complex and FYVE-2 and TOM1H-1. This suggests, that they might act as upstream components of the ESCRT machinery. Other homologues of FYVE also interact with Vps20 and Vps2 of the ESCRT III complex.

These interactions were confirmed by BiFC assay (Figure 4-2).

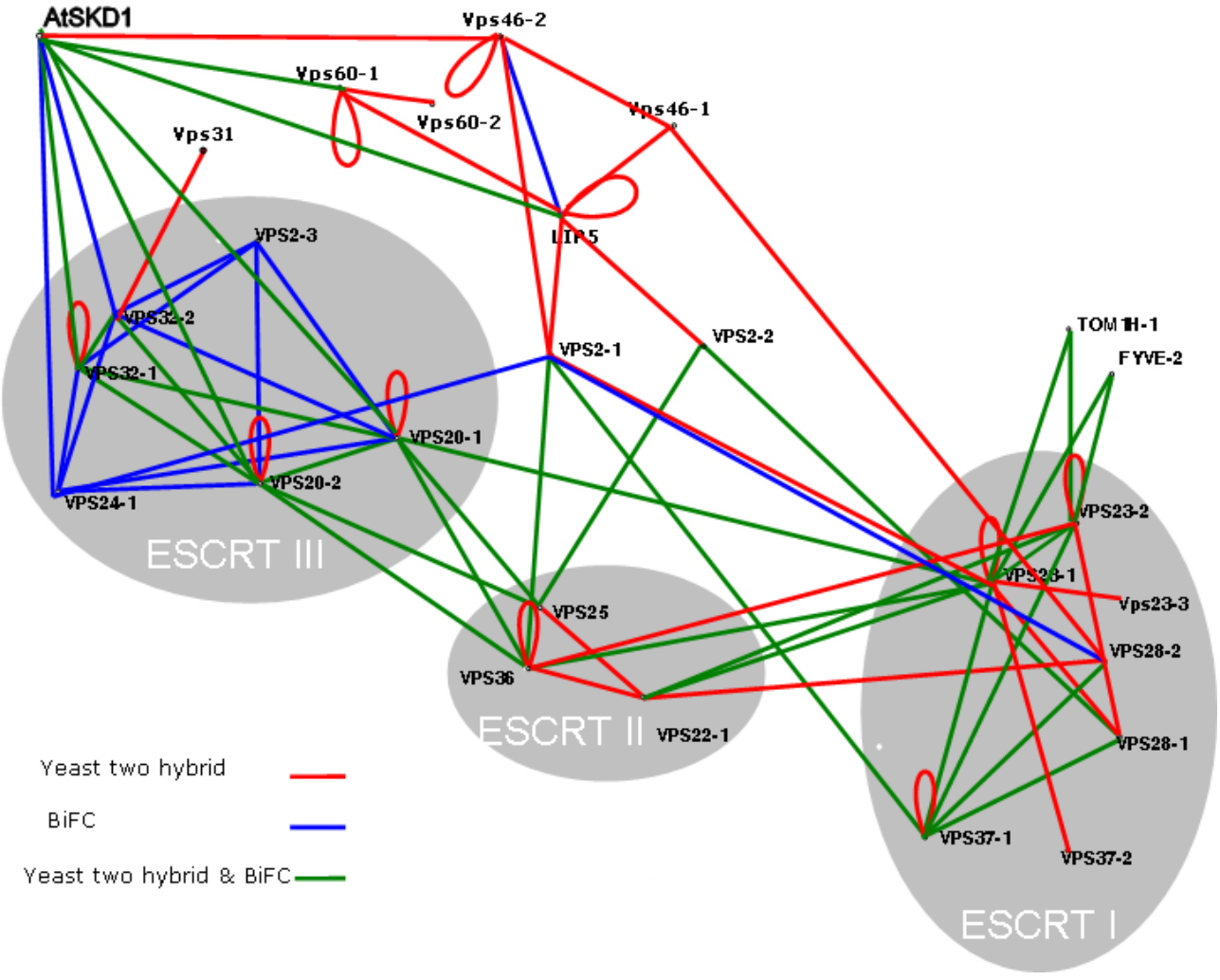

Fig 2-4: **Interaction network of the *Arabidopsis* ESCRT components**. All positive interaction found with yeast two hybrid assays (red), BiFC (blue) or with both tests (green, solid) are shown as connecting lines. Self-interactions are indicated by loops. Putative ESCRT sub-complexes are shaded in grey

2.2.7 Interactions between ESCRT I, ESCRT II and ESCRT III complexes

Yeast two-hybrid assays of the *Arabidopsis* ESCRT I and ESCRT II complexes showed that ESCRT I binds to ESCRT II and ESCRT III (Figure 4-2). The BiFC assay supported this finding. The interaction between ESCRT I and ESCRT II in plant appears to be different from yeast.

In *Arabidopsis*, the interaction between ESCRT I and ESCRT II is mediated by Vps23 of ESCRT I, whereas this interaction was not detected in yeast studies. In yeast, the interaction of the two sub-complexes is mediated by Vps28 of ESCRT I binding to Vps22 and Vps36 (Bowers et al., 2004; Teo et al., 2006). By contrast, the *Arabidopsis* ELCH/Vps23 interacts with Vps36 and Vps22-1. In yeast, no interaction between Vps23p and ESCRT II have been found using yeast two-hybrid assay or BiFC, but Vps28-2 of ESCRT I does interact with Vps22-1 of ESCRT II. BiFC has confirmed the interactions of Vps23 with Vps22 and Vps36 (Figure 4-2).

Interaction between ESCRT I and III takes place via ELCH, Vps37 and Vps28-1 that bind to Vps20-1, Vps2-1 and Vps2-2 of ESCRT III, respectively. All interactions were confirmed by BiFC.

Vps25 and Vps36 of ESCRT II interact with both homologues of Vps20 and with one of the three homologues of Vps2, Vps2-3 in both yeast two-hybrid and BiFC assays.

2.2.8 Downstream ESCRT proteins interact with each other and the ESCRT III

Studies in yeast and human detected that Vps4/SKD1, Vps46/Did2, Vps60, Bro1/Vps31 and Vta1/LIP5 are associated directly or indirectly with ESCRT III in yeast two-hybrid assays. In *Arabidopsis,* AtSKD1 also interacts with both of Vps20-1 and Vps20-2 and Vps32-1 of ESCRT III, which are small coiled-coil proteins. In addition, it also binds to Vps22-1 of ESCRT I. Vps46/Did2 is related to the ESCRT III subunits (Amerik et al., 2000). Vps4 requires Vps46/Did2 to catalyze the endosomal dissociation of ESCRT III and its factors that function downstream in yeast (Vps60, LIP5/ Vta1) (Nickerson et al.,

2006). Recruitment of Vta1 is mediated by Vps46, whereas Vps60 is recruited by Vta1 and interaction of these three proteins recruit Vps4 (Nickerson et al., 2006).

In *Arabidopsis,* two homologous sequences of Vps60 were found which have high similarity to their in yeast counterparts. Moreover, Vps60-1 shows self interaction; and it interacts with upstream ESCRT complexes like SKD1/Vps4.

Vps46 has two homologues in *Arabidopsis*, which bind to each other. Moreover, Vps46-2 has self association and interacts with Vps2-1 in ESCRT III, as well as with Vps4/SKD1 and LIP5/Vta1 in ESCRT downstream proteins. Vps46-1 interacts with Vps28-2 in ESCRT I and LIP5/Vta1.

Yeast two-hybrid assays showed that LIP5/Vta1 interacts with Vps2-1 and Vps2-2 of ESCRT-III and also binds to Vps4. In addition AtLIP5 binds to Vps60-1 and both homologues of Vps46 of *Arabidopsis thaliana*.

The Vps31 gene, is allelic to the yeast ESCRT III associated protein BRO1. Vps31/BRO1 encodes a 97,3 kDa soluble cytoplasmic protein that transiently associates with endosomes. Yeast BRO1 has a highly conserved N-terminal domain, a central coiled-coil region and a C-terminal proline-rich domain in yeast (Odorizzi et al., 2003). Vps31 in *Arabidopsis* binds to the Vps32-2 component in the ESCRT III complex (Figure 4-2) consist to yeast.

Doa4 is a member of the ESCRT machinery which acts in upstream of ESCRT complex. In yeast, a deubiquitination reaction was detected catalyzed by Doa4 interacting with Vps32-2 of ESCRT III (Nikko and Andre, 2007). In *Saccharomyces cerevisiae* Doa4 functions in the multivesicular body protein sorting pathway, and contains highly conserved C-terminal catalytic domains coupled to an N-terminal region with low similarity among to other proteins (Richter et al., 2007). Yeast two-hybrid assays could not detect any interaction between Doa4 candidate proteins and any of the ESCRT complexes in *Arabidopsis*.

2.2.9 *Arabidopsis* ESCRT components interact on endosomes

The BiFC technique not only shows interactions of proteins but also detects the intracellular localization of interacting proteins. Fluorescent signals of all positive interactions were observed in dotted structures. That these speckled structures represent

endosomes is evident from triple transformations of protoplasts with split-YFP constructs of the respective interactors and the endosomal markers Ara6 and Ara7 (Figure 5-2 A-P).

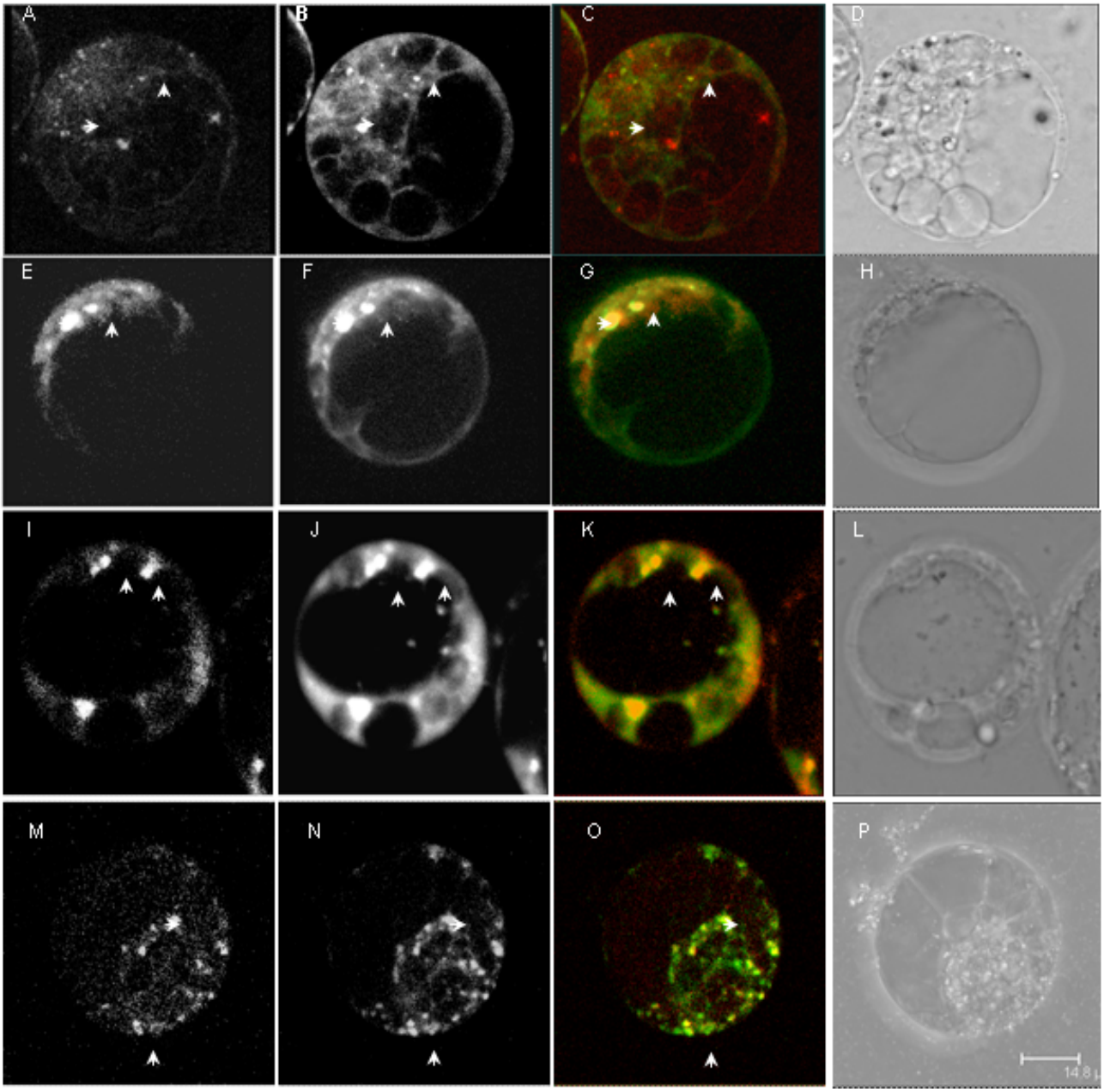

Fig 5-2: **Interaction and colocalization within and between ESCRT I and ESCRT II complexes**. A series of four pictures is shown for interaction and colocalization: the first picture of each row shows marker localization (A, E, I and M), the second the localization of BiFC interactions (B, F, J and N), the third an overlay of the first two pictures (C, G, K and O) and the fourth a bright field image of respective protoplasts (D, H, L and P). Colocalization of the interaction between ELCH and Vps37 with endosomal marker Ara6 **(A-D)** with endosomal marker Ara7 **(E-H)** and also colocalization of the interaction between ELCH and Vps36 of ESCRT II with endosomal marker Ara6 **(I-L)** with endosomal marker Ara7 **(M-P)** is shown. The arrows depict endosomal demonstrating colocalization. Bar 14,8µm.

Table 2-2: Summary of protein–protein interaction between the *Arabidopsis* Vps proteins. Result from the yeast two hybrid assays are given on the left side of each cell, while results of BiFC assay are given on the right side. ‘’+’’ and ‘’-’’ denote positive or negative results, respectively, and‘’0’’ stands for not determined

	Vps 23-1	Vps 23-2	Vps 23-3	Vps 28-2	Vps 37-1	Vps 37-2	Vps 22-1	Vps 25	Vps 36	Vps 2-1	Vps 20-1	Vps 20-2	Vps 24-1	Vps 32-2	Vps 2-3	Vps 32-1	Vps 2-2	Vps 28-1	TOM1	FYVE	Doa4	Vps 31-Bro1	Rsp5	Vps 46-1	Vps 46-2
Vps23-1	+/0	+/+	-/-	-/-	+/+	+/0	+/+	-/-	+/+	-/-	-/-	-/-	-/0	-/0	-/0	-/0	-/0	+/-	+/+	+/+	-/-	-/-	-/-	-/-	-/-
Vps23-2	+/+	+/0	-/-	-/-	+/+	-/0	+/+	-/-	+/-	+/-	-/-	-/-	-/0	-/-	-/-	-/-	-/-	+/-	+/+	+/+	-/-	-/-	-/-	-/-	-/-
Vps23-3	-/-	-/-	-/-	-/-	-/-	-/-	-/-	-/-	-/-	-/-	-/-	-/-	-/-	-/-	-/-	-/-	-/-	+/0	-/-	-/-	-/-	-/-	-/-	-/-	-/-
Vps28-2	-/-	-/-	-/-	-/-	+/+	-/0	+/-	-/-	-/-	-/+	-/0	-/0	-/0	-/0	-/0	-/0	-/-	-/-	-/0	-/0	-/-	-/-	-/-	-/-	-/-
Vps37-1	+/+	+/+	-/-	-/+	+/0	-/0	-/-	-/-	-/-	-/+	-/-	-/0	-/0	-/0	-/0	-/0	-/-	-/+	-/-	-/-	-/-	-/-	-/-	-/-	-/-
Vps37-2	+/0	-/0	-/-	-/0	-/0	-/0	-/0	-/0	-/0	-/0	-/0	-/0	-/0	-/0	-/0	-/0	-/0	-/0	-/0	-/0	-/-	-/-	-/-	-/-	-/-
Vps22-1	+/+	-/+	-/-	-/-	-/-	-/0	-/0	+/-	-/-	-/-	-/0	-/0	-/0	-/0	-/0	-/0	-/-	-/-	-/0	-/0	-/-	-/-	-/-	-/-	-/-
Vps25	-/-	-/-	-/-	-/-	-/-	-/0	-/-	-/0	-/-	-/-	+/+	+/+	-/0	-/-	-/-	-/0	+/+	-/-	-/0	-/0	-/-	-/-	-/-	-/-	-/-
Vps36	-/+	+/-	-/-	-/-	-/-	-/0	+/-	-/-	+/0	-/+	+/+	+/+	-/-	-/-	-/-	-/-	-/-	-/-	-/-	-/-	-/-	-/-	-/-	-/-	-/-
Vps2-1	-/-	-/-	-/-	-/-	+/+	-/0	-/-	-/-	+/+	-/0	-/-	-/-	-/-	-/-	-/-	-/-	-/-	-/-	-/0	-/0	-/-	-/-	-/-	-/-	+/0
Vps20-1	+/+	-/-	-/-	-/-	-/-	-/0	-/-	+/+	+/+	-/-	+/0	+/+	-/+	-/+	-/+	+/+	-/-	-/0	-/0	-/0	-/-	-/-	-/-	-/-	-/-
Vps20-2	-/-	-/-	-/-	-/-	-/-	-/0	-/-	+/+	+/+	-/-	+/+	+/0	-/+	-/+	-/+	-/+	-/-	-/0	-/0	-/0	-/-	-/-	-/-	-/-	-/-
Vps24-1	-/0	-/0	-/-	-/0	-/-	-/0	-/-	-/-	-/-	-/+	-/+	-/+	-/0	-/+	-/-	-/+	-/-	-/0	-/0	-/0	-/-	-/-	-/-	-/-	-/-
Vps32-2	-/-	-/-	-/-	-/0	-/-	-/0	-/-	-/-	-/-	-/-	-/+	+/+	-/+	-/0	-/+	-/+	-/-	-/-	-/0	-/0	-/-	-/-	-/-	-/-	-/-
Vps2-3	-/-	-/-	-/-	-/0	-/-	-/0	-/-	-/-	-/-	-/-	-/+	-/+	-/-	-/+	-/0	-/+	-/-	-/-	-/0	-/0	-/-	-/-	-/-	-/-	-/-
Vps32-1	-/-	-/-	-/-	-/-	-/-	-/0	-/-	-/-	-/-	-/-	+/+	+/+	-/+	+/+	-/+	+/0	-/-	-/-	-/0	-/0	-/-	+/0	-/-	-/-	-/-
Vps2-2	-/-	-/-	-/-	-/-	-/-	-/0	-/-	-/-	-/-	-/-	-/-	-/-	-/-	-/-	-/-	-/-	-/0	+/+	-/0	-/0	-/-	-/-	-/-	-/-	-/-
Vps28-1	-/-	-/-	-/-	-/-	+/+	-/0	-/-	-/-	-/-	-/-	-/-	-/-	-/-	-/-	-/0	-/-	+/+	-/0	-/0	-/0	-/-	-/-	-/-	-/-	-/-
TOM1	-/+	-/+	-/-	-/0	-/0	-/0	-/0	-/0	-/-	-/0	-/0	-/0	-/0	-/0	-/0	-/0	-/0	-/0	-/0	-/0	-/-	-/-	-/-	-/-	-/-
FYVE	+/+	+/+	-/-	-/0	-/0	-/0	-/0	-/0	-/-	-/0	-/0	-/0	-/0	-/0	-/0	-/0	-/0	-/0	-/0	-/0	-/-	-/-	-/-	-/-	-/-
Doa4	-/-	-/-	-/-	-/-	-/-	-/-	-/-	-/-	-/-	-/-	-/-	-/-	-/-	-/-	-/-	-/-	-/-	-/-	-/-	-/-	-/-	-/-	-/-	-/-	-/-
Vps31-Bro1	-/-	-/-	-/-	-/-	-/-	-/-	-/-	-/-	-/-	-/-	-/-	-/-	-/-	-/-	-/-	-/-	-/-	-/-	-/-	-/-	-/-	-/-	-/-	-/-	-/-
Vps46-1	-/-	-/-	-/-	+/0	-/-	-/-	-/-	-/-	-/-	-/-	-/-	-/-	-/-	-/-	-/-	-/-	-/-	-/-	-/-	-/-	-/-	-/-	-/-	-/-	+/0
Vps46-2	-/-	-/-	-/-	-/-	-/-	-/-	-/-	-/-	-/-	-/-	-/-	-/-	-/-	-/-	-/-	-/-	-/-	-/-	-/-	-/-	-/-	-/-	-/-	-/-	+/0
Vps60-1	-/-	-/-	-/-	-/-	-/-	-/-	-/-	-/-	-/-	-/-	-/-	-/-	-/-	-/-	-/-	-/-	-/-	-/-	-/-	-/-	-/-	-/-	-/-	-/-	-/-
Vps60-2	-/-	-/-	-/-	-/-	-/-	-/-	-/-	-/-	-/-	-/-	-/-	-/-	-/-	-/-	-/-	-/-	-/-	-/-	-/-	-/-	-/-	-/-	-/-	-/-	-/-
LIP5	-/-	-/-	-/-	-/-	-/-	-/-	-/-	-/-	-/-	-/-	-/-	-/-	-/-	-/-	-/-	-/-	-/-	-/-	+/+	-/-	-/-	-/-	-/-	-/-	-/-

2.3 Characterization and functional analysis of AtSKD1

2.3.1 Identification of AtSKD1/Vps4 (Suppressor of K^+ transport growth Deffect1) homolog in *Arabidopsis thaliana*

Vps4 has an essential role in the last step of the ESCRT pathway which uses the energy of ATP hydrolysis to release the ESCRT complex from the endosomal membrane (Babst et al., 1997).

Based on a Blast search, one putative AtSKD1/Vps4 homolog was identified in the *Arabidopsis* genome (At2g26700) (Winter and Hauser, 2006). The nucleotide sequence of AtSKD1 predicted a protein of 435 amino acid residues and 48.5 KDa (Haas et al., 2007). That is 54% identical and 67% similar to yeast Vps4 protein (Figure 6-2) AtSKD1 is a single gene. Production of dominant negative of it is accessable by single and double mutation in ATP binding and ATP hydrolysis domains. Therefore, the AtSKD1 is a useful tool to study the function of the ESCRT pathway.

2.3.2 AtSKD1/Vps4 interacts with its upstream and downstream proteins

In this assay AtSKD1 interacted with both homologues of Vps20-1 and Vps20-2 and one homolog of Vps32-1 in ESCRT III complex. This result was consistent with interaction data of yeast and mammals.

One sequence homologue of Vta1 was identified in *Arabidopsis* with Blast search, which is named as AtLIP5. However, this LIP5 did not bind with any Vps protein in the yeast two hybrid assays indicating that other Vps proteins might play this role in plants.

In this study Vps4 was found to interact with LIP5/Vta1, to the second homologue of Vps46 (Vps46-2) and to both homologues of Vps60 (Vps60-1 and Vps60-2).

Fig 6-2: **Sequence alignment of *Arabidopsis* SKD1 with yeast Vps4 and human SKD1**. Sequence alignment of Human SKD1, yeast Vps4, human SKD1-A and SKD1 (At2g27600) from *Arabidopsis thaliana.* Black-shaded amino acids are identical, dark grey-shaded amino acids are conserved, and light grey indicates weak similarity.

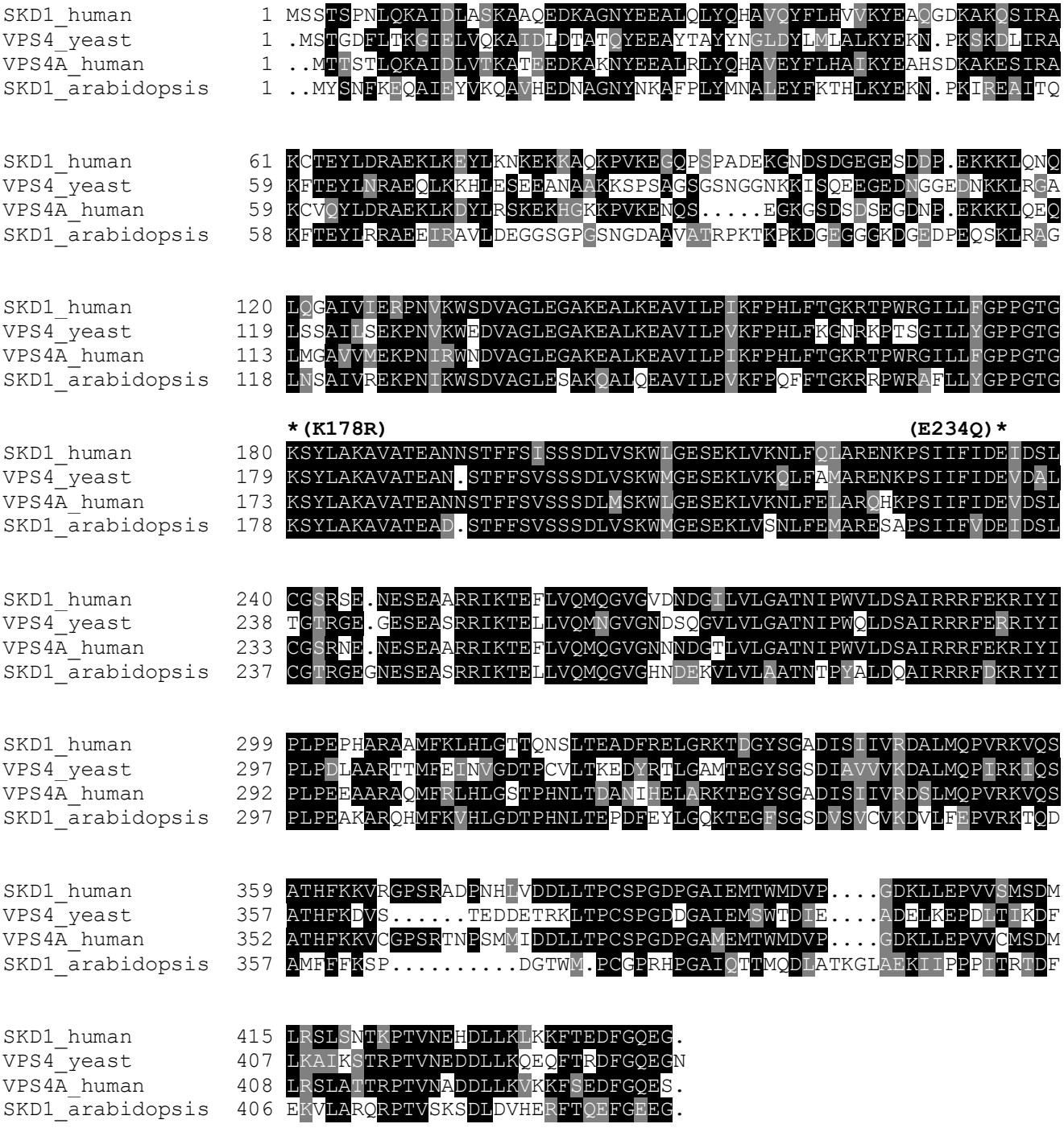

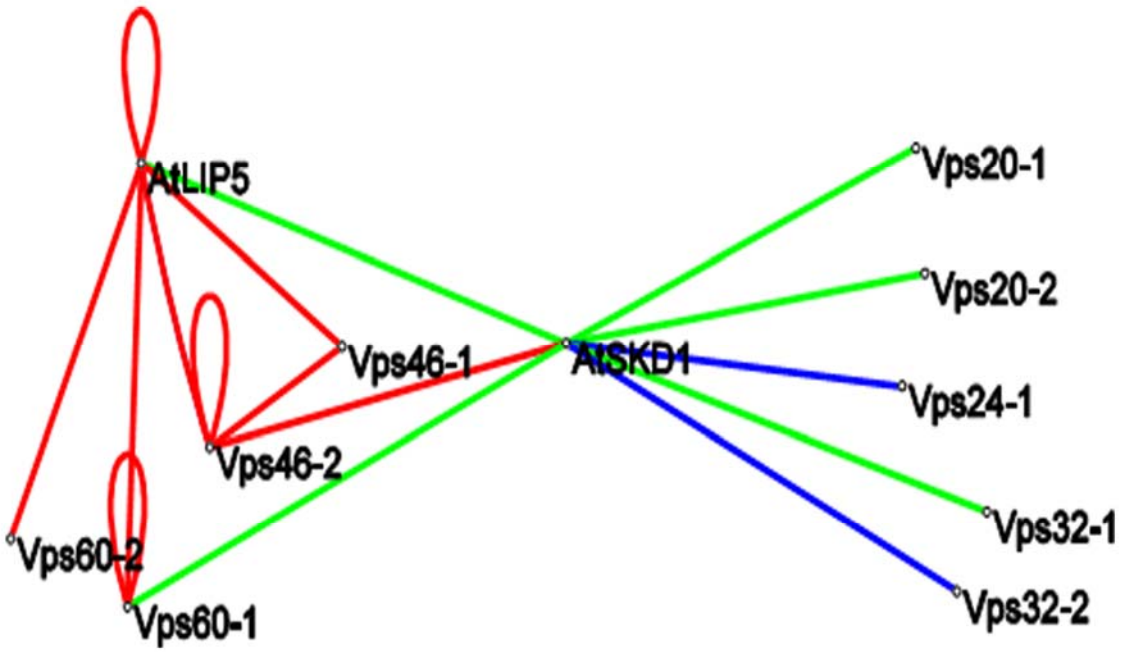

Fig 7-2: **Interaction network of AtSKD1 with Vps proteins of *Arabidopsis thaliana***. Positive interaction of AtSKD1 with ESCRT III complex in upstream and with downstream regulator proteins (Vps46, Vps60, LIP5) found with yeast two hybrid assay (red), BiFC (blue) or with both tests (green, solid) are shown as connecting lines. Self-interactions are indicated by loops

Vps46-2 and Vps 60-1 showed self interaction, AtVta1/LIP5 interacted with Vps 46-2p and Vps60-1p and Vps60-2. A summary of the detected interactions is shown in figure 7-2 and 8-2A shows interaction of AtSKD1 with ESCRT III subunits in first row (Figure 8-2 A-D), and second row is interaction AtSKD1 with downstream regulator proteins (Figure 8-2 E-H). A detailed view of bait and prey constructs and their interactions is shown in table 3-2.

The BiFC assay could confirm the interactions between AtSKD1 and homologues of Vps20, Vps32 and also with Vps24. The BiFC could confirm interaction between AtSKD1 with Vta1/LIP5 and Vps60-1 (Figure 7-2).

To identify the domains responsible for different interactions deletion analysis of AtSKD1 was performed using yeast two hybrid system. Five constructs were prepared carrying deletions in the AtSKD1 gene (Figure 8-2 B). These constructs were challenged against LIP5/ Vta1. Surprisingly, the assay showed that neither MIT nor ß-domain of AtSKD1 is necessary for interaction of AtSKD1 with Vta1 (Figure 8-2 B, C).

A

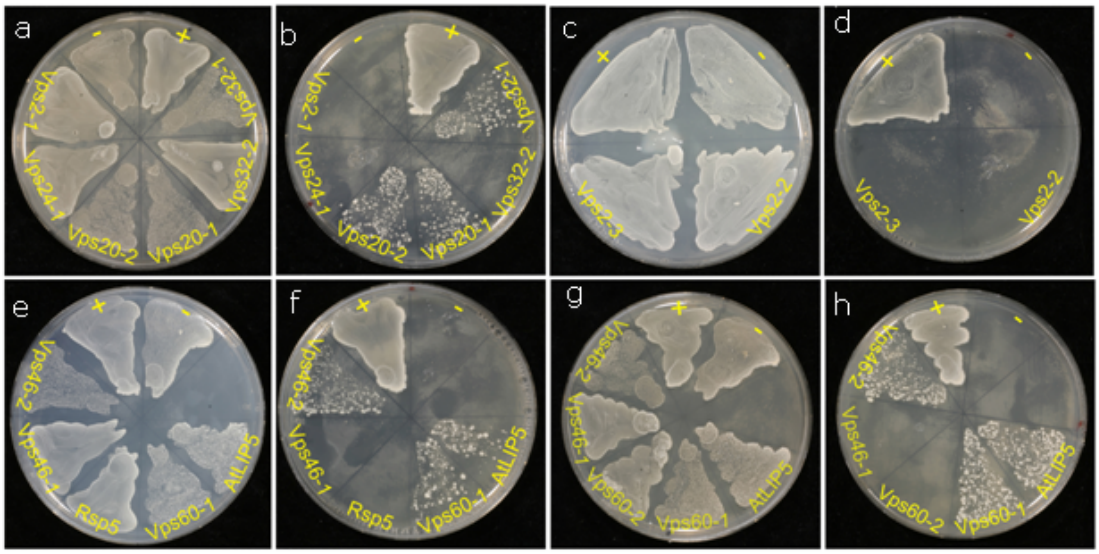
a
Vps2-1
Vps32-2
Vps24-1
Vps20-2
Vps20-1
b
Vps2-1
Vps24-1
Vps20-2
Vps20-1
Vps32-2
c
Vps2-3
Vps2-2
d
Vps2-3
Vps2-2
e
Vps46-2
Vps46-1
Rsp5
Vps60-1
AtLIP5
f
Vps46-2
Vps46-1
Rsp5
Vps60-1
AtLIP5
g
Vps46-2
Vps46-1
Vps60-2
Vps60-1
AtLIP5
h
Vps46-2
Vps46-1
Vps60-2
Vps60-1
AtLIP5

B

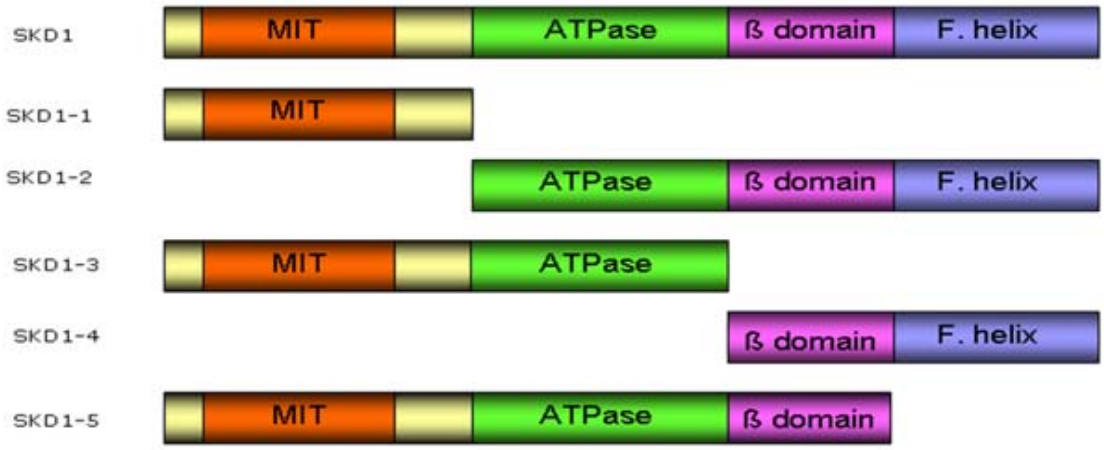
SKD1
MIT
ATPase
ß domain
F. helix
SKD1-1
MIT
SKD1-2
ATPase
ß domain
F. helix
SKD1-3
MIT
ATPase
SKD1-4
ß domain
F. helix
SKD1-5
MIT
ATPase
ß domain

C

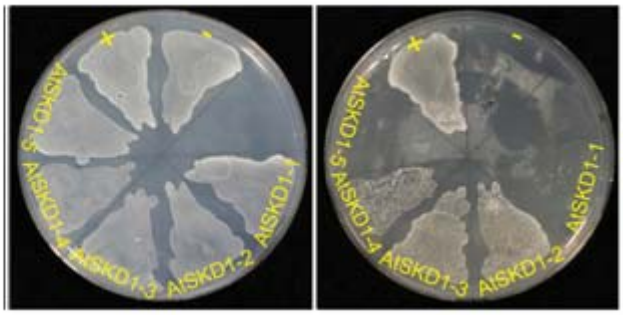
AtSKD1-5
AtSKD1-4
AtSKD1-3
AtSKD1-2
AtSKD1-1
AtSKD1-5
AtSKD1-4
AtSKD1-3
AtSKD1-2
AtSKD1-1

Complexes of Vps4 and its interacting partners were colocalized with Ara6-CFP and CFP-Ara7, early and late endosomal markers respectively, in *Arabidopsis* protoplasts (Figur 12-2).

Continued from last page

Fig8-2: **A**. **All interactions of AtSKD1 with upstream and downstream Vps proteins by yeast two hybrid**,(a-d) AtSKD1 in Bait vector interact with ESCRT III subunits in prey vector which a and c are interaction plate and b and d are selectable plate, (e and f) AtSKD1 in prey vector interact with downstream regulator proteins in Bait vector, (g and h) AtSKD1 in Bait vector and downstream regulator Vps proteins in prey vector, e and g are interaction plates, and f and h are selectable plate.
B Schematic of the full-length AtSKD1 and the truncated versions: SKD1-1 SKD1-5.
C Interaction of LIP5 with truncated AtSKD1, interaction of LIP5 in pAS (Bait) vector with truncated AtSKD1 in pACT (Prey) vector, A is interaction plate and B is selectable plate.

PAS/PACT /(pSYC/pSYN)	Vps20-1	Vps20-2	Vps24-1	Vps32-2	Vps32-1	Vps46-1	Vps46-2	Vps60-1	Vps60-2	At-SKD1	At-LIP5	Doa4
Vps20-1	0	0	0	0	0	0	0	0	0	+/+	0	0
Vps20-2	0	0	0	0	0	0	0	0	0	+/+	0	0
Vps24-1	0	0	0	0	0	0	0	0	0	-/-	0	0
Vps32-2	0	0	0	0	0	0	0	0	0	-/+	0	0
Vps32-1	0	0	0	0	0	0	0	0	0	+/+	0	0
Vps46-1	0	0	0	0	0	0	0	0	0	-/-	0	0
Vps46-2	0	0	0	0	0	0	0	0	0	-/-	0	0
Vps60-1	0	0	0	0	0	0	0	0	0	+/0	0	0
Vps60-2	0	0	0	0	0	0	0	0	0	-/-	0	0
At-SKD1	-/+	-/+	-/+	-/+	+/-	-/-	+/-	+/+	-/-	-/-	+/+	-/0
AT-LIP5	0	0	0	0	0	0	0	0	0	-/-	0	0
Doa4	0	0	0	0	0	0	0	0	0	-/-	0	0

2.3.3 ATPase assay of AtSKD1

Study of Vps4, a member of the AAA-type ATPase family in yeast and mammals, showed that Vps4 catalyzes the dissociation of ESCRT complexes from the endosomal membrane (Babst et al., 1998; Scott et al., 2005b). Domain analysis of Vps4 proteins in yeast and human showed three domains: An N-terminal MIT (N-terminal microtubule interacting and trafficking) domain, a highly conserved AAA-ATPase domain, and a C-terminal helix (Babst et al., 1998; Haas et al., 2007; Xiao et al., 2007; Hartmann et al., 2008; Yu et al., 2008). Point mutant variants of Vps4 in ATP binding or ATP hydrolysis domains were not able to hydrolyze ATP in yeast and mammalian cells and induced an endosomal sorting defects (Babst et al., 1998). AtSKD1 is a sequence homolog of yeast Vps4 in *Arabidopsis*. An amino acid change in the ATP binding domain (K178A) and another mutation in the ATP hydrolysis domain (E234Q) were induced in AtSKD1 and cloned in the bacterial expression vector pNHis with N-terminal His_6.

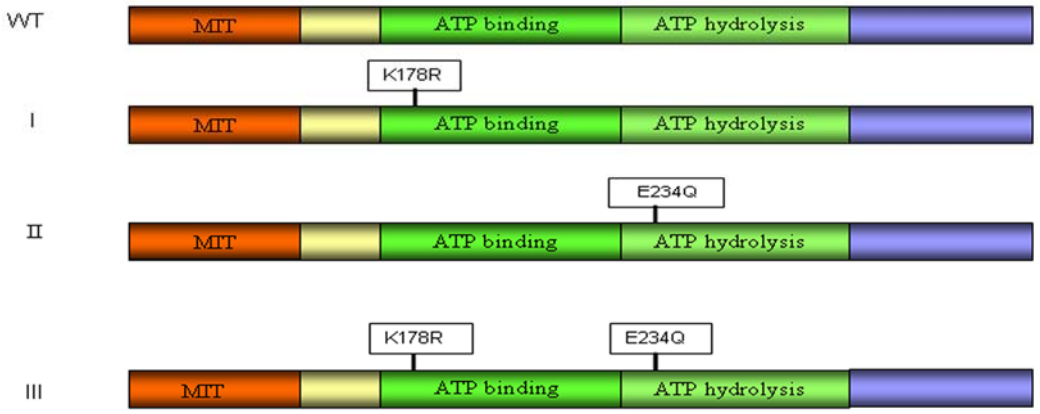

Fig 9-2 Schematic protein structure of AtSKD1. I; mutation in the ATP binding domain. **II**; mutation in the ATP hydrolyses domain. **III**; mutation in the ATP binding and hydrolyses domain

AtSKD1 and AtSKD1$^{K178A,\ E234Q,\ K178AE234Q}$ proteins were expressed in BL_{21} *E.Coli* cells. AtSKD1 is a dimer which, in the absence of ATP, but in the presence of ATP adenine nucleotide binding, changes the conformation of AtSKD1 and induces oligomerization of

AtSKD1 (Babst et al., 1998). To measure the hydrolysis activity of the AtSKD1 and its dominant negative mutants a coupled enzyme ATPase assay was used. The coupled enzyme ATPase assay is based on one molecule of NADH oxidized to NAD+ and corresponds to the production of one molecule of ADP by the motor ATPase (Huang and Hackney, 1994).

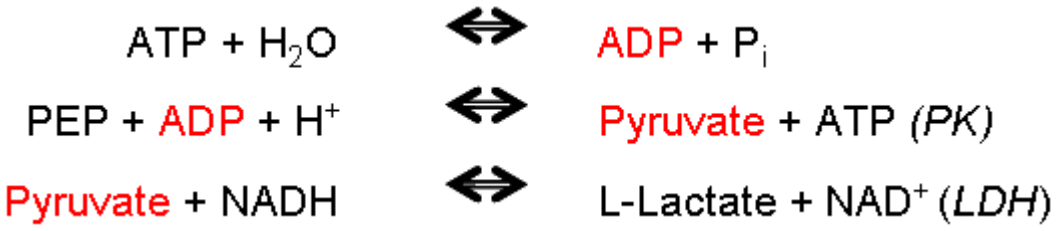

Fig. 10-2. Schematic of the coupled enzyme ATPase assay The coupled enzyme ATPase assay is based on the conversion of phosphoenolpyruvate (PEP) to pyruvate by pyruvate kinase (PK) coupled to the conversion of pyruvate to lactate by lactate dehydrogenase (LDH). The latter step requires NADH which is oxidized to NAD+. NADH absorbs strongly at 340 nm but NAD+ does not, enabling the ultilization of NADH to be followed by monitoring absorbance at 340 nm. The decrease in OD340 can be converted into ATPase activity where 1 molecule of NADH oxidized to NAD+ corresponds to the production of 1 molecule of ADP by the motor ATPase

In this assay, two different conditions were used. First, the ATPase activity of proteins was tested in different concentration of ATP, second in different concentration of lactate dehydrogenase enzyme. AtSKD1^{K178A,} AtSKD1^{E232234Q} and AtSKD1^{K178AE234Q} were not able to hydrolyze the ATP, mutation in both ATP binding or ATP hydrolysis domain abolished ATPase activity of AtSKD1, in contrast with the wild type AtSKD1 protein which hydrolyzes ATP (Figure 11-2).

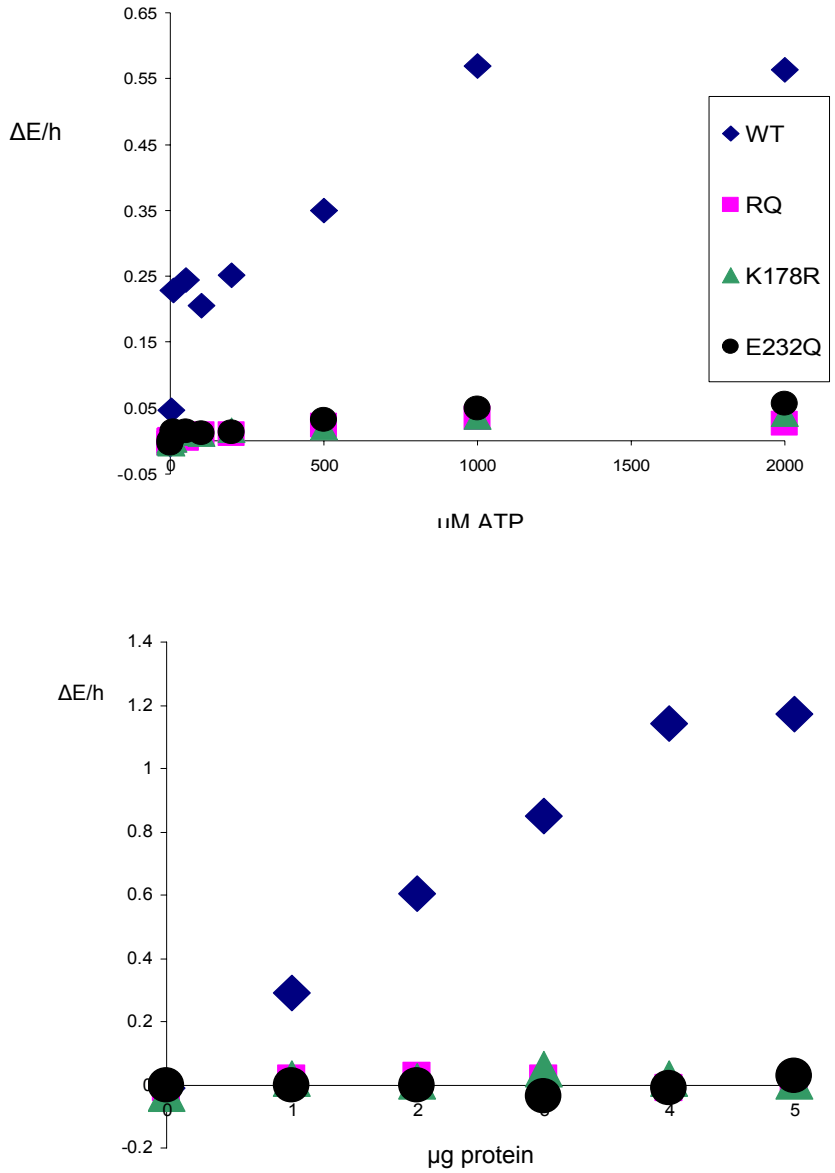

Fig 11-2: **Analysis of ATPase activity of AtSKD1, AtSKD1^{K178A}, AtSKD1^{E234Q} and AtSKD1^{K178AE234Q}**. ATPase activity of AtSKD1 and AtSKD1^{K178AE234Q} measured by oxidation of NADH to NAD **(A)** hydrolysis of AtSKD1 in different concentration of ATP (0-2000μm) **(B)** ATPase activity of AtSKD1, AtSKD1^{K178A,} AtSKD1^{E232Q} and AtSKD1^{K178AE234Q} in different concentrations of AtSKD1 and its dominate negative variants proteins.

2.3.4 AtSKD1 colocalizes with the endosomal Ara6 and Ara7 markers on MVB

Mutation in Vps proteins display the phenotype that so called class E compartment, a structure that shows both endosomal and vacuolar characteristics in yeast (Fujita et al., 2003; Finken- Eigen., 1997; Babst et al., 1998; Scott et al., 2005; Azmi et al., 2006; Katzmann et al., 2002).

To identify putative cellular defects due to the AtSKD1 malfunction, an YFP-AtSKD1 and YFP-AtSKD1^{K178AE234Q} fusion constructs was prepared, driven by the cauliflower mosaic virus promoter (CaMV35S) and YFP-AtSKD1 gene was overexpressed in *Arabidopsis* protoplasts. The YFP-AtSKD1 protein was localized in the cytoplasm and in small punctuated structure was observed which was randomly distributed along the periphery of the protoplasts (Figure 12-2 A).

To further analyze of the AtSKD1 localization, double transformations of *pro35s:YFP-AtSKD1* and *pro35s:Ara6-CFP* or *pro35S:CFP-Ara7* were done. Co localization analysis of YFP-AtSKD1 and Ara6-CFP (early endosomal marker) and CFP-Ara7 (late endosomal marker) was in punctuating structures (Figure 12-2 A-D and I-K). While the YFP-AtSKD1^{K178AE234Q} protein localized in large abnormal compartments, Double transformation of YFP-AtSKD1 ^{K178AE234Q} with Ara6 or Ara7 fused YFP colocalized in the large endosomal compartment (Figure 12-2 E-H and M-P).

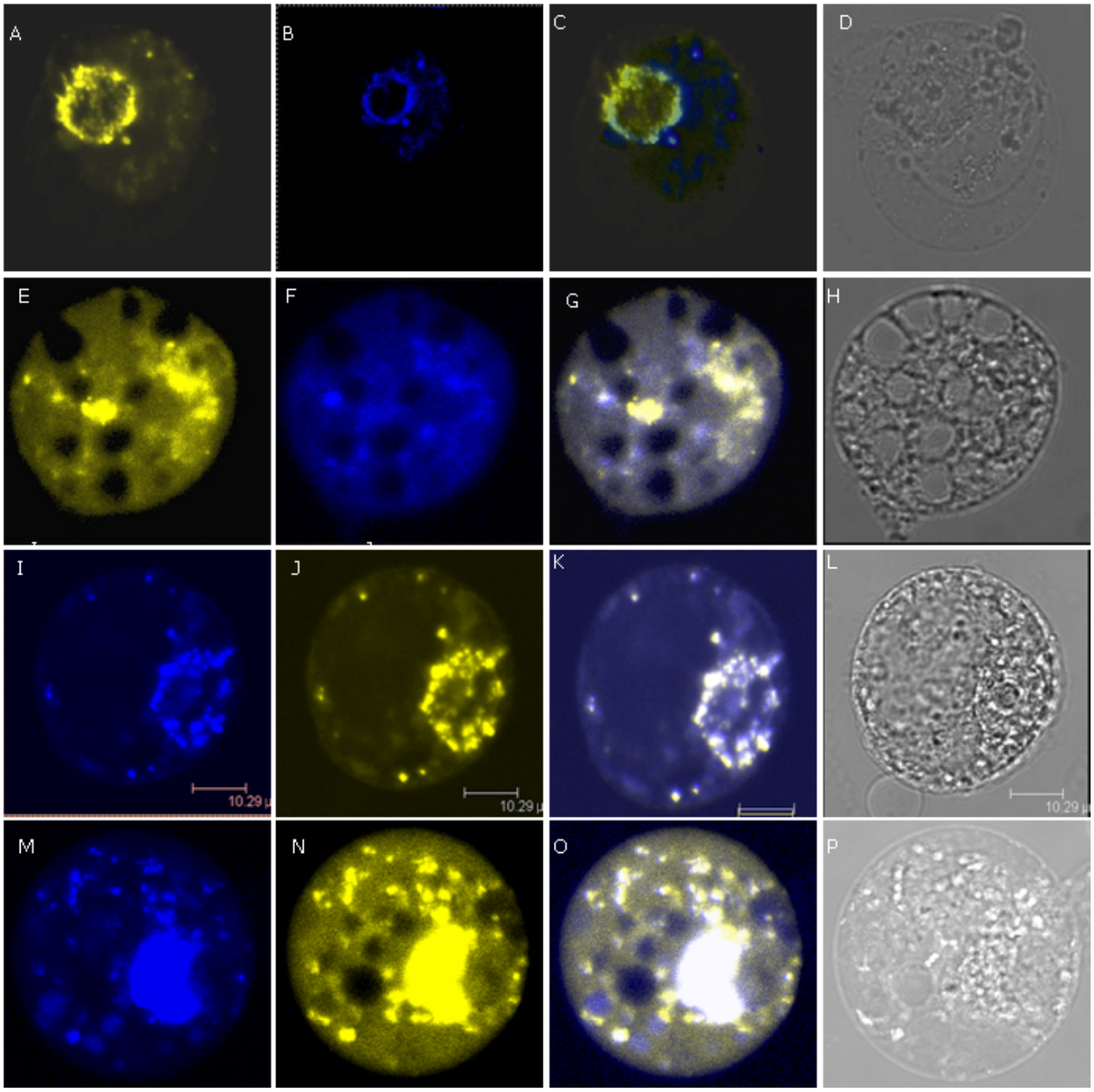

Fig12-2: **Colocalization of YFP-AtSKD1 or AtSKD1-CFP and YFP-AtSKD1^{K178AE234Q} proteins with Ara6 and Ara7 fused to CFP or YFP in *Arabidopsis* protoplast by BiFC.**
(A) YFP-AtSKD1 (**B**) Ara6-CFP-SKD1 in the dots structure **(C)** overlay of A and B **(D)** is bright field.
(E) YFP-SKD1$^{K178A-E234Q}$ **(F)** Ara6-CFP localized in abnormal large endosome like class E compartment **(G)** overlay of E and F **(H)** is bright fild
(I) AtSKD1-CFP **(J)** YFP-Ara7 in dot structures in protoplast**. (K)** Overlay of I and J **(L)** is bright field
(M) CFP-AtSKD1$^{K178A-E234Q}$ **(N)** YFP-Ara7 in endosome as large dots structures **(O)** is overlay of M and N **(P)** is bright field

2.3.5 Expression of AtSKD1 in *Arabidopsis* plants

To analyze the effect of these mutations AtSKD1 and three AtSKD1 dominant negative constructs in plants, AtSKD1^{K178A}, AtSKD1^{E234Q}, and AtSKD1$^{K178A\text{-}E234Q}$ were overexpressed under control of the CaMV35S promoter in *Arabidopsis* plants. Overexpression of AtSKD1 inactive variants caused no transformed plant, Indicating that these mutations have a lethal phenotype in *Arabidopsis thaliana* in all three cases.

2.3.5.1 Localization of AtSKD1 in root

To analyze the effect of these mutations on AtSKD1 function in plants, AtSKD1^{K178A}, AtSKD1^{E234Q}, and AtSKD1$^{K178A\text{-}E234Q}$ were overexpressed under control of the *GLABRA2* promoter in *Arabidopsis* plants. Based on previous study *GLABRA2* promoter is expressed in the non-root hair cells (atrichoblasts) preferentially in the differentiating non-hair epidermal cells within the meristematic and elongation zone in the root (Lin and Schiefelbein, 2001; Schiefelbein, 2003). *proGL2:AtSKD1-YFP* and *proGL2:AtSKD1^{K178AE234Q}-YFP* were expressed in *Arabidopsis thaliana*. Fluorescence was observed in files of atrichoblasts (Figure 13-2 A), AtSKD1-YFP and AtSKD1^{K178AE234Q}-YFP showed similar localization in cytoplasm and endosomes like trichomes. AtSKD1-YFP was localized in the cytoplasm and small doted structures spread throughout the cell that colocalized with FM4-64 on endosomes. FM4-64 is a fluorescent dye that binds the plasma membrane and is internalized by endocytosis. Roots were incubated in 2µM FM4-64, 120-150 min. After that most of FM4-64 co-localized with the YFP signal in root, suggesting that AtSKD1-YFP is targeted to an endosomal MVB compartment (Figure 13-2 A-D). Colocalization of AtSKD1^{K178AE234Q} with FM4-64 was detected in enlarged endosomal compartments (Figure 13-2 E-G).

To test the viability of the *Arabidopsis* roots FDA staining was done. FDA stained the whole cytosol exception vacuole. FDA staining of the surface cells of the root was detected as a degrading activity of fluorescien diacetate by cellular sterases and subsequent accumulation derived fluorescein whitin cells. Large numbers of atrichoblast cells of *proGL2:AtSKD1^{K178AE234Q}-YFP* expressed lines showing no deviation in vacuolization from wild type, only a few atrichoblast cells showed vacuolar fragmentation (Figure 13-2 E and F).

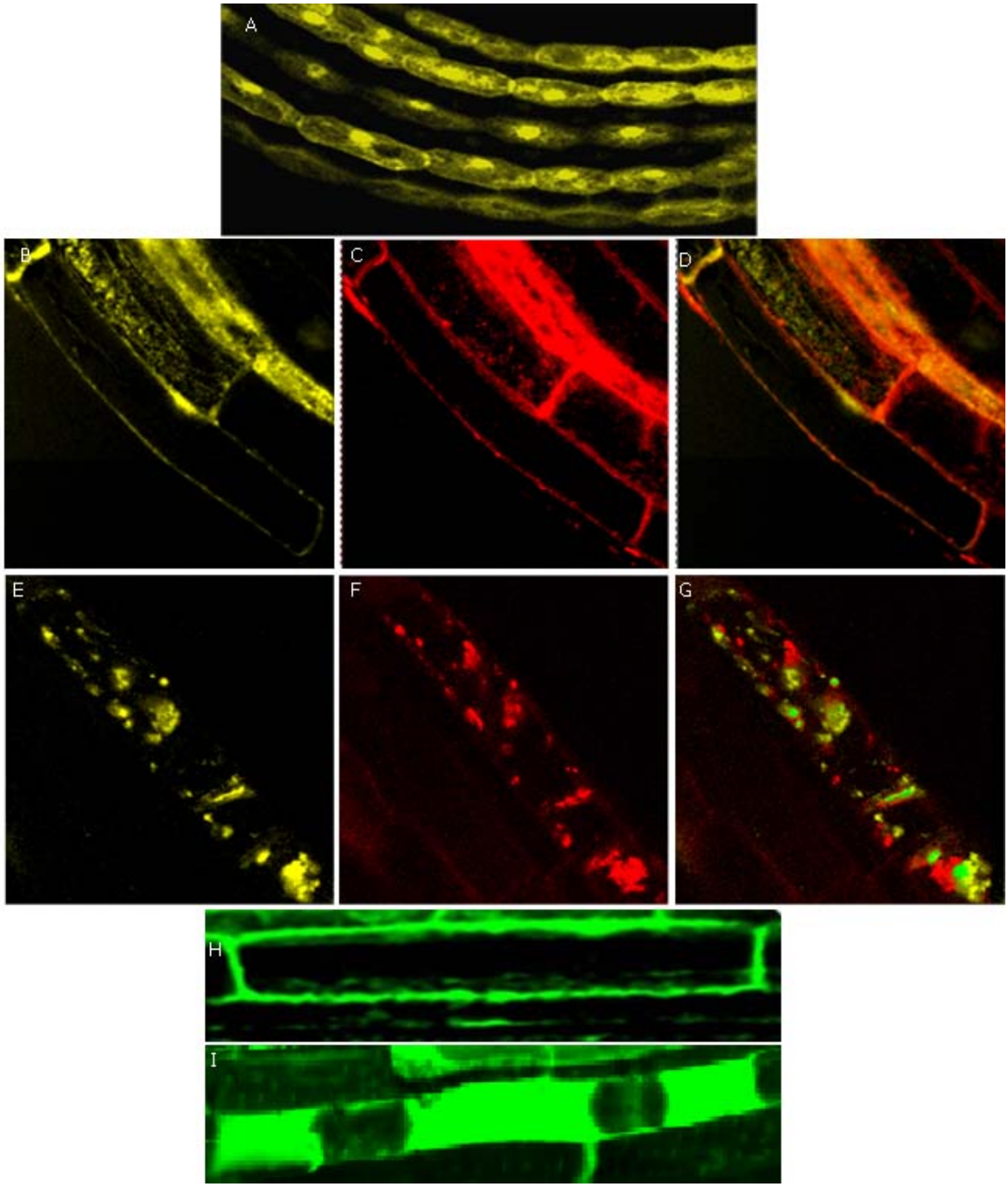

Fig 13-2: **Localization of AtSKD1-YFP and AtSKD1^{K178AE234Q}-YFP in root epidermal cells.**
Confocal laser-scanning micrographs of *proGl2:AtSKD1:YFP* and *proGL2:SKD1^{K178AE234Q}:YFP* in the *Arabidopsis* root.
A) YFP signal showing *ProGL2:AtSKD1-YFP* expressed in hairless cells like a files in the root. **(B)** Localization of AtSKD1-YFP which colocalized with **(C)** FM4-64 into the root cytoplasm and endosomes. **(D)** Overlay of A and B **(E)** colocalization of AtSKD1^{K178AE234Q}-YFP with **(F)** FM4-64, the big doted structure with AtSKD1^{K178AE234Q}-YFP was also stained by FM4-64.
.**(H-I)** Confocal laser-scanning micrographs of FDA-stained *proGL2:AtSKD1* and *proGL2SKD1^{K178AE234Q}* roots **(H)** FDA-stained *proGL2:SKD1:YFP* root, note that the cytoplasm is stained. **(I)** FDA-stained AtSKD1^{K178AE234Q} roots; note that the vacuole fragmentation is visible in atrichoblasts

2.3.5.2 Ectopic expression of AtSKD1 and its dominant negatives in trichomes

To avoid the lethality problem of overexpression of AtSKD1 mutants and analyze the role of AtSKD1 in development, AtSKD1 and its inactive mutants were combined with the trichome specific *GLABRA2* promoter (GL2) and transformed into *Arabidopsis* plants. Homozygous lines showed over- and underbranched trichomes (Figure 14-2 A-B and Table 4-2). In addition, the misexpression lines of the *ProGL2:AtSKD1*^{K17A}, *ProGL2:AtSKD1*^{E234Q} and *ProGL2:AtSKD1*^{K17AE234Q} 5 days old trichomes collapsed and died (Figure 14-2 C), whereas the trichomes of the *ProGL2:AtSKD1* misexpresion lines were viable. This phenotype was stronger in the double mutant AtSKD1^{K178AE234Q} overexpression lines. Remarkably, expression of wildtype AtSKD1 also induces higher percentage of four-branched and also lower branched trichomes compared to wild type (table4-2).

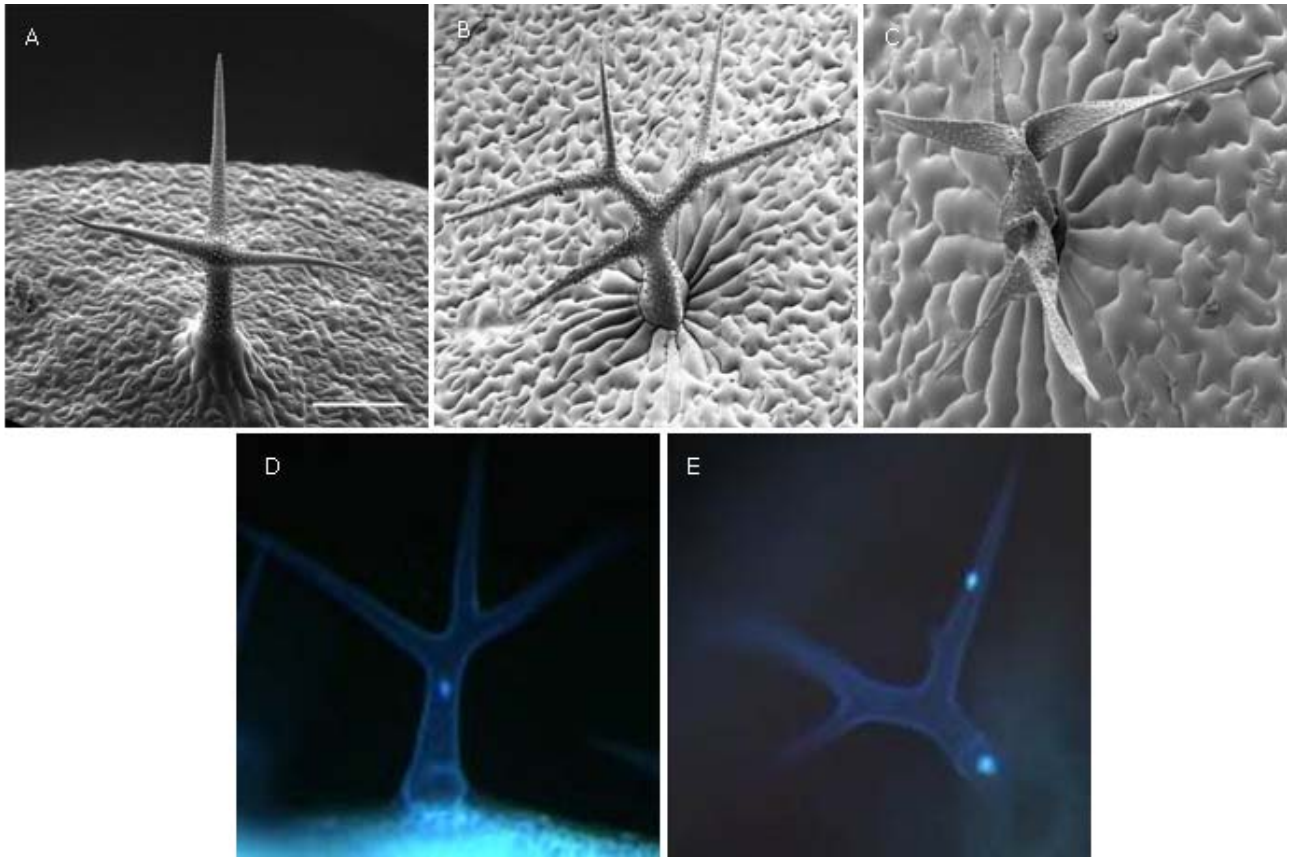

Fig 14-2: **Phenotype of the AtSKD1 dominant negatives in *Arabidopsis* trichome**. **(A)** Scanning-electron micrographs of a mature unicellular wild-type trichome **(B)** Scanning-electron micrographs of a mature overbranched trichome **(C)** Dead trichome of *ProGL2:AtSKD1*^{K178AE234Q} transgenic line.
(D, E) Light micrograph of DAPI-stained
(D) Wild type trichome with single nucleus **(E)DAPI** staining of trichome in *ProGL2:AtSKD1*^{K178AE234Q} transgenic line detected multiple nuclei trichomes

Since cell size is often correlated with the degree of cellular polyploidization, the DNA of trichomes were stained with the 4,6 Diamidino-2-phenylindol (DAPI). DAPI is a nucleic acid specific dye but stains cell wall as well as nuclei (Figure 14-2 D and E). To show the DNA content of trichomes, leaves three and four were stained with DAPI, and trichomes were visualized by epi-fluorescent microscopy. The DNA content of the trichomes were measured by quantifying the fluorescence of DAPI stained nuclei. No significant difference could be detected in the DNA content in comparison to wild type trichomes (table 4-2). However I found an increased occurrence of multiple nuclei in trichomes at

the frequency of 1.7%, 4.27% and 5.82% in AtSKD1^{K178A}, AtSKD1^{E234Q} and AtSKD1^{K178AE234Q} overexpression lines respectively.

Table 4-2: Effect of *proGL2:AtSKD1^{K178AE234Q}* on trichome branching.
Statistics of trichome branch numbers, cluster frequencies and multiple nuclei of Wild type and dominant negative AtSKD1 versions. n: total trichomes

Genotype	No of branches					Multiple nuclei %	n
	1	2	3	4	5		
Col	0	3.8	90.67	5.44	0	0	451
proGL2:AtSKD1	0	11.73	78.01	10.25	0	0	1352
proGL2:AtSKD1^{K178R}	0.059	16.77	62.82	19.28	0.976	1.7 (2-nucl.)	1458
proGL2:AtSKD1^{E234Q}	0.18	27.092	54.5	14.979	3.097	3.4 (2-nucl) 0.8 (3-nucl) 0.07 (4-nucl)	1358
*proGL2:**AtSKD1$^{K178R-E234Q}$***	0	10.776	54.226	28.598	5.978	4.3 (2-nucl) 1.4 (3-nucl) 0.12 (4-nucl)	1642

2.3.5.3 Localization of AtSKD1 and its dominant negatives variants in trichomes

To analyze whether the ATPase dominant negatives of AtSKD1 cause vacuolar protein sorting defect YFP was fused to the C-terminus of wtAtSKD1 and AtSKD1^{K178AE234Q} and the constructs were expressed in *Arabidopsis* under the control of the GL2 promoter. In homozygous lines, YFP fluorescence was analyzed by Confocal laser scanning microscopy.

In the *proGl2:AtSKD1-YFP* transgenic lines fluorescence signal was detected in the cytoplasm of unbranched and newly developed two-branched trichomes. In mature

trichomes fluorescence could be detected not only as dispersed in the cytoplasm (Figure 15-2 A-D) but also in small punctuated structures (Figure 15-2 D-E). In *proGl2:AtSKD1*^{K178AE234Q}*-YFP* transgenic lines fluorescence signal was visible as big dots in young trichomes (figure 15-2 F-I).

To determine the function of AtSKD1 in the endocytic pathway, the mature trichome of *proGL2:SKD1*^{K178AE234Q}*-YFP* expressing plants were stained with FM4-64, a fluorescent dye that binds to the plasma membrane and is internalized by endocytosis. Leaves were incubated in 2µM FM4-64 for 120-150 min. Afterwards most of FM4-64 co localized with SKD1^{K178AE234Q}-YFP in trichomes, compared with the staining of *proGL2:AtSKD1-YFP* plants the FM4-64 was internalized by endocytosis already after ten minutes. this suggestes that AtSKD1^{K178AE234Q}-YFP is targeted to an endosomal MVB compartment (Figure 16-2 A-C) but delays in endocytosis in dominant negatives lines in compared with the wild type suggests a defect in endocytosis of FM4-64 in AtSKD1 ^{K178AE234Q} transgentic lines.

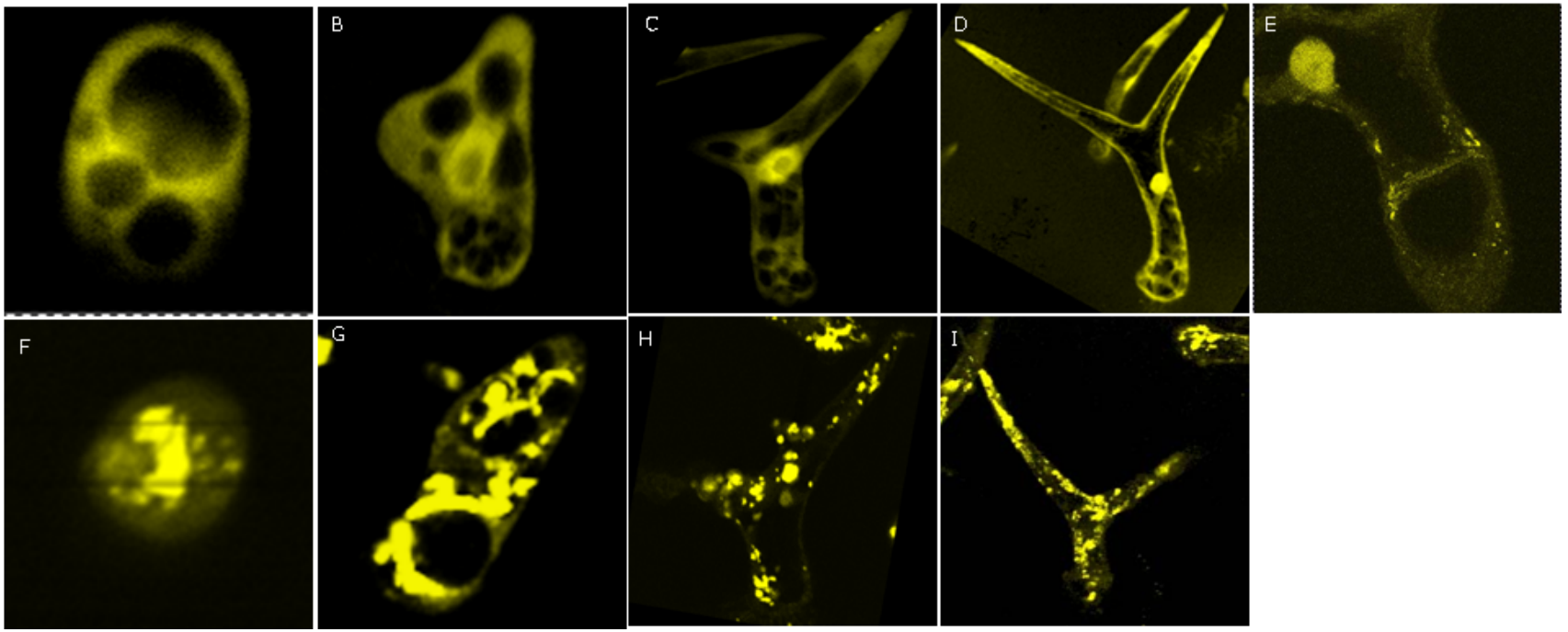

Fig 15-2: **Localization of AtSKD1-YFP and AtSKD1^{K178AE234Q} -YFP in trichome .**
(A-I) Confocal laser scanning micrograph of a **(A-C)** young and **(D-E)** mature trichome of *ProGL2:AtSKD1-YFP* expressing plants. Note that the YFP signal can be observed in the endosomes and the cytoplasm of trichomes. **(E)** The endosomal localization in the trichome is shown in a close up. **(F-G)** young trichome of *ProGL2:AtSKD1^{K178AE234Q}-YFP,* the YFP signal can be observed in the endosome and the cytoplasm of trichomes as large doted structure. **(H-I)** Localization and distribution of *ProGL2:AtSKD1^{K178AE234Q}-YFP* fusion protein in misexpressing plants. In young leaves, all trichomes show a YFP signal in cytoplasm and endosomes. In old leaves, Localization and distribution of YFP fusion protein in whole trichome in *ProGL2:SKD1^{K178AE234Q}* misexpressing plants are on the endosome. While the endosomal signal is evenly distributed in the basal part of mature trichomes

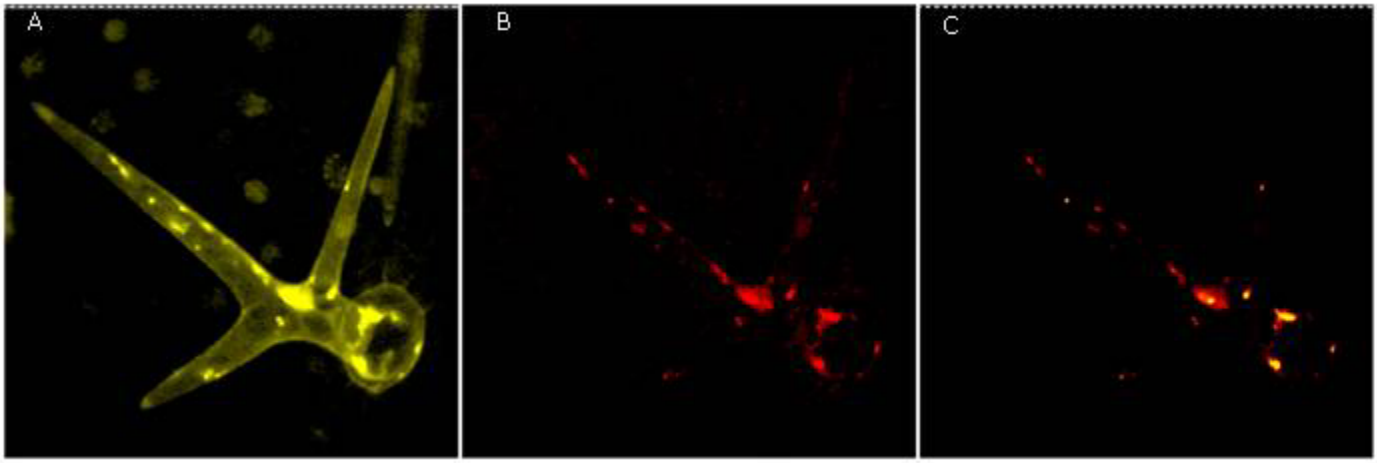

Fig 16-2: **Co localization of AtSKD1^{K178AE234Q}-YFP with FM4-64 in trichome.**
Confocal-laser-scanning micrographs of a mature trichome. **(A)** Localization of AtSKD1^{K178AE234Q}-YFP fusion protein in *proGL2: **AtSKD1**^{K178AE234Q}**-YFP*** misexpressing plant which shows big doted structure **(B)** localization of FM4-64 as endosomal dye. Most of the AtSKD1^{K178AE234Q}-YFP positive compartments were loaded with FM4-6 **(C)** overlay of A and B

In mature trichomes dominant negative AtSKD1 is localized in the big punctuated structures and interestingly, it was not only in cytoplasmic part around the main vacuole of the cell but this structure was also expanded in whole trichome cell (Figure 15-2 I). The central vacuole was no distinguishable.

2.3.6 Mutation in AtSKD1 induces vacuole defects in trichomes

The five days old trichomes on the leaves of the dominant negative AtSKD1 transgenic lines were collapsed and fell over. To test whether the fallen trichomes died, the trichomes were stained with FDA. FDA stains the cytosol of living cells resulting in a negative stain of vacuoles (Figure17-2 A-I).

Wild type *Arabidopsis* and the *proGl2:AtSKD1* transgenic lines showed a similar FDA staining pattern on trichome development (Figure 17-2 A-C).

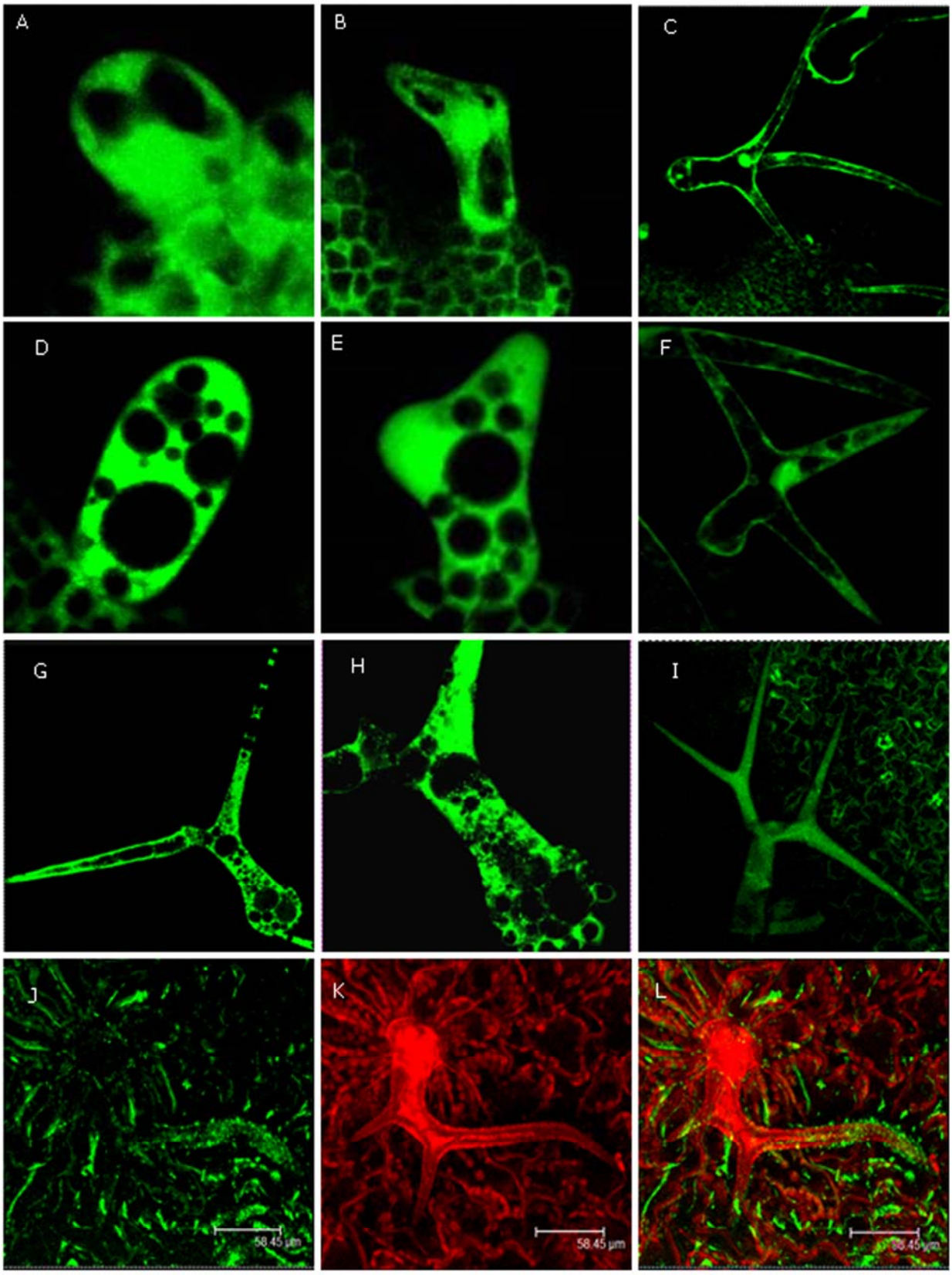
A
B
C
D
E
F
G
H
I
J
K
L
58.45 µm
58.45 µm

FDA Staining of *proGL2:AtSKD1*^{K178AE234Q} lines indicated normal vacuolization indistinguishable from wild type in the young trichomes, but formation of large vacuoles in the *proGL2:AtSKD1*^{K178AE234Q} line was transient. After the large vacuole formation (Figure 17-2 D-F), vacuole fragmentation was begun from the sides of trichome branches and stem of trichomes then extended to the whole cell and huge numbers of small vacuoles were produced (Figure 17-2 G, and H). After that the trichomes completely lost their vacuoles. Finally, the cells were collapsed (Figure 17-2 I).

The collapsed trichomes did not show any FDA staining and appearing dead (Figure 17-2 J). To determine the cell death, Propidium Iodide staining was used. Frequently, cells displaying a high Autofluorecence were found, which is indicative of the production of large amounts of phenolic compounds which is often correlated with cell death (Figure17-2 K and L).

To find, vacuole fragmentation is a defect in vacuole biogenesis, or in the maintenance of vacuole, a genetic analysis of 40 leaves were done by FDA staining. This analysis detected that the vacuole fragmentation in *proGl2:AtSKD1*^{K178AE234Q} lines are correlated to age of trichomes in different positions of leaves. Different classes of vacuole were detected by this analysis. The class one and two of vacuoles were found in base of leave with small vacuoles (Figure 17-2 D,E), trichomes with the class three vacuoles that are large central vacuoles were placed in the middle part of the leaf (Figure 17-2 F). trichomes with fragmentized vacuole were classified in the class four which were located in close to tip of the leaf (Figure 17-2 G,H). Finally collapsed trichomes sit at tip of the leaf (Figure 17-2 H).

Continued from last page:

Fig 17-2: Analysis of vacuole fragmentation in AtSKD1 dominant negative by FDA staining. Confocal-laser-scanning micrographs of FDA-stained *proGL2:AtSKD1* and *proGL2:AtSKD1*^{K178AE234Q} trichomes; (**A-C**) FDA staining of young rosette leaves of *proGL2:AtSKD1* expressing plant shows that in young leaves, the cytoplasm of almost all trichomes and the vacuoles are small. In mature trichomes, the FDA signal is detected in the endosomes and cytoplasm of trichomes the cytoplasmic region around the vacuole and the thin lining of the cytoplasm is stained, indicating that the cell is alive. (**D-I**) trichomes of young rosette leaf of *proGL2:SKD1*^{K178AE234Q} is stained by FDA. (**D-F**) In young leaves, the cytoplasm of all trichome show FDA signal in the whole cell since vacuoles are small. In mature trichomes, the FDA signal is detected in cytoplasm of trichomes. the cytoplasmic region around the vacuole and the thin lining of the cytoplasm is stained, indicating that the cell is alive (**G**) Vacuole fragmentation in mature trichomes, after vacuole development was completed that produce many small vacuoles (**H**) trichomes lost vacuoles and Collapsed **(I)** cell death in trichome after completely lost vacuole **(J)** Propidium iodide staining of *proGL2:SKD1*^{K178AE234Q} indicates that membranes are not intact any more and that the cell is dead **(K)** overlay of I and J

3. Discussion

3.1 The ESCRT pathway in *Arabidopsis thaliana*

The ESCRT pathway plays a role in monoubiqutin dependent vacuolar protein degradation. Most of its known components are conserved in yeast, mammals and plants. However, detailed functional analysis of ESCRT components is available mostly in yeast and mammals. The first part of present work, It is focused on analysis of the protein-protein interactions between *Arabidopsis thaliana* ESCRT orthologs. The results showed that the interactions within and between ESCRT complexes are conserved also in *Arabidopsis*. In addition, novel interactions were identified between ESCRT I and ESCRT III pathway components. Our data could also confirm the recent finding that ELCH, the *Arabidopsis* ortholog of yeast Vps23 and human TSG101 also plays a conserved role (Spitzer et al., 2006).

The second part of the thesis studies the regulatory function of AtSKD1 in the MVB (multi-vesicular body) pathway. The results indicate that SKD1 acts in the late steps of the ESCRT pathway in *Arabidopsis,* since single and double mutation in ATPase domain of AtSKD1 gene can block the sorting of proteins and induce cell death. The data suggest that AtSKD1 might also act as a regulator of cytokinesis.

These findings open a new view on the functions of AtSKD1 especially with respect to cell viability and the regulation of the cell cycle in *Arabidopsis thaliana.*

3.2 The MVB pathway is highly conserved during the eukaryotic development

Based on sequence comparison it was revealed that the *Arabidopsis* genome encodes members of the ESCRT protein sorting pathway (Winter and Hauser, 2006, Spitzer et al., 2006). We performed systematic yeast two hybrid and BiFC analyses between the ESCRT components and found that the ESCRT core complex in *Arabidopsis* is conserved with that of mammals and yeast, but shows closer similarity to mammals than to yeast. According to our data, one major difference between ESCRT complexes in

Arabidopsis and yeast is that interactions between *Arabidopsis* ESCRT I and II components are based on the interactions between Vps23 with Vps22 and Vps36 in contrast to interactions between Vps 28 with Vps22 and Vps36 in yeast. The difference can be supported by the special structure of yeast Vps36 protein, which contains two NZF zinc-finger regions that are missing from plant and animal counterparts (Babst et al., 2002; Alam et al., 2004; Slagsvold et al., 2005);.

ELCH is a member of the ESCRT I complex in *Arabidopsis* and it interacts with components of all three ESCRT I, II and III complexes. ELCH also binds to TOM1 and FYVE upstream ESCRT pathway components. These results confirm that ELCH plays a central role in the MVB pathway in *Arabidopsis*. In contrast, yeast Vps23 interacts with the upstream Vs27/Hrs complex, only with Mvb12 subunit of ESCRT I, and there is no evidence of its interaction with ESCRT II and ESCRT III complex (Bishop and Woodman, 2000; Bowers et al., 2004; Chu et al., 2006). Considering all these results, that ELCH directly interacts with upstream subunits and downstream ESCRT I, II and III components, and also previous studies which indicated that ELCH binds to ubiquitin and also interacts with other ESCRT I components on endosomes (Spitzer et al., 2006), strongly confirms the idea that ESCRT pathway exists and conserves in plants.

These results in *Arabidopsis* are consistent with TSG101 function in mammals including binding with ubiquitin, localization in endosomes and interaction with ESCRT I components. In addition, study of TSG101 revealed abnormalities in the cytoskeleton, cytokinesis in *tsg101* mutant cells and defective in protein trafficking within the endosomal system (Babst et al., 2000).

In plants, initial cargo recognition appears to be different from yeast and mammals as no Vps27-Hse1 complex has been identified in the *Arabidopsis* genome so far. But two genes families were identified that together are similar to the Vps27 and Hrs domain in yeast and mammals. Members of the TOM1 protein family included a VHS and a GAT domain similar to Hrs protein in human, which has been identified as an interactor of TSG101, and other family member had a FYVE domain similar to the Vps27 protein of yeast. Binding of these two proteins to ELCH subunit which takes place on endosomes, suggests that FYVE and TOM1 proteins or the whole families of these might perform

ESCRT 0 function in plants. Moreover, with respect to the interaction pattern of the plants and animals; my data suggested a difference in the recruitment of cargo proteins.

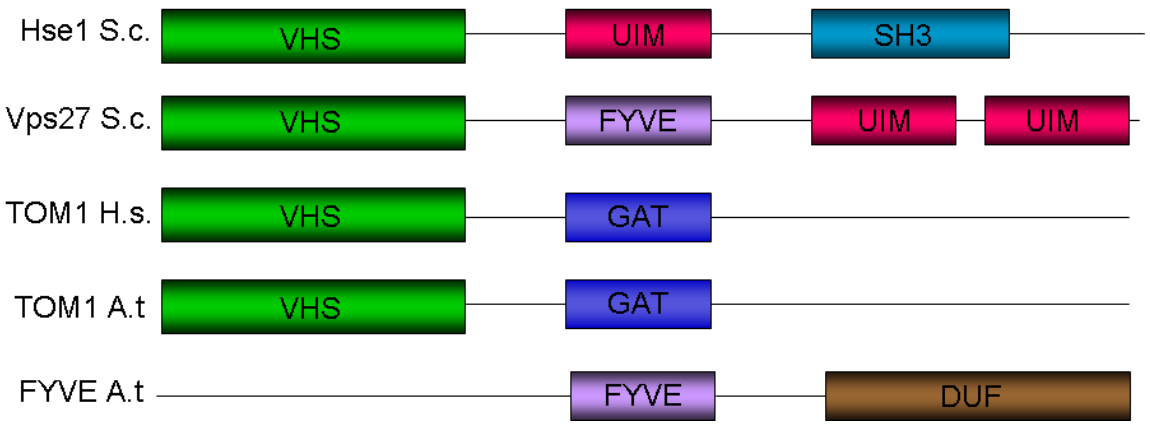

Fig 1.3 The domain structures of ESCRT upstream proteins. The domain structures of yeast HseI (Hse S.c.) and Vps27 (Vps27 S.c.) are compared with the human TOM1 (TOM1 H.s.) and the *Arabidopsis* TOM1 (TOM1 A.t.) and FYVE (FYVE A.t) homologs. Abbreviations: VHS: "VPS27/Hrs/STAM), UIM: "ubiquitin interacting motive", FYVE: "Fab1, YOTB, ZK632.12,Vac1, EEA1)", SH3: "Src homolog 3)", GAT: "GGA and TOM1", DUF: "domain of unknown function"

A further noteworthy point is that the Vps2-3 (At1g03950) is set into the putative ESCRT III structure, while Vps2-1 and Vps2-2 show interactions only with members of the putative ESCRT I and ESCRT II complexes and Vps46 in the downstream of ESCRT complexes. Most of the interactions were observed in yeast two hybrids and BiFC systems, but the interactions in the ESCRT III sub-complexes mostly were not detected in yeast to hybrid assays. It is unclear whether this is due to masking of interaction interfaces by the used tags or whether the putative role of ESCRT III as an endosomal coat requires membranes for some interactions to occur.

Taken together these results suggest the presence of an ESCRT protein-sorting pathway in plants similar to the yeast and mammalians ESCRT pathway.

3.3 The role of AtSKD1 in the MVB pathway in *Arabidopsis thaliana*

Vps4 plays a key role in the regulation of MVB sorting in yeast and mammals. Vps4 is responsible for the removal of ESCRT complexes from the endosome. Based on

sequence similarity one ortholog of Vps4 has been identified in the *Arabidopsis* genome, AtSKD1, which encodes a protein that is expressed in all plant tissues. Point mutations in the ATP-binding and ATP-hydrolysis domains compromise the function of Vps4 and block the MVB pathway in mammals and yeast. The corresponding lysin and glutamic acid residues in ATP binding and ATP hydrolyses domains are conserved in yeast, mammals and also in *Arabidopsis;* therefore generation of the dominant-negative mutants of AtSKD1 ortholog provides a useful tool to study its interfere with the MVB pathway also in plants.

3.3.1 AtSKD1 is a functional homolog of Vps4 in *Arabidopsis thaliana*

Binding of AtSKD1 to *Arabidopsis* homologues of ESCRT III components including the small coiled-coil proteins of Vps20, Vps32 and Vps24 and binding also to ESCRT III accessory proteins including Vps46 and Vps60 suggested that recruitment of AtSKD1 might be mediated by ESCRT III activity.

In addition, LIP5 is an ortholog of Vta1 which is an activator of ATP-hydrolysis activity of Vps4 protein in yeast. By amino acid sequence alignment based on the similarity in the VSL region which is conserved region in Vta1 homologs across evolution including yeast, human and *Arabidopsis,* LIP5 an ortholog of Vta1 was found in *Arabidopsis* (Lottridge et al., 2006; Haas et al., 2007) . Furthermore binding of AtSKD1 with ESCRT III accessory proteins (Vps46 and Vps60) and also LIP5 suggests the regulatory role of these proteins on AtSKD1 activity in *Arabidopsis* as it has been described that Vps4 is recruited via interactions with Vps46 and Vps60 and enhance ATPase activity of Vps4 in mammals and yeast(Azmi et al., 2006; Lottridge et al., 2006; Nickerson et al., 2006).

Taken together, present study shows interaction of AtSKD1 with regulator proteins downstream of ESCRT complexes suggested the AtSKD1 could be functional homolog of Vps4 in plants. These results are consistent with the data of mammalian and yeast studies which demonstrated that Vps46/Did2 recruits Vta1 (AtLIP5), and Vta1 recruits Vps60. Interaction between Vta1 and accessory ESCRT III proteins (Vps46 and Vps60) recruit Vps4. in addition interaction of Vps4 with Vta1 promotes assembly and disassembly of ESCRT III complex (Xiao et al., 2008; Lottridge et al., 2006).

To identify the interacting surfaces of AtSKD1 and LIP5, deletion analysis of AtSKD1 protein has been performed. Surprisingly neither the MIT domain nor the ß domain of AtSKD1 could interact with LIP5 in *Arabidopsis.* Therefore other domains might play a role in this interaction, for instance the ATPase domain or the C-terminal domain is also necessary for interaction between AtSKD1 and LIP5 in *Arabidopsis*.

3.3.2 AtSKD1 functions in the protein sorting pathway

Transient expression of pro*35S:YFP-AtSKD1* in *Arabidopsis* protoplasts revealed endosomal localization of AtSKD1 besides the cytoplasmic signal, whereas AtSKD1 dominant negatives localized on big dot-like structures that based on colocalization studies can be deformed endosomal compartments, as observed in class E Vps mutant of *S.cerevisiae* (Babst et al., 1997). Thereby, the relevance of change in the size of the endosome in dominant negatives AtSKD1, and also blocked transport of CPY marker to vacuole in AtSKD1 dominant negative in protoplast (Channa Keshavaiah, unpubished data) can explain the defect in the sorting of cargo proteins in the MVB pathway which accumulates cargo proteins on endosomes, which are not able deliver to vacuole for degradation. Cotransformation of the AtSKD1 dominant negative with a vacuolar marker CPY in *Arabidopsis* protoplast could help to clarify AtSKD1 function in the vacuole trafficking pathway (Channa keshavaiah, unpublished observation). Accumulation of the vacuolar marker CPY in an aberrant endosomal compartment in AtSKD1^{K178AE234Q} protoplast cells shows mis-sorting of vacuolar marker in the trafficking pathway to the vacuole, resulting in an accumulation of CPY on endosomes in comparison with the wild type AtSKD1, which displays wild type morphology and normal vacuolar sorting phenotypes. It appears AtSKD1, like its equivalent ortholog in yeast might have a essential role in sorting machinery.

Interestingly, a single amino acid substitution in ATPase domain of AtSKD1 is enough to completely block protein sorting. In this context, expression of the AtSKD1-YFP and AtSKD1$^{K178A\&\ E234Q}$-YFP in *Arabidopsis* plants allowed to follow localization of them in trichome and root cells of homozygous transgenic lines. The analysis could confirm the observation in protoplast that AtSKD1-YFP localized on endosomes in root and trichome

(Figure 11-2, 14-2). Taken together, the data suggest that AtSKD1^{K178AE234Q}–YFP expressed in plants cells indicates the phenotype closely related to class E Vps protein. Furthermore, very low speed internalization of the FM4-64 to the endosome of the root and trichomes in the dominant negative AtSKD1 transgenic lines in compare to the wild type AtSKD1 suggest a role of the AtSKD1 protein in the endocytic pathway in *Arabidopsis*. Accumulation of endocytic markers in the class E compartment in Vps mutants was described in yeast (Raymond et al., 1992; Piper et al., 1995). Accumulation of endocytic and biosynthetic proteins in a class E mutant can induce a secondary defect in endocytosis of proteins which suggests the function of AtSKD1 in endocytic pathway. Taken together, the results predict AtSKD1 function in the endocytosis and sorting of cargo proteins in *Arabidopsis* like Vps4 in yeast.

3.4 Cytokinesis needs a functional AtSKD1

Our finding that AtSKD1 dominant negatives are exhibited an increasing in the nucleus predicts that AtSKD1 also could be involved in regulation of endoreplication of trichomes. The deregulation of observed branch number in trichomes could be a function of cell size and DNA content. The formation of supernumerary in *Arabidopsis* often is accompanied by additional rounds of endoreplication, but the genetic analysis of nuclear DNA content of dominant negative AtSKD1 did not detect any significant difference of DNA content in all dominant negatives lines compare with wild type. A multiple nuclei phenotype was observed in transgenic lines of dominant negatives AtSKD1, suggest role of AtSKD1 in cytokinesis since defects in cytokinesis are manifested by the appearance of multinucleated cell. This phenotype of AtSKD1 mutant is similar to ELCH, a first protein in ESCRT pathway indicating that mutation in this gene induces a cell division defect where the cell contains multiple nuclei (Spitzer et al., 2006). Its human ortholog TSG101 is a component of ESCRT I complex, which is involved in the sorting of monoubiqutylated proteins into the MVB pathway inducing a mitotic defect and producing multiple nuclei cells, which suggested a regulatory role of this protein in the cell cycle (Xie et al., 1998), which functions in the late stages of cell division.

Based on a previous study on endosomal sorting in yeast, AtSKD1 function in the last step in the MVB pathway which mediates the disassembly and recycling of the ESCRT complex from endosomal membranes whereas, the ELCH functions in the early steps in the recognition of ubiquitylated cargo poteins. Taken together, these two genes, which belong to MVB pathway, show a similar phenotype. It is conceivable that there is a common characteristic effect of the ESCRT machinery in plants. This is a supposition from mammalian study that ESCRT machinery play a role in late stages of cytokinesis which mediates essential membrane fission for efficient separation of the daughter cells in the last step of cell division (Carlton and Martin-Serrano, 2007). Further analysis needs to address these questions whether AtSKD1 plays an essential role in cell division, and how it is involved in this function and whether AtSKD1 has direct role in the cell cycle.

In my finding miss-expression of AtSKD1 dominant negatives causes alterations in the endomembrane system, Fragmentation of vacuoles, mis-sorted membrane proteins through accumulated in prevacuolar compartments, and early cell death are the other phenotypes of mutation in ATP binding or ATP hydrolysis domains.

3.5 Ectopic expression of AtSKD1 induces the vacuolar fragmentation and cell death

3.5.1 Vacuole maintenance is defected in the AtSKD1 mutants

Arabidopsis cells have a large central vacuole that is created by the combination of lytic vacuoles and protein storage vacuoles (Rojo et al., 2001). Vacuolar disruption usually occurs by nutrient limitation conditions or by osmotic stress, which results in the fragmentation of vacuoles into numerous small vacuolar vesicles (Wickner et al., 2002 (Wickner, 2002); (Bryant and Stevens, 1998; Otegui et al., 2005); (Marty, 1999)).

One criterion to monitor cell maintenance is the extension of cell vacuolization. Fragmentized vacuoles were found in the AtSKD1^{K178AE234Q} transgenic lines to be associated with severe growth and abnormalities of trichomes. Defective vacuole organization was prominent in AtSKD1 dominant negative transgenic lines. In AtSKD1 dominant negatives transgenic lines enlarged vacuoles which presumably were created by the

fusion of existing small vacuoles (Owen and Makaroff., 1995) subsequently were fragmentized after development and large central vacuoles formation. The fragmentized vacuoles phenotype shows that dominant negatives of AtSKD1 are similar to those found in class B Vps mutants of *S.cerevisiae* and that Vps mutant of Aspergillus Oryzae impair vacuole biogenesis (Price et al., 2000),(Ohneda et al., 2005).

Whether AtSKD1 controls vacuolar maintenance and cell death by different pathways or whether vacuole fragmentation in AtSKD1 mutations is a consequence of cell death is unclear.

There are two emphases as to why the vacuoles are disrupted in these mutants: firstly, when ATPase activity of AtSKD1 was blocked in transgenic lines of AtSKD1 dominant negatives blocked ATPase activity of AtSKD1, and also defects protein sorting pathway. Previous study in yeast has described that many enzymes which are involved in the maintenance of vacuole, deliver to the vacuole by this sorting pathway such as vacuolar proton pump activity (V-ATPase pump). Disruptions in V-ATPase pump which induces fission reaction of vacuoles could impair the biogenesis of vacuoles (Baars et al., 2007). In order to understand whether dominant negatives AtSKD1 impair vacuole biogenesis, FDA staining of transgenic lines of AtSKD1 dominant negatives exhibited that the biogenesis of the vacuoles were not impaired in lacking ATPase activity in these transgenic lines and developed normally, as in wild type trichomes. In these transgenic lines, vacuole development is preceded, and enlarged vacuoles presumably are created by the fusion of preexisting small vacuoles (Owen and Makaroff 1995). Large central vacuole structure was transient in the trichomes of AtSKD1 dominant negative transgenic lines. Vacuole disruption was initiated in young trichomes after large central vacuole formation, which started from the edge and stem of the trichome and developed to whole trichome.

In yeast, Multivesicular bodies frequently are found close to the vacuole, but they are regarded as prevacuolar compartments that fuse to the vacuole. Mutation in proteins involved in the MVB pathway accumulates cargo proteins in enlarged endosomal compartments. However, analysis of the transient expression of the AtSKD1^{K178A}, AtSKD1^{E234Q}, and AtSKD1^{K178AE234Q} in *Arabidopsis* protoplast detected vacuolar fragmentation and extended abnormal compartments after 24 hours. This data suggests a

second possibility for the disruption of the vacuole. The presence of trafficking pathway in another direction from the vacuole to the endosomes might be conceivable when a vacuole receives MVB membranes by vesicles fusion and has to reduce its membrane again to maintain the equilibrium which precedes vacuole fission and therefore adds a vacuole membrane to the endosome.

3.5-2 Cell death; the last chapter of AtSKD1 mutation

Ectopic expression of the AtSKD1 in the trichome causes cell death. To understand more about trichome death; the vacuoles of the trichomes were assayed, using FDA staining which stains living cells. Cell death was the last phenotype which could be observed in the trichomes of the dominant negative AtSKD1 transgenic lines. There are two explanations for the cell death. First, whether vacuole fragmentation in AtSKD1 dominant negatives causes cell death. Second; cell death precedes vacuole fragmentation. As judge by the relative timing of effect, the primary defect of these mutations is vacuole fragmentation, which starts immediately after the large central vacuole developed from the sides of the branches. This process continued more than a day, until the trichome cell lost the whole vacuole, leading to the cell's death (Figure 13-2). Whereas the last vacuolar vesicles present in the cell, trichomes are survive and stand up when cells lost whole vacuoles, trichomes collapsed and dead. In the last step when there is no vacuole in the trichome, it does not stain with FDA, which means it is no longer alive. FDA staining of the trichomes of AtSKD1 dominant negatives indicates that the vacuolar defects precede the initiation of cell death.

Now the question arises as to how the vacuole disruption induces cell death?

There are many routes for committing suicide in eukaryotic cells. Programmed cell death (PCD), which is regulated by a vacuolar processing enzyme (VPE), where a cystein proteinase induces vacuolar disruption, causing a subsequent degradation of the cytoplasmic structures which lead to cell death (Kuroyanagi et al., 2005). The proteases also are vacuolar processing enzymes which, when activated, form a residue in the lytic vacuoles that mediates the activation of other vacuolar enzymes and the disruption the tonoplast in the culminating phase of developmental and induces programmed cell death

(Hatsugai et al., 2004; Nakaune et al., 2005; Bozhkov and Jansson, 2007). Apoptosis is a type of programmed cell death. The main executioners in apoptosis are caspases (aspartat-specific cystein proteinase).

Now the main question is which kind of cell death is induced in AtSKD1 dominant negatives plants? What is the relation between blocked ATPase activity of AtSKD1 dominant negatives and fragmentation of vacuoles?

ATPase activity of AtSKD1 is blocked by mutation in ATPase domain of SKD1. How this mutation disrupts maintenance of large vacuole in *Arabidopsis* is in not clear. It has been reported recently that ELCH interacts with VHA-a3, which is an isoform of VHA-a in *Arabidopsis* (Spitzer et al., 2006). On the other hand, as known from a previous study of the activity of Vacuolar H-ATPase as a potential regulator of vacuolar morphology, membrane dynamics is necessary for maintenance of vacuole (Baars et al., 2007). Taken together, it is suggested that the MVB sorting pathway is related to vacuolar ATPase activity, as described in *elch* mutant plant that misregulation of V-ATPase results in a cell division defect (Spitzer, PhD thesis 2007). How does AtSKD1 ATPase malfunction induce vacuole disruption? One idea is the AtSKD1 mutation can alter the proton pump activity of the VHA protein that induces vacuolar fragmentation and that finally cell death occurs, with consideration to previous results which indicated that the vacuolar ATPase activity is involved in the sorting of biosynthetic cargo and receptor mediated endosytosis (Nishi and Forage., 2002), and that the trafficking of VHA proteins also is done by the MVB pathway. On the other hand, the ESCRT pathway also is involved in both functions by internalizing of cargo proteins from endosomes into luminal vesicles, and also by the direct interaction of V-ATPase and ELCH, suggesting that V-ATPase could be involved in ESCRT sorting machinery. Thereby, mutation in AtSKD1, which abolishes MVB sorting machinery, might eliminate V-ATPase function, resulting in a reduction of vacuole maintenance, causing vacuole rupture and finally, cell death through the loss of the vacuole.

4. Materials and Methods

4.1 MATERIAL

4.1.1 Chemicals and antibiotics

All used chemicals and antibiotics in analytical quality have been used from Sigma-Aldrich (Taufkirchen), Boehringer Mannheim (Mannheim), Serva (Heidelberg), Merck (Darmstadt), Qiagen (Hilden), Roth (Karlsruhe).

4.1.2 Enzymes and molecular biological materials

Restriction enzymes were used from MBI-fermentas (St.Leon-Rot), New England Biolabs (Frankfurt/Main) and Roche (Mannheim). Primers were generated by ARK Scientific and Invitrogen (Karlsruhe).

4.1.3 Cloning vectors

The following vectors were used in this work:

pACT-GW (clontech) was used as prey vector in yeast two hybrid assay.

pAS-GW (clontech) was used as a bait vector in yeast two hybrid assay.

pSYC-GW was used for bimolecular flurecent complementation assay contain split of C-terminal of YFP.

pSYN-GW was used for BiFC assay contain N-terminal of YFP.

pGEM-T easy (Promega) for PCR-product clonings.

pDONR 201vector (Invitrogen) was used as a donor in gateway based clonings.

pAM-PAT-GW as a binary gateway target vector containing a CaMV 35S promoter. Cassette and BASTA resistance (GenBank accession AY027531).

pAM-PAT-GW as a binary gateway target vector containing a GLABRA 2 promoter cassette and BASTA resistance.

pENSG-CFP a binary gateway target vector containing a CaMV 35S promoter cassette, the CFP protein and confering resistance to BASTA.

pENSG-YFP a binary gateway target vector containing a CaMV 35S promoter cassette, the YFP protein and confering resistance to BASTA.
pEearlyGate 201(N-HA) (Early *et al*., 2006) a binary gateway target vector containing a CaMV 35S promoter cassette, the YFP protein and conferring resistance to BASTA.
pN-His() for standard clonings and PCR-product clonings contains T7 promoter and Ampicilin resistance.

4.1.4 Antibiotics

Ampicillin (Amp) 100 mg/ml in H2O
Gentamycin (Gent) 15 mg/ml in H2O
Kanamycin (Kan) 50 mg/ml in H2O
Rifampicin (Rif) 100 mg/ml in DMSO
Those stock solutions (1000x) stored at –20ºC. Aqueous solutions were sterile filtrated.

4.1.5 Bacterial strains

For standard cloning the *Escherichia coli* strains DH5alpha and XL1blue were used, the DB3,1 strain, which is resistant to the *ccdB* gene, was used for the Gateway Entry, Donor and Destination vectors. For plant transformation *Agrobacterium tumefaciens* strains GV3101 were used. The gateway cloning required the usage of a modified strained of GV3101. For yeast-two hybrid assays, the strain AH 109 was used. The BL21, strain which is resistant to chloramphenicel was used for protein expression.

4.1.6 Plant lines

In this study Columbia (Col) ecotypes were used. The mutants of Vps4/SKD1 are in col background.

4.2 Methods

4.2.1 Plant work

4.2.1.1 Plant growth conditions

Seeds were sawn on humid freshly prepared *Arabidopsis* culture soil, covered with a plastic lid and stored for three to seven days at 4°C. *Arabidopsis thaliana* plants were grown under long-day conditions (16 h of light, 8 h of darkness) between 18 and 25 ºC under standard greenhouse conditions and the lid was removed after three to four days.

4.2.1.2 Plant transformation

Plants were transformed according to the "floral dip" method (Clough and Bent, 1998). To grow (achive) strong plants, these were allowed to grow at 18°C untill the first flowers appeared at stalks of approximately 10 cm in length. Five days before plant transformation a 5 ml of the Agrobacteria clone preculture in YEB medium was incubated for two days at 28°C. This preculture was used to inoculate the final 500 ml culture which was then incubated again for three days at 28°C. Before transformation 5% sucrose and 0.05% Silwett L-77 were added to the culture. Plants were dipped in this solution for approximately 20-30 seconds and after that covered with a lid. The lid was removed on the next day after those plants were treated as usual.

4.2.1.3 Selection of transformants

The seeds of transgenic plants carrying in their T-DNA a kanamycin or a hygromycin resistance were selected on half strong MS-Agar plates with 50 µg/ml kanamycin or 25 µg/ml hygromycin, respectively. Transgenic plants containing the BASTA resistance were grown on soil for 10 to 15 days. The seedlings were sprayed with a 0.001 % BASTA solution, the spraying was repeated after 3 to 7 days.

4.2.1.4 Seed sterilization

The surface of the seeds was sterilized by 15 min incubation in 95% Ethanol and after that incubated 15 min in a 3% $NaClO_3$ solution containing 0.1% triton X-100. Then the seeds were washed two to three times with striele watter s and than plated under the clean bench on MS-Agar plates (1% Murashige-Skoog salts, 1% sucrose, 0.7% agaragar, pH5.7) were used without antibiotic or with kanamycin (50 µg/ml) or hygromycin (25 g/ml). Plants were grown under long day conditions (16 h photoperiod and 22ºC).

4.2.1.5 DAPI staining

For DAPI stainings leafs were incubated overnight in 70% Ethanol at RT. Leaves were incobated under vaccum (0.6 bar) for 30 min in a DAPI solution (in final solution 0.25µg/ml DAPI in H2O) Leafs were washed in 70% EtOH at 4ºC to reduce background after that wash with H2O.

For DNA measurements of trichomes, rosette leaves were vacuum infiltrated for 30 min in formaldehyde solution (3.7% formaldehyde in PBST) then incubated 2h at 4ºC.

Samples were washed two times for 15 min in PBST. Then leaves were vacuum infiltrated in DAPI solution (0.25µg/ml, 5% DMSO in H_2o) for 15 min and incubated overnight in DAPI solution at 4ºC thereafter leaves were washed two times in PBST.

4.2.1.6 Propidium iodide staining

Plant material (leaves and roots) was incubated for 5 minutes in 100 µg/ml Propidium iodide in H2O. After that the samples where washed with H2O, mounted on a slide and analyzed under the microscope with UV excitation.

4.2.1.7 Fluoresceine diacetate staining

Plant material was incubated for 5 minutes in H2O contain 100 µg/ml and FDA. Afterwards the samples where washed with H2O and mounted on a slide and analysed under the microscope with UV excitation

4.2.1.8 8 Microscopy

Light and epifluorescence microscopy was performed using a LEICA-DMRE microscope using DIC optics (LEICA). Images were taken using a high resolution KY-F70 3-CCD

JVC camera and frame grabbing DISKUS software (DISKUS, Technisches Büro, Königswinter). Confocal laser scanning microscopy (CLSM) was done with a Leica TCS-SP2 confocal microscope together with the Leica-software (Leica Microsystems, Heidelberg). Sections in steps of 1 or 2 µm were taken and eventually integrated by Leica Confocal Software Lite 2.05 (LCS, Leica Microsystems, Heidelberg). For fluorescence microscopy plants were embedded with tab water and covered with a coverslide. Transversal sections were carried out with plants embedded in 4% low-melting agarose and hand sectioned using a razor blade as described by Kim *et al.* (2003). Images were assembled and processed using Adobe Photoshop 6.0 and Microsoft Power-Pointsoftware.

4.2.2 Molecular-biological methods

4.2.2.1Genomic DNA preparation from plant tissue

To gain high-quality genomic DNA, the CTAB-preparation was used (Rogers and Bendich., 1988). Plant material (single rosette or cauline leave) was grinded and 200 µl of extraction buffer (2 % (w/v) CTAB, 1,4 M NaCl, 20 mM EDTA, 100 mM Tris/HCl pH 8.0, 0.2 % bmercaptoethanol) was added and incubated for 30 minutes at 65 °C. After addition of 150 µl Chloroform/Isoamylalcohol (24:1) and careful shaking, the probes were centrifuged for 15 minutes at 4000 rpm. The aqueous phase was transferred into a new tube and mixed with 200 µl isopropanol and centrifuged for 15 min. at 4000 rpm. The pellet was washed with 70 % Ethanol and dried, afterwards the pellet was resolved in 20 µl 20 mM Tris/HCl pH 8.0.

4.2.2.2 Plasmid DNA preparation from bacteria

Plasmid preparation was performed using a column pEQ-LAB Plasmid Miniprep KitI (PEQLAB Biotechnology GmbH, Erlangen) according to the manufacturer's protocol.

4.2.2.3 DNA-manipulation

DNA manipulation and cloning were carried out according to Sambrock et

al.(Sambrook et al., 1989) or Ausubel (Ausubel, 1994), using standard procedures. All PCR-amplified fragments were sequenced prior to further investigation.

PCR-Primers and constructs were designed using the Vector NTI-suite 7.1 software (Invitrogen, Karlsruhe).

4.2.2.4 Plasmid construction

Full length cDNA for PCR and sequent BP reaction were obtained from RIKEN Genomic Sciences Center (Sakurai et al 2005, Seki et al 1998, Seki et al 2002). Ara6 and Ara7 were a gift from Takashi Ueda and have been described earlier (Ueda et al 2004, Ueda et al 2001).Vps22-2 and Vps23-2 and Vps23-3 were amplify directly from Arabidopsis genomic DNA. Gene specific primers incorporating attB1 and attB2 sequences were purchased from Invitrogen.

The coding sequence of Vps genes were amplified by PCR reactions with primer incorporating attB1 and attB2 sequences (Invitrogen) and introduced into the pDONR201by BP clonase reaction according to manufacturers instructions (Invitrogen). The resulting pDONR 201 clones were transformed into the E. coli strain DH5-alpha and sequenced. DNA fragments were transferred to the destination vectors pAS, pACT for yeast two hybrid analysis and to pENSG-YFP and pENSG-CFP for localization studies by LR clonase reaction according to the manufacture instructions (Invitrogen). The product of recombination reaction (LR reaction) was used to transform Arabidopsis protoplast as described later.

4.2.2.5 BiFC constructs

The BiFC assay is a generally applicable for the visualization of a variety of protein complexes in living cells and organisms.

All Vps candidate genes were fused to N-terminus of the split YFP parts and were amplified without stop codon and introduced into pDONR201 after sequencing the resulting clones were used for LR recombination reaction into the destination vectors pSPYNE and pSPYNc (Wlter et al 204) and subsequent transformation into Arabidopsis protoplasts. Negative controls were carried out for each experiment by cotransforming and empty vector containing only the appropriate split YFP part together with the

respective gene:spliYFP fusion and by expression of non-interacting transcription factors AtMYB51(At1g18570) in pSPYNE and bHLH133(At2g20095) in pSPYCE to exclude non-specific association caused by high local concentrations of non interacting partners (Gigolashvili et al 2007, Lalonde et al 2008). Experiments were performed in a reciprocal manner at least three times.

Two proteins are said to interact when the protoplasts expressing the fusion proteins present an emission of light due to the reconstituted YFP protein.

4.2.2.6 Protoplast preparation and transformation

To create the protoplasts, 50 mL of cell suspension culture (Clombia type growing in MS medium supplemented with, MS powder: 4,3g, sucrose: 30g, vitamin B5: 4 mL, NAA: 0,5 mg, kinetin 0,1 mG, pH 5,5) was spinned down at 1500 rpm for 5 minutes. 50 mL of enzyme solution (1% cellulase, 0,2% mazerozym in MS-0,34M Glucose manitol medium (MS powder 4,3 g, glucose 30,5 g, mannitol: 30,5g, pH 5,5) was added to the pellet in two steps of 25 mL each(Mathur and Koncz, 1998). The suspension was transferred to two large petridishes (diameter: 145 mm, height: 20 mm) and shaken in the dark for 4 hours at 50 rpm. Subsequently, the protoplasts were made ready for transformation transferred to two Falkon tubes and were spinned down at 800 rpm. The pellets were resuspended in 25 mL MS-0,34M Glucose manitol medium and spinned down like described previously. The pellet was resuspended in 5mL of MS-0,28M sucrose medium (MS powder: 4,3 g.L-1, 0,28M sucrose, pH 5,5) and centrifuged at 800 rpm for 5 minutes. The supernatant containing the protoplasts was then ready for transformation. Each transformation required to mix 50 ìL of protoplasts and 15 ìg of DNA with 150 ìL PEG solution (25% PEG 6000, 0,45 M mannitol, 0,1M Ca(NO3)2, pH 9) in a 2 mL Eppendorf tube. The mix was incubated 20 minutes in the dark and the PEG was washed away by the means of two subsequent additions of 500 ìL of 0,275 M Ca(NO3)2. The transformed protoplasts were centrifuged at 800 rpm for 7 minutes and transferred to 500 ìL MS 0,34 M glucose mannitol solution (Magyar *et al.,* 2005). The Eppendorf tube was left laying for 16 hours at 23^{o}C in the dark before observation of the protoplasts.

4.2.2.7 Yeast two-hybrid assay

Fusions with the GAL4 activation domain and the GAL4 DNA-binding domain were performed in the pACT and pAS plasmids (Clontech): Full-length *all Vps candidat genes* were fused to the GAL4 activation domain in the pACT plasmid and to the GAL4 DNA-binding domain in the pAS plasmid. Few used constructs and empty vectors did not show any self activation in yeasts. The yeasts were transformed using a standard AcLi/ssDNA/PEG method (Gietz et al 1995). Interactions were analyzed on synthetic dropout medium lacking leucine and tryptophan and on synthetic dropout medium lacking leucine, tryptophan and histidine supplemented with 3mM 3-amino-1,2,4-triazole(3-AT) (Sigma- Aldric, Munich Germany). Two proteins are said to interact when a population of yeast transformed with them fused either to the GAL4 activation domain or the GAL4 DNA-binding domain has acquired the ability to grow on histidine lacking media. SNF1 and SNF4 were used as positive controls (Fields and Song 1989). All experiments were repeated at least three times and performed in a reciprocal manner.

4.2.2.8 Blunt-end ligation

For blunt-end ligations the DNA was either cut with blunt-cutters. The vector was cut with a blunt-cutter and gel purified. After the fill-in reaction the fragment was ligated into the blunt site of the vector in room temperature over night. Additionally 0,1 units of the enzyme was added for digesting the vector. The ligase was inactivated by heating the reaction to 65ºC and 0.5 units of the enzyme, used to digest the vector, was added and incubated at optimal temperature. As negative control the same reaction with all conditions preserved was done in parallel but the insert was replaced by water.

4.2.3 Basic protein techniques (SDS-PAGE, Western blotting)

See “Molecular Cloning: A Laboratory Manual (Third Edition) By Joseph Sambrook,

Peter MacCallum Cancer Institute, Melbourne, Australia; David Russell, University of

Texas Southwestern Medical Center, Dallas”

4.2.3.1 Protein extraction and purification

At SKD1 and its dominant negatives were cloned into the invitrogen pTRCHis Vector and have expressed in BL21 *E.coli*.

Bacteria transformed with His vector contain AtSKD1 and its dominant negatives are grown in LB medium containing 100 µg/ml ampicillin at 28°C. At OD_{600} = 0.6, cells are induced by addition of IPTG (inducer isopropyl-â-thiogalactoside) final concentration 0,5 mM and left at 10°C overnight. The suspension is then centrifuged (30 min., 7500 rpm) and the pellet resuspended in PBS lysis Buffer (10 mM imidazol, 0.3M NaCl, 50mM NaH_2Po_4, 2mM DTT (Invitrogen) and the cell suspension sonicated 3 X 10 seconds. The cells are pelleted by centrifugation at 17000rpm for 20 min, using a Sorvall centrifuge equipped with an SS34 rotor. The supernatant is loaded on a Ni-NTA-Agarose column (Nichel nitrilotriacetic resin), washed with washing Buffer (20 mM imidazol, 0.3M NaCl, 50mM NaH_2Po_4, 2mM DTT) and eluted with elution Buffer (200 mM imidazol, 0.3M NaCl,50mM NaH_2Po_4, 2mM DTT).

4.2.3.2 Western blotting

The extracted protein was loaded on a gel (separation gel: 12% acrylamide (Rotigel30), 1M Tris pH 8,8 and SDS 10% in H2O) and ran for 60 minutes under 20 mA. The blot was carried on under semi-dry conditions to a Roti-PVDF membrane (Carl Roth GmbH, Karsruhe) according to the manufacturer's instructions.

The membrane was blocked for 1 hour in 5% milk dissolved in phosphate buffered saline-tween (PBST: 8 g of NaCl 0.2 g of KCl, 1.44 g of Na_2HPO_4, 0.24 g of KH_2PO_4 , 2 ml of tween-20 in 1L of H2O; pH 7,2). The first antibody (Roche) 1:2000 was applied over night at 4°C in 5% milk in PBST. The blot was washed three times in PBT:

for 10 minutes. The second antibody was applied for 90 minutes at room temperature in 5% milk in PBST. The blot was washed three times in PBST for 10 minutes. Finally, the detection was performed with the kit ECL Western Blotting Analysis system (Amersham Biosciences, UK) following the instructions given by the manufacturers.

4.3 Image processing

All images were processed using Adobe Photoshop 6.0 software.

4.4 Sequence analysis

DNA and protein sequence analysis was performed using the Vector NTI® software from invitrogen™. Multiple sequence alignment was done using CLUSTALW from the NPS@ Web server. NPS@ is part of the Pôle Bioinformatique Lyonnais. For coiled-coil domain analysis the COILS program was used (Lupas et al., 1991).

http://www.invitrogen.com

http://npsa-pbil.ibcp.fr/cgi-bin/npsa_automat.pl?page=npsa_clustalw.html

http://www.ch.embnet.org/software/COILS_form.html

5. References

Alam, S.L., and Sundquist, W.I. (2007). Structural biology: ESCRT service. Nature 447, 921-922.

Alam, S.L., Sun, J., Payne, M., Welch, B.D., Blake, B.K., Davis, D.R., Meyer, H.H., Emr, S.D., and Sundquist, W.I. (2004). Ubiquitin interactions of NZF zinc fingers. Embo J 23, 1411-1421.

Azmi, I., Davies, B., Dimaano, C., Payne, J., Eckert, D., Babst, M., and Katzmann, D.J. (2006). Recycling of ESCRTs by the AAA-ATPase Vps4 is regulated by a conserved VSL region in Vta1. J Cell Biol 172, 705-717.

Azmi, I.F., Davies, B.A., Xiao, J., Babst, M., Xu, Z., and Katzmann, D.J. (2008). ESCRT-III family members stimulate Vps4 ATPase activity directly or via Vta1. Dev Cell 14, 50-61.

Baars, T.L., Petri, S., Peters, C., and Mayer, A. (2007). Role of the V-ATPase in regulation of the vacuolar fission-fusion equilibrium. Mol Biol Cell 18, 3873-3882.

Babst, M. (2005). A protein's final ESCRT. Traffic 6, 2-9.

Babst, M., Sato, T.K., Banta, L.M., and Emr, S.D. (1997). Endosomal transport function in yeast requires a novel AAA-type ATPase, Vps4p. Embo J 16, 1820-1831.

Babst, M., Wendland, B., Estepa, E.J., and Emr, S.D. (1998). The Vps4p AAA ATPase regulates membrane association of a Vps protein complex required for normal endosome function. Embo J 17, 2982-2993.

Babst, M., Odorizzi, G., Estepa, E.J., and Emr, S.D. (2000). Mammalian tumor susceptibility gene 101 (TSG101) and the yeast homologue, Vps23p, both function in late endosomal trafficking. Traffic 1, 248-258.

Babst, M., Katzmann, D.J., Estepa-Sabal, E.J., Meerloo, T., and Emr, S.D. (2002). Escrt-III: an endosome-associated heterooligomeric protein complex required for mvb sorting. Dev Cell 3, 271-282.

Bishop, N., and Woodman, P. (2000). ATPase-defective mammalian VPS4 localizes to aberrant endosomes and impairs cholesterol trafficking. Mol Biol Cell 11, 227-239.

Bowers, K., Lottridge, J., Helliwell, S.B., Goldthwaite, L.M., Luzio, J.P., and Stevens, T.H. (2004). Protein-protein interactions of ESCRT complexes in the yeast Saccharomyces cerevisiae. Traffic 5, 194-210.

Bozhkov, P., and Jansson, C. (2007). Autophagy and cell-death proteases in plants: two wheels of a funeral cart. Autophagy 3, 136-138.

Bracha-Drori, K., Shichrur, K., Katz, A., Oliva, M., Angelovici, R., Yalovsky, S., and Ohad, N. (2004). Detection of protein-protein interactions in plants using bimolecular fluorescence complementation. Plant J 40, 419-427.

Bryant, N.J., and Stevens, T.H. (1998). Vacuole biogenesis in Saccharomyces cerevisiae: protein transport pathways to the yeast vacuole. Microbiol Mol Biol Rev 62, 230-247.

Carlton, J.G., and Martin-Serrano, J. (2007). Parallels between cytokinesis and retroviral budding: a role for the ESCRT machinery. Science 316, 1908-1912.

References

Chu, T., Sun, J., Saksena, S., and Emr, S.D. (2006). New component of ESCRT-I regulates endosomal sorting complex assembly. J Cell Biol 175, 815-823.

Eastman, S.W., Martin-Serrano, J., Chung, W., Zang, T., and Bieniasz, P.D. (2005). Identification of human VPS37C, a component of endosomal sorting complex required for transport-I important for viral budding. J Biol Chem 280, 628-636.

Fields, S., and Song, O. (1989). A novel genetic system to detect protein-protein interactions. Nature 340, 245-246.

Finken-Eigen, M., Rohricht, R.A., and Kohrer, K. (1997). The VPS4 gene is involved in protein transport out of a yeast pre-vacuolar endosome-like compartment. Curr Genet 31, 469-480.

Gigolashvili, T., Berger, B., Mock, H.P., Muller, C., Weisshaar, B., and Flugge, U.I. (2007). The transcription factor HIG1/MYB51 regulates indolic glucosinolate biosynthesis in Arabidopsis thaliana. Plant J 50, 886-901.

Gruenberg, J., Griffiths, G., and Howell, K.E. (1989). Characterization of the early endosome and putative endocytic carrier vesicles in vivo and with an assay of vesicle fusion in vitro. J Cell Biol 108, 1301-1316.

Haas, T.J., Sliwinski, M.K., Martinez, D.E., Preuss, M., Ebine, K., Ueda, T., Nielsen, E., Odorizzi, G., and Otegui, M.S. (2007). The Arabidopsis AAA ATPase SKD1 is involved in multivesicular endosome function and interacts with its positive regulator LYST-INTERACTING PROTEIN5. Plant Cell 19, 1295-1312.

Harter, C., and Wieland, F. (1996). The secretory pathway: mechanisms of protein sorting and transport. Biochim Biophys Acta 1286, 75-93.

Hartmann, C., Chami, M., Zachariae, U., de Groot, B.L., Engel, A., and Grutter, M.G. (2008). Vacuolar protein sorting: two different functional states of the AAA-ATPase Vps4p. J Mol Biol 377, 352-363.

Hatsugai, N., Kuroyanagi, M., Yamada, K., Meshi, T., Tsuda, S., Kondo, M., Nishimura, M., and Hara-Nishimura, I. (2004). A plant vacuolar protease, VPE, mediates virus-induced hypersensitive cell death. Science 305, 855-858.

Hawes, C.R., Brandizzi, F., and Andreeva, A.V. (1999). Endomembranes and vesicle trafficking. Curr Opin Plant Biol 2, 454-461.

Huang, T.G., and Hackney, D.D. (1994). Drosophila kinesin minimal motor domain expressed in Escherichia coli. Purification and kinetic characterization. J Biol Chem 269, 16493-16501.

Hulskamp, M., Schnittger, A., and Folkers, U. (1999). Pattern formation and cell differentiation: trichomes in Arabidopsis as a genetic model system. Int Rev Cytol 186, 147-178.

Jou, Y., Chou, P.H., He, M., Hung, Y., and Yen, H.E. (2004). Tissue-specific expression and functional complementation of a yeast potassium-uptake mutant by a salt-induced ice plant gene mcSKD1. Plant Mol Biol 54, 881-893.

Jurgens, G. (2004). Membrane trafficking in plants. Annu Rev Cell Dev Biol 20, 481-504.

Kim, H.L., and Kim, J.A. (2000). Purification of clathrin assembly protein from rat liver. Exp Mol Med 32, 222-226.

Kirchhausen, T., Bonifacino, J.S., and Riezman, H. (1997). Linking cargo to vesicle formation: receptor tail interactions with coat proteins. Curr Opin Cell Biol 9, 488-495.

Kornfeld, S., and Mellman, I. (1989). The biogenesis of lysosomes. Annu Rev Cell Biol 5, 483-525.

Kostelansky, M.S., Schluter, C., Tam, Y.Y., Lee, S., Ghirlando, R., Beach, B., Conibear, E., and Hurley, J.H. (2007). Molecular architecture and functional model of the complete yeast ESCRT-I heterotetramer. Cell 129, 485-498.

Kuroyanagi, M., Yamada, K., Hatsugai, N., Kondo, M., Nishimura, M., and Hara-Nishimura, I. (2005). Vacuolar processing enzyme is essential for mycotoxin-induced cell death in Arabidopsis thaliana. J Biol Chem 280, 32914-32920.

Leung, K.F., Dacks, J.B., and Field, M.C. (2008). Evolution of the multivesicular body ESCRT machinery; retention across the eukaryotic lineage. Traffic 9, 1698-1716.

Lin, Y., and Schiefelbein, J. (2001). Embryonic control of epidermal cell patterning in the root and hypocotyl of Arabidopsis. Development 128, 3697-3705.

Lottridge, J.M., Flannery, A.R., Vincelli, J.L., and Stevens, T.H. (2006). Vta1p and Vps46p regulate the membrane association and ATPase activity of Vps4p at the yeast multivesicular body. Proc Natl Acad Sci U S A 103, 6202-6207.

Lupas, A.N., and Martin, J. (2002). AAA proteins. Curr Opin Struct Biol 12, 746-753.

Marty, F. (1999). Plant vacuoles. Plant Cell 11, 587-600.

Matlack, K.E., Mothes, W., and Rapoport, T.A. (1998). Protein translocation: tunnel vision. Cell 92, 381-390.

Mellman, I. (1996). Endocytosis and molecular sorting. Annu Rev Cell Dev Biol 12, 575-625.

Miller, E.A., Lee, M.C., and Anderson, M.A. (1999). Identification and characterization of a prevacuolar compartment in stigmas of nicotiana alata. Plant Cell 11, 1499-1508.

Mukherjee, S., Ghosh, R.N., and Maxfield, F.R. (1997). Endocytosis. Physiol Rev 77, 759-803.

Nakaune, S., Yamada, K., Kondo, M., Kato, T., Tabata, S., Nishimura, M., and Hara-Nishimura, I. (2005). A vacuolar processing enzyme, deltaVPE, is involved in seed coat formation at the early stage of seed development. Plant Cell 17, 876-887.

Nickerson, D.P., West, M., and Odorizzi, G. (2006). Did2 coordinates Vps4-mediated dissociation of ESCRT-III from endosomes. J Cell Biol 175, 715-720.

Nikko, E., and Andre, B. (2007). Split-ubiquitin two-hybrid assay to analyze protein-protein interactions at the endosome: application to Saccharomyces cerevisiae Bro1 interacting with ESCRT complexes, the Doa4 ubiquitin hydrolase, and the Rsp5 ubiquitin ligase. Eukaryot Cell 6, 1266-1277.

Odorizzi, G., Babst, M., and Emr, S.D. (1998). Fab1p PtdIns(3)P 5-kinase function essential for protein sorting in the multivesicular body. Cell 95, 847-858.

Odorizzi, G., Katzmann, D.J., Babst, M., Audhya, A., and Emr, S.D. (2003). Bro1 is an endosome-associated protein that functions in the MVB pathway in Saccharomyces cerevisiae. J Cell Sci 116, 1893-1903.

Ogura, T., and Wilkinson, A.J. (2001). AAA+ superfamily ATPases: common structure--diverse function. Genes Cells 6, 575-597.

Ohneda, M., Arioka, M., and Kitamoto, K. (2005). Isolation and characterization of Aspergillus oryzae vacuolar protein sorting mutants. Appl Environ Microbiol 71, 4856-4861.

Okita, T.W., and Rogers, J.C. (1996). Compartmentation of Proteins in the Endomembrane System of Plant Cells. Annu Rev Plant Physiol Plant Mol Biol 47, 327-350.

Otegui, M.S., Noh, Y.S., Martinez, D.E., Vila Petroff, M.G., Staehelin, L.A., Amasino, R.M., and Guiamet, J.J. (2005). Senescence-associated vacuoles with intense proteolytic activity develop in leaves of Arabidopsis and soybean. Plant J 41, 831-844.

Piper, R.C., Cooper, A.A., Yang, H., and Stevens, T.H. (1995). VPS27 controls vacuolar and endocytic traffic through a prevacuolar compartment in Saccharomyces cerevisiae. J Cell Biol 131, 603-617.

Prag, G., Lee, S., Mattera, R., Arighi, C.N., Beach, B.M., Bonifacino, J.S., and Hurley, J.H. (2005). Structural mechanism for ubiquitinated-cargo recognition by the Golgi-localized, gamma-ear-containing, ADP-ribosylation-factor-binding proteins. Proc Natl Acad Sci U S A 102, 2334-2339.

Price, A., Seals, D., Wickner, W., and Ungermann, C. (2000). The docking stage of yeast vacuole fusion requires the transfer of proteins from a cis-SNARE complex to a Rab/Ypt protein. J Cell Biol 148, 1231-1238.

Puertollano, R. (2005). Interactions of TOM1L1 with the multivesicular body sorting machinery. J Biol Chem 280, 9258-9264.

Raymond, C.K., Howald-Stevenson, I., Vater, C.A., and Stevens, T.H. (1992). Morphological classification of the yeast vacuolar protein sorting mutants: evidence for a prevacuolar compartment in class E vps mutants. Mol Biol Cell 3, 1389-1402.

Richter, C., West, M., and Odorizzi, G. (2007). Dual mechanisms specify Doa4-mediated deubiquitination at multivesicular bodies. Embo J 26, 2454-2464.

Rohn, W.M., Rouille, Y., Waguri, S., and Hoflack, B. (2000). Bi-directional trafficking between the trans-Golgi network and the endosomal/lysosomal system. J Cell Sci 113 (Pt 12), 2093-2101.

Rojo, E., Gillmor, C.S., Kovaleva, V., Somerville, C.R., and Raikhel, N.V. (2001). VACUOLELESS1 is an essential gene required for vacuole formation and morphogenesis in Arabidopsis. Dev Cell 1, 303-310.

Scheuring, J., and Schramm, V.L. (1997). Kinetic isotope effect characterization of the transition state for oxidized nicotinamide adenine dinucleotide hydrolysis by pertussis toxin. Biochemistry 36, 4526-4534.

Schiefelbein, J. (2003). Cell-fate specification in the epidermis: a common patterning mechanism in the root and shoot. Curr Opin Plant Biol 6, 74-78.

Scott, A., Gaspar, J., Stuchell-Brereton, M.D., Alam, S.L., Skalicky, J.J., and Sundquist, W.I. (2005a). Structure and ESCRT-III protein interactions of the MIT domain of human VPS4A. Proc Natl Acad Sci U S A 102, 13813-13818.

Scott, A., Chung, H.Y., Gonciarz-Swiatek, M., Hill, G.C., Whitby, F.G., Gaspar, J., Holton, J.M., Viswanathan, R., Ghaffarian, S., Hill, C.P., and Sundquist, W.I. (2005b). Structural and mechanistic studies of VPS4 proteins. Embo J 24, 3658-3669.

Slagsvold, T., Aasland, R., Hirano, S., Bache, K.G., Raiborg, C., Trambaiolo, D., Wakatsuki, S., and Stenmark, H. (2005). Eap45 in mammalian ESCRT-II binds ubiquitin via a phosphoinositide-interacting GLUE domain. J Biol Chem 280, 19600-19606.

Spitzer, C., Schellmann, S., Sabovljevic, A., Shahriari, M., Keshavaiah, C., Bechtold, N., Herzog, M., Muller, S., Hanisch, F.G., and Hulskamp, M. (2006). The Arabidopsis elch mutant reveals functions of an ESCRT component in cytokinesis. Development 133, 4679-4689.

Stuchell, M.D., Garrus, J.E., Muller, B., Stray, K.M., Ghaffarian, S., McKinnon, R., Krausslich, H.G., Morham, S.G., and Sundquist, W.I. (2004). The human endosomal sorting complex required for transport (ESCRT-I) and its role in HIV-1 budding. J Biol Chem 279, 36059-36071.

Szymanski, D.B., Jilk, R.A., Pollock, S.M., and Marks, M.D. (1998). Control of GL2 expression in Arabidopsis leaves and trichomes. Development 125, 1161-1171.

Tanaka, H., Fujita, H., Katoh, H., Mori, K., and Negishi, M. (2002). Vps4-A (vacuolar protein sorting 4-A) is a binding partner for a novel Rho family GTPase, Rnd2. Biochem J 365, 349-353.

Teo, H., Perisic, O., Gonzalez, B., and Williams, R.L. (2004). ESCRT-II, an endosome-associated complex required for protein sorting: crystal structure and interactions with ESCRT-III and membranes. Dev Cell 7, 559-569.

Teo, H., Gill, D.J., Sun, J., Perisic, O., Veprintsev, D.B., Vallis, Y., Emr, S.D., and Williams, R.L. (2006). ESCRT-I core and ESCRT-II GLUE domain structures reveal role for GLUE in linking to ESCRT-I and membranes. Cell 125, 99-111.

Vajjhala, P.R., Wong, J.S., To, H.Y., and Munn, A.L. (2006). The beta domain is required for Vps4p oligomerization into a functionally active ATPase. Febs J 273, 2357-2373.

Wickner, W. (2002). Yeast vacuoles and membrane fusion pathways. Embo J 21, 1241-1247.

Winter, V., and Hauser, M.T. (2006). Exploring the ESCRTing machinery in eukaryotes. Trends Plant Sci 11, 115-123.

Xiao, J., Xia, H., Yoshino-Koh, K., Zhou, J., and Xu, Z. (2007). Structural characterization of the ATPase reaction cycle of endosomal AAA protein Vps4. J Mol Biol 374, 655-670.

Yeo, S.C., Xu, L., Ren, J., Boulton, V.J., Wagle, M.D., Liu, C., Ren, G., Wong, P., Zahn, R., Sasajala, P., Yang, H., Piper, R.C., and Munn, A.L. (2003). Vps20p and Vta1p interact with Vps4p and function in multivesicular body sorting and endosomal transport in Saccharomyces cerevisiae. J Cell Sci 116, 3957-3970.

Yoshimori, T., Yamagata, F., Yamamoto, A., Mizushima, N., Kabeya, Y., Nara, A., Miwako, I., Ohashi, M., Ohsumi, M., and Ohsumi, Y. (2000). The mouse

SKD1, a homologue of yeast Vps4p, is required for normal endosomal trafficking and morphology in mammalian cells. Mol Biol Cell 11, 747-763.

Yu, Z., Gonciarz, M.D., Sundquist, W.I., Hill, C.P., and Jensen, G.J. (2008). Cryo-EM structure of dodecameric Vps4p and its 2:1 complex with Vta1p. J Mol Biol 377, 364-377.

6. Appendix
6.1 list of primers

List of Primers which were used in this study

Name of Primer	sequences(5'-3)
RSP5-4g12570	GGGGACAAGTTTGTACAAAAAAGCAGGCTTCATGACTCTAAGCCGTTCA
RSP5-4g12570	GGGGACCACTTTGTACAAGAAAGCTGGGTCTCACCATTTACCGAAACT
Vps22-4g27040	GGGGACAAGTTTGTACAAAAAAGCAGGCTTCATGCGACGACGACCAGGA
Vps22-4g27040	GGGGACCACTTTGTACAAGAAAGCTGGGTCTTAAGTATCAGATCCGAT
Vps23-1-ELCH-3g12400	GGGGACAAGTTTGTACAAAAAAGCAGGCTTCATGGTTCCCCCGCCGTCTAAT
Vps23-1-ELCH-3g12400	GGGGACCACTTTGTACAAGAAAGCTGGGTCTCATGAATGTAACCTACC
CC1-2g06530	GGGGACAAGTTTGTACAAAAAAGCAGGCTTCATGATGAATTCAATCTTC
CC1-2g06530	GGGGACCACTTTGTACAAGAAAGCTGGGTCTCACATTTTTCTAAGGTT
Doa4-2g40930	GGGGACAAGTTTGTACAAAAAAGCAGGCTTCATGGCGGAGGTATCGATGG
Doa4-2g40930	GGGGACCACTTTGTACAAGAAAGCTGGGTCCAATGAGTTGCAGGGATA
Vps22-4-2g22890	GGGGACAAGTTTGTACAAAAAAGCAGGCTTCATGGCTACATCTCTTCAAAC
Vps22-4-2g22890	GGGGACCACTTTGTACAAGAAAGCTGGGTCTCATTCGTAGTTTGGCTCG
Vps22-5-4g27030	GGGGACAAGTTTGTACAAAAAAGCAGGCTTCATGGCTGTATCACTTCCAAC
Vps22-5-4g27030	GGGGACCACTTTGTACAAGAAAGCTGGGTCTTATGCTTGGTTGTTGGAG
Vps22-3-1g62190	GGGGACAAGTTTGTACAAAAAAGCAGGCTTCATGGCTGTATCATTTCAAAC
Vps22-3-1g62190	GGGGACCACTTTGTACAAGAAAGCTGGGTCTTAAATCTTTGTAAAGAAA
Vps22-short-3g31960	GGGGACAAGTTTGTACAAAAAAGCAGGCTTCATGACATTTGTAAGAATCC
Vps22-short-3g31960	GGGGACCACTTTGTACAAGAAAGCTGGGTCTCAGAATCTTGTTGCCAAC
VHs7(repeat)-5g16880	GGGGACAAGTTTGTACAAAAAAGCAGGCTTCATGGGTGACAATCTTATG
VHs7(repeat)-5g16880	GGGGACCACTTTGTACAAGAAAGCTGGGTCTCATGTGAGGTTAGCGGT
VHs7(long)-5g16880	GGGGACCACTTTGTACAAGAAAGCTGGGTCTGTCTGCTCAGCAGTAAAGCTTCTTACAGGCACATC
VHs12-4g11740	GGGGACAAGTTTGTACAAAAAAGCAGGCTTCATGGCGACACCGAATCAGG
VHs12-4g11740	GGGGACCACTTTGTACAAGAAAGCTGGGTCCTAGATAAGCTCAAGGAAC
VHs11-3g43230	GGGGACAAGTTTGTACAAAAAAGCAGGCTTCATGGCTACTCTCAACGGAA
VHs11-3g43230	GGGGACCACTTTGTACAAGAAAGCTGGGTCTTACGGGCGCAAACGAGCA
VHs10-1g29800	GGGGACAAGTTTGTACAAAAAAGCAGGCTTCATGTTAGAACCTGATCATG
VHs10-1g29800	GGGGACCACTTTGTACAAGAAAGCTGGGTCTTAGTCTTCAGACAATGGA
VHs8-1g06210(of gene)	ATGGACAAATTGAAGATAGCAGAATGGGGAGAGAAG
VHs8-1g06210(of gene)	TCAATCCATATTCCATAGACATTTGTTAAGGAAAA
VHs6-5g63640	ATGGCTGCGGAGCTTGTAAGTTCTGCAACAAGTGAG
VHs6-5g63640	TCAGTCACTGAAGTCTACGCTTCCACTGCGTGAGC

Appendix

VHs5-1g21380	ATGGCGAATAATGCGGCTGCTTGTGCTGAGAGGGCTAC
VHs5-1g21380	TCAAAACGGTTTGTTGTTCTGATTGTTGGGTTTGG
CC2-5g44560	ATGAACATTTTCAAGAAGAAGACCACTCCCAAAGATGC
CC2-5g44560	TCAGATTCGTCGTAGCGAAGCCAACCTCTTCTCAA
Vps36-5g04920(midel of gene)	GGGGACAAGTTTGTACAAAAAAGCAGGCTTCAGGGGATTTTGATGGCTT
	GGGGACCACTTTGTACAAGAAAGCTGGGTCCAACTCTGTCCCACGAGC
N-yfp-f	CCGCCCTGAGCAAAGACCCAACG
X-CFP-R	GGTTCAGCGTGTCCGGCGGGGCG
X-YFP-R	AGTTCAGCGTGTCCGGCGAGGGCG
AtRSP-4g12570(1000-1700)	GTCTTTTGTTGAATGAGTTAGCTCAGAATTC
AtRSP-4g12570(1000-1700)	AATATCTCCTGACATACCAGATAGAACCAT
AtRSP-4g12570(500-2200)	GTCTTTTGTTGAATGAGTTAGCTCAGAATTC
AtRSP-4g12570(500-2200)	AATATCTCCTGACATACCAGATAGAACCAT
Vps2-2g06530(without Stop)	GGGGACCACTTTGTACAAGAAAGCTGGGTCCATTTTTCTAAGGTTATCCA
Vps2-5g44560(without Stop)	GGGGACCACTTTGTACAAGAAAGCTGGGTCGATTCGTCGTAGCGAAGCCA
Vps2-1g03950(without Stop)	GGGGACCACTTTGTACAAGAAAGCTGGGTCTCTAAGCGCCGCCAACCGCT
Vps20-5g63880(without Stop)	GGGGACCACTTTGTACAAGAAAGCTGGGTCAGCCGGCAAAGGTTCTTCGA
Vps20-5g09260(without Stop)	GGGGACCACTTTGTACAAGAAAGCTGGGTCAGCTTCCAAAGGTTCTTCAA
Vps24-5g22950(without Stop)	GGGGACCACTTTGTACAAGAAAGCTGGGTCGGATCTAACTTTAGCGAGCC
Vps32-2g19830(without Stop)	GGGGACCACTTTGTACAAGAAAGCTGGGTCGAGAGCCATCTCAGCTTGTA
Vps32-4g29160(without Stop)	GGGGACCACTTTGTACAAGAAAGCTGGGTCGAGGGCCATCTCAGCCTGTA
Vps4-2g27600(without Stop)	GGGGACCACTTTGTACAAGAAAGCTGGGTCACCTTCTTCTCCAAACTCCT
YFP-gate	GGGGACCACTTTGTACAAGAAAGCTGGGTCTTACTTGTACAGCTCGTCCA
Vps4-YFP(1168)	GGGCTTGCCGAAAAGATTATTCCAC
Vps37-2g36680(repair373)	TGCAGAATAATCCGTACATC
Vps37-2g36680(repair379)	TTCTGCATTGGTTTCTGAGC
vps37(repari373)	GAAACCAATGCAGAATAATCCGTAC
vps37(repari390	GTACGGATTATTCTGCATTGGTTTC
T-GABI-specific-vps4	CTTTGATTGTTCAGGATCTTCTCC
T-GABI-PCR-VPS4	CCCATTTGGACGTGAATGTAGACAC
T-GABI-Seq-VPS4	ATATTGACCATCATACTCATTGC
Lprimer(gene specific)for tarnsposonGT-5-43334	CTGATCAAGAGCATAGGGTGTATTGGTTG
RB-GABI line	GTGGATTGATGTGATATCTCC
Transposon(DS3-1)	ACCCGACCGGATCGTATCGGT
Uprimer(gene specific)for tarnsposonGT-5-43334	GGCTAAGGCTGTTGCCACTGAAGC
Uprimer(gene specific)forGABI598A07	GACCTTGTACTTAATATATTTGAATGGTGG
INRA-RB(TDNA)	CTGATACCAGACGTTGCCCGCATAA
INRA-LB(TDNA)	CGTGTGCCAGGTGCCCACGGAATAGT
Vps27(29infarme)nostopR	GGGGGACCACTTTGTACAAGAAAGCTGGGTCTCACTCTGTGTGATTTGG
Vps27(45)nostopR	GGGGACCACTTTGTACAAGAAAGCTGGGTCCTAGATAAGCTCAAGG
Vps23-2second(10)F	GGGGACAAGTTTGTACAAAAAAGCAGGCTTCATGGCTCCTCCTCCGGCGAA

Appendix

Vps23-2second(10)R	GGGGACCACTTTGTACAAGAAAGCTGGGTCTCACGAATGCAACCTAGCTG
Vta1-new-4g26750F	GGGGACAAGTTTGTACAAAAAAGCAGGCTTCATGGCTAGTAACGCTGCAAGGGTTGTCGCT
Vta1-new-4g26750R	GGGGACAAGTTTGTACAAAAAAGCAGGCTTCATGTCGAACCCAAACGAACCAGCCAGG
Rsp5-new	GGGGACAAGTTTGTACAAAAAAGCAGGCTTCATGACTCTAAGCCGTTCATCAGCCGACGAT
Rsp5-new	GGGGGACCACTTTGTACAAGAAAGCTGGGTCTCACCATTTACCGAAACTGGAGCTGACATG
Vta1-4g26750(mips)	GGGGACAAGTTTGTACAAAAAAGCAGGCTTCATGTCGAACCCAAACGAACCAGCCAGG
Vta1-4g26750(mips)	GGGGACCACTTTGTACAAGAAAGCTGGGTCTCAGTGACCGGCACCGGCCGATGGA
Rsp5-of 500(middel)	TATGCAGAGCACAGAGCATCCTGTAGCTTG
Rsp5 of2100(middel)	CCTGTTCTTGCTGTTAACAGCCTTGAGTTT
Rsp5 o1031(middel)	CAGGGCCTAGTTTCTGTGACTTTCAGAAAG
Vta1-4g26750(mips)NO STOP	GGGGACCACTTTGTACAAGAAAGCTGGGTCGTGACCGGCACCGGCCGATGGA
Vta1-4g26750(middle450)	AAGCCCACTCCAGGTGATCCTGTGG
first part of Vta1 No Stop codon	GGGGACCACTTTGTACAAGAAAGCTGGGTCTGCCTCTGCAACCTTCTCAGGCCCT
first part of Vta1 WITH Stop codon	GGGGACCACTTTGTACAAGAAAGCTGGGTCTCATGCCTCTGCAACCTTCTCAGGCCCT
YFP	GGGGACCACTTTGTACAAGAAAGCTGGGTCTTACTTGTACAGCTCGTCCATGCCG
At4g34150(47)F	GGGGACAAGTTTGTACAAAAAAGCAGGCTTCATGTCGATGATGGCGGGTATACAAG
At4g34150(47)R	GGGGACCACTTTGTACAAGAAAGCTGGGTCCTAGTATGGAGGAGGTGGGTATTGT
At1g21440(48)F	GGGGACAAGTTTGTACAAAAAAGCAGGCTTCATGGCGGCCAAATCCACTTCACTCT
At1g21440(48)R	GGGGACCACTTTGTACAAGAAAGCTGGGTCTTATTTTGTTTCCCCTAGAGCGTTT
At4g27610(49)F	GGGGACAAGTTTGTACAAAAAAGCAGGCTTCATGAGTACACGAAGAAATGGC
At4g27610(49)R	GGGGACCACTTTGTACAAGAAAGCTGGGTCCTACAATAAGTTTTGGAGCTGTGAG
At1g08370(50)F	GGGGACAAGTTTGTACAAAAAAGCAGGCTTCATGTCTCAAAACGGGAAGATAATCC
At1g08370(50)R	GGGGACCACTTTGTACAAGAAAGCTGGGTCTCATTGTTGAAGTGCATTTTGTAAA
At3g23280(51)F	GGGGACAAGTTTGTACAAAAAAGCAGGCTTCATGGGACAACAGCAATCAAAAGGGG
At3g23280(51)R	GGGGACCACTTTGTACAAGAAAGCTGGGTCTCAGACACGGTACAGCTTAATAACC
At1g15060(52)F	GGGGACAAGTTTGTACAAAAAAGCAGGCTTCATGGCAGACACTGTTAAGCT
At1g15060(52)R	GGGGACCACTTTGTACAAGAAAGCTGGGTCTTAAACGGAAATGGCATCCT
At2g20890(53)F	GGGGACAAGTTTGTACAAAAAAGCAGGCTTCATGGCTGCAACTGCAATCTCTTCTC
At2g20890(53)R	GGGGACCACTTTGTACAAGAAAGCTGGGTCCTAAGATTTCCGTTCAACCAAGAAA
At4g24370(54)F	GGGGACAAGTTTGTACAAAAAAGCAGGCTTCATGAGGAGAGGAGGCAAGGAAGAAG
At4g24370(54)R	GGGGACCACTTTGTACAAGAAAGCTGGGTCTTAAGGTTTAACATCTCTAGTTGAA
At3g49490(55)F	GGGGACAAGTTTGTACAAAAAAGCAGGCTTCATGACCGATGGATTTCGCTATAATG
At3g49490(55)R	GGGGACCACTTTGTACAAGAAAGCTGGGTCTCAATCATCCTTGATGACATGTTCC
At1g51690(56)F	GGGGACAAGTTTGTACAAAAAAGCAGGCTTCATGAACGGTGGTGATGAGGTCGTCG
At1g51690(56)R	GGGGACCACTTTGTACAAGAAAGCTGGGTCTTAAGCATAGTACATGTACAAGCTA

Appendix

At3g62720(57)F	GGGGACAAGTTTGTACAAAAAAGCAGGCTTCATGATAGAGAAGTGTATAGGAGCGC
At3g62720(57)R	GGGGACCACTTTGTACAAGAAAGCTGGGTCTCACGTCGTCGTCGTACTAAGCTTG
At1g77060(58)F	GGGGACAAGTTTGTACAAAAAAGCAGGCTTCATGTCGATGTTAATGGCTGTC
At1g77060(58)R	GGGGACCACTTTGTACAAGAAAGCTGGGTCTCATGATTTGGTTGTCCCAAGAGCG
At2g20580(59)F	GGGGACAAGTTTGTACAAAAAAGCAGGCTTCATGGCTCCAACTCAGGATCCCAACA
At2g20580(59)R	GGGGACCACTTTGTACAAGAAAGCTGGGTCTCACTCCTCTCTGTAGTCTGGGTTC
At2g20580(59from450)F	GGTCATGAATATGTCAGGAATTTAGCTGG
At2g20580(59from2190)R	GCTGGAGAGGTTCCGAAGCATCCCGGC
At2g20580(59from922)F	GCAGATGATGATGACCGGGAAGCCC
At2g20580(59from1726)R	CCTGTTTGCCCAGGTATAGAAGTCC
At1g77060(58from350)F	CATCATTGCAGATGCTGATACCGGT
At3g62720(57from432)F	GGCGCCAAACAAGCCTAGGGTTCTT
At1g51690(56of416)F	CCATCAAGTTTTGGAAGGTTCAAGA
At1g51690(56of1127)R	GGACCTGCGTCCATGTTGATGTCCC
At3g49490(55of435)F	GCCTACCTACAGCTCAGCTACCTTAGCTCC
At3g49490(55of913)F	CTTCCCTATCCGGTAGTTGGCTCGCC
At3g49490(55of1320)F	CCAACCAACCAAGAGTCTTGTAATC
At3g49490(55of24240)R	GAGCTTGCGCTCTGTTTCCTGCTCC
At3g49490(55of2029)R	GGTTCCTGCATAAAGCTTACTGCATCCGCAG
At3g23280(51of428)F	CGGCCCTACCTTTCTCGACTTATTTGCTCCGC
At1g08370(50of413)F	CCAAGGTTAACCAGAAGCCAAAGGCCTC
At4g27610(49of416)F	CTCCTGATCGCCTGGAACTTCCCCC
Vps4YFP(451)F	CCTGTCAAGTTTCCACAGTTCTTCA
Vps4YFP(1560)R	GAAGAAGTCGTGCTGCTTCATGTGG
Vps4 with NcoI siteF	AAACCATGGCAATGTACAGCAATTTCAAGGAACAAG
Vps4 with EcoR1 siteF	AAAGAATTCCAATGTACAGCAATTTCAAGGAACAAG
Vps4 With Stopcodon with XmaIsiteR	AAACCCGGGTCAACCTTCTTCTCCAAAC
Vps4 no Stopcodon withXmaI siteR	AAAaCCCGGGACCTTCTTCTCCAAACTCC
Vps4 With Stopcodon withBamHIsiteR	AAAGGATCCTCAACCTTCTTCTCCAAACCTCC
Vps4 noStopcodon with BamHI siteR	AAAAGGATCCACCTTCTTCTCCAAACCTCC
Vps4 With Stopcodon with SalI siteR	AAAGTCGACTCAACCTTCTTCTCCAAAC
Vps4 noStopcodon with SalI siteR	AAAaGTCGACACCTTCTTCTCCAAAC
Vta1with EcoR1 siteF	AAAGAATTCCAATGTCGAACCCAAACGAACCAGCCAGGGC
Vta1 with NcoI siteF	AAACCATGGcaATGTCGAACCCAAACGAACCAGCCAGG
Vta1With Stopcodon with XmaIsiteR	AAACCCGGGTCAGTGACCGGCACCGGCC
Vta1noStopcodon with XmaI siteR	AAAaCCCGGGGTGACCGGCACCGGCC
Vta1 With Stopcodon with SalI siteR	AAAGTCGACTCAGTGACCGGCACCGGCC
Vta1noStopcodon with SalI siteR	AAAaGTCGACGTGACCGGCACCGGCC
Vps4YFP(847)F	CGGCGACGTTTTGACAAGCGTATCT
Tom1 with XmaIsiteF	AAACCCGGGCAATGAGGCCTTCTTGTGCTT
Tom1 withBamHI siteR	AAAGGATCCCTACGGCTGCCTGTCCACT
Tom1 with BamHI site NostopR	AAAGGATCCCGGCTGCCTGTCCACTGTA
Fyvewith XmaIsiteF	AAACCCGGGCAATGGCTACTCTCAACGGAA
Fyve withBamHI siteR	AAAGGATCCTTACGGGCGCAAACGAGCA
Fyve withBamHI siteNostopR	AAAGGATCCCGGGCGCAAACGAGCATAG
Elch with XmaIsiteF	AAACCCGGGCAATGGTTCCCCCGCCGTCTAAT

Appendix

Elch with BamHI siteR	AAAGGATCCTCATGAATGTAACCTACCT
Elch with BamHI site Nostop R	GGGGACAAGTTTGTACAAAAAAGCAGGCTTCATGAGCGAAACCG
At4g26410(61)	AAGCAACCGGCG
At4g26410(61)	GGGGACCACTTTGTACAAGAAAGCTGGGTCTCAGACGGAAACTC CTAGGTCCGAC
At5g22450(60)	GGGGACAAGTTTGTACAAAAAAGCAGGCTTCGAAACTCTCGTTTT TTTATTTCAGGTT
At5g22450(60)	GGGGACCACTTTGTACAAGAAAGCTGGGTCTTATCCAAACATAA ACGAGAGATCA
Tom1 withKpnIsiteF	AAAGGTACCATGAGGCCTTCTTGTGCTT
Tom1 with XmaIsite NostopR	AAAACCCGGGCGGCTGCCTGTCCACTGTA
Fyvewith KpnI siteF	AAAGGTACCATGGCTACTCTCAACGGAA
Fyve withXmaI siteNostopR	AAAACCCGGGCGGGCGCAAACGAGCATAG
Elch with KpnI siteF	AAAGGTACCATGGTTCCCCCGCCGTCTAAT
Elch withXmaI site Nostop R	AAAACCCGGGTGAATGTAACCTACCT
INRA-RB primer	TCACGGGTTGGGGTTTCTACAGGAC
INRA-LB primer	CGTGTGCCAGGTGCCCACGGAATAGT
NASC-DS3-1	ACCCGACCGGATCGTATCGGT
GABI-KAT-gene specific primer(Vps4)	CTTTGATTGTTCAGGATCTTCTCC
GABI-KAT T-DNA primer	CCCATTTGGACGTGAATGTAGACAC
T7 pro	TAATACGACTCACTATAGG
T7 Term	GCTAGTTATTGCTCAGCG
Vps4(truncate3)F	ATGTACAGCAATTTCAAGGAACAAGCGA
Vps4(truncate3)R	TCATTGTGTTTTACGAACAGGTTCAAAC
Vps4(truncate5)F	ATGTACAGCAATTTCAAGGAACAAGCGA
Vps4(truncate5)R	TCATGGTGGAATAATCTTTTCGGCAAGC
Vps4(truncate5)F	GGGGACAAGTTTGTACAAAAAAGCAGGCTTCATGTACAGCAATT TCAAGGAACAAGCGA
Vps4(truncate5)R	GGGGACCACTTTGTACAAGAAAGCTGGGTCTCATGGTGGAATAA TCTTTTCGGCAAGC

6.2. List of constructs

Name	Name of the Gene	Name of the Vector	*Source of the Gene*	Comments	Scientist
pDONR201		pDONR		Kan	Schellmann
PAS		PAS		Amp	Schellmann
PACT		PACT		Amp	Schellmann
PAS-SNF1		PAS-SNF1		Amp	Schellmann
SNF4		SNF4		Amp	Schellmann
pda08063	At2g06530(1)	RAFL	*Arabidopsis thaliana*	Amp	RIKEN
pda03672	At1g03950(3)	RAFL	*Arabidopsis thaliana*	Amp	RIKEN
pda11165	At5g63880(4)	RAFL	*Arabidopsis thaliana*	Amp	RIKEN
pda00736	At4g27040(5)	RAFL	*Arabidopsis thaliana*	Amp	RIKEN
pda04818	At3g12400(9)	RAFL	*Arabidopsis thaliana*	Amp	RIKEN
S63073	At2g38830(11)	RAFL	*Arabidopsis thaliana*	Amp	RIKEN
BX829104	At4g19003(12)	RAFL	*Arabidopsis thaliana*	Amp	RIKEN
pda09962	At4g21560(13)	RAFL	*Arabidopsis thaliana*	Amp	RIKEN
pda06592	At5g04920(15)	RAFL	*Arabidopsis thaliana*	Amp	RIKEN
pda01520	At2g27600(19)	RAFL	*Arabidopsis thaliana*	Amp	RIKEN
pda02568	At5g22950(20)	RAFL	*Arabidopsis thaliana*	Amp	RIKEN
pda11629	At5g01760(24)	RAFL	*Arabidopsis thaliana*	Amp	RIKEN
U61829	At1g76970(25)	RAFL	*Arabidopsis thaliana*	Amp	RIKEN
pda01151	At1g21380(26)	RAFL	*Arabidopsis thaliana*	Amp	RIKEN
pda04967	At5g63640(27)	RAFL	*Arabidopsis thaliana*	Amp	RIKEN
pda05496	At5g16880(28)	RAFL	*Arabidopsis thaliana*	Amp	RIKEN
pda03494	At1g06210(29)	RAFL	*Arabidopsis thaliana*	Amp	RIKEN
pda02482	At2g19830(32)	RAFL	*Arabidopsis thaliana*	Amp	RIKEN
pda01247	At4g29160(33)	RAFL	*Arabidopsis thaliana*	Amp	RIKEN
pda11379	At1g17730(34)	RAFL	*Arabidopsis thaliana*	Amp	RIKEN
pda04291	At1g73030(35)	RAFL	*Arabidopsis thaliana*	Amp	RIKEN
pda00333	At5g04850(37)	RAFL	*Arabidopsis thaliana*	Amp	RIKEN
pda08881	At2g40930(42)	RAFL	*Arabidopsis thaliana*	Amp	RIKEN
pda07144	At1g29800(43)	RAFL	*Arabidopsis thaliana*	Amp	RIKEN
pda06166	At3g43230(44)	RAFL	*Arabidopsis thaliana*	Amp	RIKEN
pda02179	At4g11740(45)	RAFL	*Arabidopsis thaliana*	Amp	RIKEN

CD3-687		pEarly gate 201		Kan+Chl	
CD3-688		pEarly gate 202		Kan+Chl	
CD3-689		pEarly gate 203		Kan+Chl	
CD3-690		pEarly gate 204		Kan+Chl	
CD3-692		pEarly gate 206		Kan+Chl	
CD3-694		pEarly gate 208		Kan+Chl	
ENS-YFP:VPS4-II	VPS4II(mutation in234aa)	ENS-YFP		Amp	Mojgan
ENS-YFP:VPS4-III	VPS4III(mutation in 178,234aa)	ENS-YFP		Amp	Mojgan
ENS-CFP:VPS4	VPS4	ENS-CFP	*A. thaliana*	Amp	Mojgan
ENS-CFP:VPS4II	VPS4II	ENS-CFP		Amp	Mojgan
ENS-CFP:VPS4III	VPS4III	ENS-CFP		Amp	Mojgan
EXS-YFP:VPS4I	VPS4I(mutation in 178aa)	EXS-YFP		Amp	Mojgan
EXS-YFP:VPS4II	VPS4II	EXS-YFP		Amp	Mojgan
EXS-YFP:VPS4III	VPS4III	EXS-YFP		Amp	Mojgan
EXS:CFP:VPS4	VPS4	EXS:CFP	*A. thaliana*	Amp	Mojgan
EXS:CFP:VPS4I	VPS4I	EXS:CFP		Amp	Mojgan
EXS:CFP:VPS4 II	VPS4II	EXS:CFP		Amp	Mojgan
EXS:CFP:VPS4 III	VPS4III	EXS:CFP		Amp	Mojgan
35S:VPS4	VPS4	pAMPAT-35S	*A. thaliana*	Amp	Mojgan
35S:VPS4I	VPS4I	pAMPAT-35S		Amp	Mojgan
35S:VPS4II	VPS4II	pAMPAT-35S		Amp	Mojgan
35S:VPS4III	VPS4III	pAMPAT-35S		Amp	Mojgan
GL2:VPS4	VPS4	pGL2-pAMPAT	*A. thaliana*	Amp	Mojgan
GL2:VPS4 I	VPS4I	pGL2-pAMPAT		Amp	Mojgan
GL2:VPS4 II	VPS4II	pGL2-pAMPAT		Amp	Mojgan
GL2:VPS4 III	VPS4III	pGL2-pAMPAT		Amp	Mojgan
At2g06530 in pDOR201	At2g06530	pDONR201	*A. thaliana*	Kan	Mojgan
At5g44560 in pDONR201	At5g44560(2)	pDONR201	*A. thaliana*	Kan	Mojgan
At1g03950 in pDONR201	At1g03950	pDONR201	*A. thaliana*	Kan	Mojgan
At5g63880 in pDONR201	At5g63880	pDONR201	*A. thaliana*	Kan	Mojgan
At4g27040 in pDONR201	At4g27040	pDONR201	*A. thaliana*	Kan	Mojgan
At2g22890 in pDONR201	At2g22890(8)	pDONR201	*A. thaliana*	Kan	Mojgan
At3g12400 in pDONR201	At3g12400	pDONR201	*A. thaliana*	Kan	Mojgan
At2g38830 in pDONR201	At2g38830	pDONR201	*A. thaliana*	Kan	Mojgan
At4g19003 in pDONR201	At4g19003	pDONR201	*A. thaliana*	Kan	Mojgan

At4g21560 in pDONR201	At4g21560	pDONR201	*A. thaliana*	Kan	Mojgan
At4g05000 in pDONR201	At4g050008(14)	pDONR201	*A. thaliana*	Kan	Mojgan
At5g04920 in pDONR201	At5g04920	pDONR201	*A. thaliana*	Kan	Mojgan
At3g53120 inpDONR201	At3g53120(16)	pDONR201	*A. thaliana*	Kan	Mojgan
At2g36680 inpDONR201	At2g36680(17)	pDONR201	*A. thaliana*	Kan	Mojgan
At5g09260 in pDONR201	At5g09260(18)	pDONR201	*A. thaliana*	Kan	Mojgan
At2g27600 in pDONR201	At2g27600	pDONR201	*A. thaliana*	Kan	Mojgan
At5g22950 inpDONR201	At5g22950	pDONR201	*A. thaliana*	Kan	Mojgan
At5g01760 in pDONR201	At5g01760	pDONR201	*A. thaliana*	Kan	Mojgan
At1g76970 in pDONR201	At1g76970	pDONR201	*A. thaliana*	Kan	Mojgan
At1g21380 in pDONR201	At1g21380	pDONR201	*A. thaliana*	Kan	Mojgan
At5g63640 in pDONR201	At5g63640	pDONR201	*A. thaliana*	Kan	Mojgan
At5g16880 in pDONR201	At5g16880	pDONR201	*A. thaliana*	Kan	Mojgan
At2g19830 inpDONR201	At2g19830	pDONR201	*A. thaliana*	Kan	Mojgan
At4g29160 in pDONR201	At4g29160	pDONR201	*A. thaliana*	Kan	Mojgan
At1g17730 in pDONR201	At1g17730	pDONR201	*A. thaliana*	Kan	Mojgan
At1g73030 in pDONR201	At1g73030	pDONR201	*A. thaliana*	Kan	Mojgan
At3g10640 in pDONR201	At3g10640(36)	pDONR201	*A. thaliana*	Kan	Mojgan
At5g04850 in pDONR201	At5g04850	pDONR201	*A. thaliana*	Kan	Mojgan
At2g40930 in pDONR201	At2g40930	pDONR201	*A. thaliana*	Kan	Mojgan
At1g29800 in pDONR201	At1g29800	pDONR201	*A. thaliana*	Kan	Mojgan
At3g43230 in pDONR201	At3g43230	pDONR201	*A. thaliana*	Kan	Mojgan
Vps2 in pEarly Gate201	At2g06530	pEarly gate 201	*A. thaliana*	Kan	Mojgan
Vps2 in pEarly Gate201	At5g44560	pEarly gate 201	*A. thaliana*	Kan	Mojgan
Vps2 in pEarly Gate201	At1g03950	pEarly gate 201	*A. thaliana*	Kan	Mojgan
Vps20 in pEarly Gate201	At5g63880	pEarly gate 201	*A. thaliana*	Kan	Mojgan
Vps22 in pEarly Gate201	At4g27040	pEarly gate 201	*A. thaliana*	Kan	Mojgan
Vps22 in pEarly Gate201	At2g22890	pEarly gate 201	*A. thaliana*	Kan	Mojgan
Vps23 in pEarly Gate201	At3g12400	pEarly gate 201	*A. thaliana*	Kan	Mojgan

Vps23 in pEarly Gate201	At2g38830	pEarly gate 201	*A. thaliana*	Kan	Mojgan
Vps25 in pEarly Gate201	At4g19003	pEarly gate 201	*A. thaliana*	Kan	Mojgan
Vps28 in pEarly Gate201	At4g21560	pEarly gate 201	*A. thaliana*	Kan	Mojgan
Vps28 in pEarly Gate201	At4g05000	pEarly gate 201	*A. thaliana*	Kan	Mojgan
Vps36 in pEarly Gate201	At5g04920	pEarly gate 201	*A. thaliana*	Kan	Mojgan
Vps37 in pEarly Gate201	At3g53120	pEarly gate 201	*A. thaliana*	Kan	Mojgan
Vp37 in pEarly Gate201	At2g36680	pEarly gate 201	*A. thaliana*	Kan	Mojgan
Vps20 in pEarly Gate201	At5g09260	pEarly gate 201	*A. thaliana*	Kan	Mojgan
Vps4 in pEarly Gate201	At2g27600	pEarly gate 201	*A. thaliana*	Kan	Mojgan
Vps24 in pEarly Gate201	At5g22950	pEarly gate 201	*A. thaliana*	Kan	Mojgan
Vps27 in pEarly Gate201	At5g01760	pEarly gate 201	*A. thaliana*	Kan	Mojgan
Vps27 in pEarly Gate201	At1g76970	pEarly gate 201	*A. thaliana*	Kan	Mojgan
Vps27 in pEarly Gate201	At1g21380	pEarly gate 201	*A. thaliana*	Kan	Mojgan
Vps27 in pEarly Gate201	At5g63640	pEarly gate 201	*A. thaliana*	Kan	Mojgan
Vps27 in pEarly Gate201	At5g16880	pEarly gate 201	*A. thaliana*	Kan	Mojgan
Vps32 in pEarly Gate201	At2g19830	pEarly gate 201	*A. thaliana*	Kan	Mojgan
Vps32 in pEarly Gate201	At4g29160	pEarly gate 201	*A. thaliana*	Kan	Mojgan
Vps46 in pEarly Gate201	At1g17730	pEarly gate 201	*A. thaliana*	Kan	Mojgan
Vps46 in pEarly Gate201	At1g73030	pEarly gate 201	*A. thaliana*	Kan	Mojgan
Vps60i 2 in pEarly Gate201	At3g10640	pEarly gate 201	*A. thaliana*	Kan	Mojgan
Vps60 in pEarly Gate201	At5g04850	pEarly gate 201	*A. thaliana*	Kan	Mojgan
Doa4 in pEarly Gate201	At2g40930	pEarly gate 201	*A. thaliana*	Kan	Mojgan

Vps27 in pEarly Gate201	At1g29800	pEarly gate 201	*A. thaliana*	Kan	Mojgan
Vps27 in pEarly Gate201	At3g43230	pEarly gate 201	*A. thaliana*	Kan	Mojgan
Vps2 in pEarly Gate202	At2g06530	pEarly gate202	*A. thaliana*	Kan	Mojgan
Vps2 in pEarly Gate202	At5g44560	pEarly gate202	*A. thaliana*	Kan	Mojgan
Vps2 in pEarly Gate202	At1g03950	pEarly gate202	*A. thaliana*	Kan	Mojgan
Vps20 in pEarly Gate202	At5g63880	pEarly gate202	*A. thaliana*	Kan	Mojgan
Vps22 in pEarly Gate202	At4g27040	pEarly gate202	*A. thaliana*	Kan	Mojgan
Vps222 in pEarly Gate202	At2g22890	pEarly gate202	*A. thaliana*	Kan	Mojgan
Vps23 in pEarly Gate202	At3g12400	pEarly gate202	*A. thaliana*	Kan	Mojgan
Vps23 in pEarly Gate202	At2g38830	pEarly gate202	*A. thaliana*	Kan	Mojgan
Vps25 in pEarly Gate202	At4g19003	pEarly gate202	*A. thaliana*	Kan	Mojgan
Vps28 in pEarly Gate202	At4g21560	pEarly gate202	*A. thaliana*	Kan	Mojgan
Vps28 in pEarly Gate202	At4g05000	pEarly gate202	*A. thaliana*	Kan	Mojgan
Vps362 in pEarly Gate202	At5g04920	pEarly gate202	*A. thaliana*	Kan	Mojgan
Vps37 in pEarly Gate202	At3g53120	pEarly gate202	*A. thaliana*	Kan	Mojgan
Vps372 in pEarly Gate202	At2g36680	pEarly gate202	*A. thaliana*	Kan	Mojgan
Vps20 in pEarly Gate202	At5g09260	pEarly gate202	*A. thaliana*	Kan	Mojgan
Vps4 in pEarly Gate202	At2g27600	pEarly gate202	*A. thaliana*	Kan	Mojgan
Vps24 in pEarly Gate202	At5g22950	pEarly gate202	*A. thaliana*	Kan	Mojgan
Vps27 in pEarly Gate202	At5g01760	pEarly gate202	*A. thaliana*	Kan	Mojgan
Vps27 in pEarly Gate202	At1g76970	pEarly gate202	*A. thaliana*	Kan	Mojgan
Vps27 in pEarly Gate202	At1g21380	pEarly gate202	*A. thaliana*	Kan	Mojgan

Vps27 in pEarly Gate202	At5g63640	pEarly gate202	*A. thaliana*	Kan	Mojgan
Vps27 in pEarly Gate202	At5g16880	pEarly gate202	*A. thaliana*	Kan	Mojgan
Vps32 in pEarly Gate202	At2g19830	pEarly gate202	*A. thaliana*	Kan	Mojgan
Vps322 in pEarly Gate202	At4g29160	pEarly gate202	*A. thaliana*	Kan	Mojgan
Vps462 in pEarly Gate202	At1g17730	pEarly gate202	*A. thaliana*	Kan	Mojgan
Vps46 in pEarly Gate202	At1g73030	pEarly gate202	*A. thaliana*	Kan	Mojgan
Vps602 in pEarly Gate202	At3g10640	pEarly gate202	*A. thaliana*	Kan	Mojgan
Vps60 in pEarly Gate202	At5g04850	pEarly gate202	*A. thaliana*	Kan	Mojgan
Doa4 in pEarly Gate202	At2g40930	pEarly gate202	*A. thaliana*	Kan	Mojgan
Vps27 in pEarly Gate202	At1g29800	pEarly gate202	*A. thaliana*	Kan	Mojgan
Vps27 in pEarly Gate202	At3g43230	pEarly gate202	*A. thaliana*	Kan	Mojgan
Vps2 in pEarly Gate203	At2g06530	pEarly gate 203	*A. thaliana*	Kan	Mojgan
Vps2 in pEarly Gate203	At5g44560	pEarly gate 203	*A. thaliana*	Kan	Mojgan
Vps2 in pEarly Gate203	At1g03950	pEarly gate 203	*A. thaliana*	Kan	Mojgan
Vps20 in pEarly Gate203	At5g63880	pEarly gate 203	*A. thaliana*	Kan	Mojgan
Vps22 in pEarly Gate203	At4g27040	pEarly gate 203	*A. thaliana*	Kan	Mojgan
Vps22 in pEarly Gate203	At2g22890	pEarly gate 203	*A. thaliana*	Kan	Mojgan
Vps23 in pEarly Gate203	At3g12400	pEarly gate 203	*A. thaliana*	Kan	Mojgan
Vps23 in pEarly Gate203	At2g38830	pEarly gate 203	*A. thaliana*	Kan	Mojgan
Vps25 in pEarly Gate203	At4g19003	pEarly gate 203	*A. thaliana*	Kan	Mojgan
Vps28 in pEarly Gate203	At4g21560	pEarly gate 203	*A. thaliana*	Kan	Mojgan
Vps28 in pEarly Gate203	At4g05000	pEarly gate 203	*A. thaliana*	Kan	Mojgan

Vps362 in pEarly Gate203	At5g04920	pEarly gate 203	*A. thaliana*	Kan	Mojgan
Vps37 in pEarly Gate203	At3g53120	pEarly gate 203	*A. thaliana*	Kan	Mojgan
Vps37 in pEarly Gate203	At2g36680	pEarly gate 203	*A. thaliana*	Kan	Mojgan
Vps20 in pEarly Gate203	At5g09260	pEarly gate 203	*A. thaliana*	Kan	Mojgan
Vps4 in pEarly Gate203	At2g27600	pEarly gate 203	*A. thaliana*	Kan	Mojgan
Vps24 in pEarly Gate203	At5g22950	pEarly gate 203	*A. thaliana*	Kan	Mojgan
Vps27 in pEarly Gate203	At5g01760	pEarly gate 203	*A. thaliana*	Kan	Mojgan
Vps27 in pEarly Gate203	At1g76970	pEarly gate 203	*A. thaliana*	Kan	Mojgan
Vps27 in pEarly Gate203	At1g21380	pEarly gate 203	*A. thaliana*	Kan	Mojgan
Vps27 in pEarly Gate203	At5g63640	pEarly gate 203	*A. thaliana*	Kan	Mojgan
Vps27 in pEarly Gate203	At5g16880	pEarly gate 203	*A. thaliana*	Kan	Mojgan
Vps32 in pEarly Gate203	At2g19830	pEarly gate 203	*A. thaliana*	Kan	Mojgan
Vps322 in pEarly Gate203	At4g29160	pEarly gate 203	*A. thaliana*	Kan	Mojgan
Vps462 in pEarly Gate203	At1g17730	pEarly gate 203	*A. thaliana*	Kan	Mojgan
Vps462 in pEarly Gate203	At1g73030	pEarly gate 203	*A. thaliana*	Kan	Mojgan
Vps602 in pEarly Gate203	At3g10640	pEarly gate 203	*A. thaliana*	Kan	Mojgan
Vps60 in pEarly Gate203	At5g04850	pEarly gate 203	*A. thaliana*	Kan	Mojgan
Doa4Vps2 in pEarly Gate203	At2g40930	pEarly gate 203	*A. thaliana*	Kan	Mojgan
Vps27 in pEarly Gate203	At1g29800	pEarly gate 203	*A. thaliana*	Kan	Mojgan
Vps27 in pEarly Gate203	At3g43230	pEarly gate 203	*A. thaliana*	Kan	Mojgan
ESCARTIII without stop codon in pDONR201	At2g06530(1)	pDONR201	*A. thaliana*	Kan	Mojgan

ESCARTIII without stop codon in pDONR201	At5g44560(2)	pDONR201	*A. thaliana*	Kan	Mojgan
ESCARTIII without stop codon in pDONR201	At1g03950(3)	pDONR201	*A. thaliana*	Kan	Mojgan
ESCARTIII without stop codon in pDONR201	At5g63880(4)	pDONR201	*A. thaliana*	Kan	Mojgan
ESCARTIII without stop codon in pDONR201	At5g09260(18)	pDONR201	*A. thaliana*	Kan	Mojgan
ESCARTIII without stop codon in pDONR201	At5g22950(20)	pDONR201	*A. thaliana*	Kan	Mojgan
ESCARTIII without stop codon in pDONR201	At2g19830(32)	pDONR201	*A. thaliana*	Kan	Mojgan
ESCARTIII without stop codon in pDONR201	At4g29160(33)	pDONR201	*A. thaliana*	Kan	Mojgan
Vps4 without stop codon in pDONR201	At2g27600(19)	pDONR201	*A. thaliana*	Kan	Mojgan
PSYC		PSYC		Amp	Mojgan
PSYN		PSYN		AMP	Mojgan
ESCARTIII in pSYC	At2g06530(1)	pSYC	*A. thaliana*	AMP	Mojgan
ESCARTIII in pSYC	At5g44560(2)	pSYC	*A. thaliana*	AMP	Mojgan
ESCARTIII in pSYC	At1g03950(3)	pSYC	*A. thaliana*	AMP	Mojgan
ESCARTIII in pSYC	At5g63880(4)	pSYC	*A. thaliana*	AMP	Mojgan
ESCARTIII in pSYC	At5g09260(18)	pSYC	*A. thaliana*	AMP	Mojgan
ESCARTIII in pSYC	At5g22950(20)	pSYC	*A. thaliana*	AMP	Mojgan
ESCARTIII in pSYC	At2g19830(32)	pSYC	*A. thaliana*	AMP	Mojgan
ESCARTIII in pSYC	At4g29160(33)	pSYC	*A. thaliana*	AMP	Mojgan
Vps4 in pSYC	At2g27600(19)	pSYC	*A. thaliana*	AMP	Mojgan
ESCARTIII in pSYN	At2g06530(1)	PSYN	*A. thaliana*	AMP	Mojgan
ESCARTIII in pSYN	At5g44560(2)	PSYN	*A. thaliana*	AMP	Mojgan
ESCARTIII in pSYN	At1g03950(3)	PSYN	*A. thaliana*	AMP	Mojgan
ESCARTIII in pSYN	At5g63880(4)	PSYN	*A. thaliana*	AMP	Mojgan
ESCARTIII in pSYN	At5g09260(18)	PSYN	*A. thaliana*	AMP	Mojgan
ESCARTIII in pSYN	At5g22950(20)	PSYN	*A. thaliana*	AMP	Mojgan
ESCARTIII in pSYN	At2g19830(32)	PSYN	*A. thaliana*	AMP	Mojgan
ESCARTIII in pSYN	At4g29160(33)	PSYN	*A. thaliana*	AMP	Mojgan
Vps4 in pSYN	At2g27600(19)	PSYN	*A. thaliana*	AMP	Mojgan

Erklärung

Ich versichere, dass ich die von mir vorgelegte Dissertation selbständig angefertigt, die benutzten Quellen und Hilfsmittel vollständig angegeben und die Stellen der Arbeit – einschließlich Tabellen, Karten und Abbildungen -, die anderen Werken im Wortlaut oder dem Sinn nach entnommen sind, in jedem Einzelfall als Entlehnung kenntlich gemacht habe; dass diese Dissertation noch keiner anderen Fakultät oder Universität zur Prüfung vorgelegen hat; dass sie – abgesehen von unten angegebenen Teilpublikationen – noch nicht veröffentlicht worden ist sowie, daß ich eine solche Veröffentlichung vor Abschluß des Promotionsverfahrens nicht vornehmen werde. Die von mir vorgelegte Dissertation ist von Prof. Dr. Martin Hülskamp betreut worden.

Mojgan shahriari

Lebenslauf

Persönliche Daten

Name	Mojgan Shahriari
Geburtsdatum	11.09.1971
Geburtdort	Kordkoy, Iran
Staatsangehörigkeit	iranisch

Schulbildung

1984 - 1988	Enghelab Gymnasium in Gorgan, Iran

Studium

1989 – 1993	Universität Azad in Tehran, Abschluss B.Sc. Biologie
1994 – 1997	Wissenschaften und Forschungen von Azad Universität in Teheran
6/2004 – 11/2008	Ph.D. Studentin an der Universität zu Köln, Deutschland

Letzte Projekte

Isolierung von Mycobacterium tuberculosis-Stämmen von verschiedenen iranischen Patienten durch DNA-Fingerabdrücke (RFLP)-Methode (M.Sc. Diplomarbeit, Es geschah in Pasture-Institut, Iran).
Klassifizierung der iranischen Oliven mit Hilfe molekularer Marker (RAPD & SSR).
Bestimmung der Rhizoctonia solani Haplotyp mittels molekularer Marker (PBR).

Promotionsarbeit

Molekular-und zellbiologische Analysen der ESCRT System in *Arabidopsis thaliana*

Wissenschaftliche Ausbildung

14.-21.9.2000	Besuch im Workshop zum Thema “Theory and Practical Recombinant DNA” Agricultural Biotechnology Research Institute der Iran (ABRII)
16.-20.02.2002	Besuch im Workshop zum Thema “Application of DNA Molecular markers on Agriculture and Natural Resources”

(As a instructor) Department of Natural Resources, Universität Gilan. Somesara, Iran.

06.-16.02.2000 Besuch im Workshop zum Thema ”Preliminary software and Applied statistic”.
Agricultural education center of Garmsar ,Iran

September 2000 Besuch in “ Application of Bioinformation in Molecular Biology“
Research Center of Biochemistry and Biophysics of Tehran University, Iran

28.06-03.07.2001 Besuch im Workshop zum Thema "In-situ-Hybridisierung"
Agricultural Biotechnology Research Institute of Iran (ABRII). Karaj, Iran.

25.12.2001 Besuch im Workshop zum Thema “ Lab Bio safety“
Agricultural Biotechnology research Institute of Iran (ABRII).

19.-24.05.2002 Besuch in einem regionalen spezialisierten Trainings-Kurs auf “Application of DNA markers for crop Improvement”. (This workshop preformed by ABRII and ICARDA)
Agricultural Biotechnology Research institute of Iran (ABRII). Karaj, Iran.

Publikation

The *Arabidopsis* elch mutant reveals functions of an ESCRT component in cytokinesis. (Development. 2006,133: 4679-4689)
Multi –drag resistant strains of Mycobacterium tuberculosis cultured from Patients in Tehran genetically belong to distinct cluster (Scand J Infect Dis. 2003; 35(1):47-51).

Genetic diversity of Iranian Olive Germplasm by RAPD marker. Proceedings of The Second National Biotechnology Congress.(9^{th} -11^{th} Oct. 2001)

Classification of Iranian wheat (Triticum thaoudar) population using, RAPD marker. Proceedings of The Second National Biotechnology Congress.(9^{th} -11^{th} Oct. 2001).

Evaluation of abiotic tolerance genes Expression (GST, APX and SOD) in Wheat and Barley. Proceedings of the first Cellular and Molecular Biology Congress, Shahid Chamran University of Ahvaz. Iran. (27th -29^{th} Feb. 2003).

	Hordeum vulgare cultivar Azar2 glutathione-S-transferase (GST) mRNA, partial cds gi|34979591|gb|AY377972.1|[34979591] Submitted on NCBI at 02-SEP-2003
	Single Nucleotide polymorphisms (SNP) in Ascorbate Peroxidase gene in Hordium Vulgare.(May 20-22. 2003) 8th Iranian Genetics Congress,page288.
Manuskript	The Arabidopsis thaliana ESCRT protein interaction network is involved in cytokinesis
In Vorbereitung	Trichome specific expression of dominant negative Arabidopsis AtSKD1 versions leads to multinuclear trichome cells